ABSTRACT

MCVEIGH, DOREEN MIRIAM ANNE. Potential Larval Dispersal and Population Connectivity of Deep-Sea Methane Seep Invertebrates. (Under the direction of Dr. David B. Eggleston).

Since their discovery, deep-sea chemosynthetic ecosystems have been novel systems within which to test the generality of paradigms developed for shallow-water species. The first part of this study explored the roles of larval behavior, pelagic larval duration (PLD), and spawning locations on dispersal potential of seep invertebrates. The goal was to assess the dispersal trajectories of the polychaete, *Lamellibrachia luymesi*, the gastropod, *Bathynerita naticoidea*, and the crustacean, *Alvinocaris muricola* among seep-sites in the Gulf of Mexico (GOM) and Western Atlantic Ocean (WAO) using a coupled biophysical model. Larval particles were programmed with species-specific PLDs and swimming behaviors that best matched empirical data, and released into a flow field that accurately characterizes climatological conditions at ~7-kilometer horizontal resolution. While there was variation, the overall trend was consistent, with the greatest dispersal observed for *A. muricola*, followed by *B. naticoidea*, and *L. luymesi*. *L. luymesi* mean particle distance travelled was significantly higher when released from western GOM (274 km ± 0.82), followed by the eastern GOM (171 km ± 0.82). *B. naticoidea* mean particle distance travelled was significantly higher when released from western GOM (670 km ± 1.27), followed by WAO (287 km ± 1.27), northern WAO (286 km ± 1.27), central GOM (241 km ± 0.15), and western GOM (268 km ± 1.27). *A. muricola* mean particle distance travelled was significantly higher when released from eastern GOM (854 km ± 2.53), followed by central GOM (846 km ± 1.27), western GOM (757 km ± 1.27), WAO (616 km ± 1.27), and northern WAO (612 km ± 1.27). In Chapter 2, the dissertation explored potential larval dispersal and

population connectivity of the deep-sea mussel, "*Bathymodiolus" childressi* among three methane seep sites in the Gulf of Mexico. Three possible larval dispersal simulations were evaluated: (1) demersal drift of larvae, (2) variable larval vertical distribution with near surface dispersal, and (3) variable larval vertical distribution with near-surface dispersal. Particles with Simulation 3 behavior had the greatest dispersal distance (1173 km $\pm$2.00), followed by Simulation 2 (921 km $\pm$2.00), and Simulation 1 behavior (237 km $\pm$1.43). In Chapter 3, the dissertation quantified potential population connectivity using Lagrangian Particle Density Functions (LPDFs) and connectivity matrices for the five methane seep species. There were marked differences in the strength of larval dispersal pathways and LPDFs among the different species and release sites, with a majority of larval particles remaining near their natal site. The LPDFs of particles released from the GOM with surface seeking "*B." childressi* behavior readily dispersed throughout the eastern GOM and WAO. Conversely, *L. luymesi* and "*B." childressi* demersal drifting particles were spatially constrained to the northern and western GOM, with no connection to the WAO. The majority of *A. muricola* and *B. naticoidea* particles released from WAO dispersed south of the release sites along the shelf-break depth contour toward the Caribbean (southward). Patterns of population connectivity varied greatly among species, with the greatest amount of connectivity by *B. naticoidea* and *A. muricola*, and the least amount of connectivity exhibited by surfacing seeking *"B." childressi* and *L. luymesi*. Despite the extensive dispersal of particles, no other sites exhibited any degree of connectivity. These results are the first known attempt to use empirically observed behavior of larval seep invertebrates to assess dominant pathways and connectivity in a coupled biophysical model, and assess self-recruitment from release sites despite wide variation in PLD and behavior. Collectively, the

three chapters of this dissertation provide an initial and quantitative understanding of the potential population connectivity for four species of methane seep invertebrates found throughout the GOM and WAO and the significance of coupled biophysical models to test connectivity hypotheses.

Potential Larval Dispersal and Population Connectivity of Deep-Sea Methane Seep Invertebrates.

by
Doreen Miriam Anne McVeigh

A dissertation submitted to the Graduate Faculty of
North Carolina State University
in partial fulfillment of the
requirements for the degree of
Doctor of Philosophy

Marine, Earth, and Atmospheric Sciences

Raleigh, North Carolina

2016

APPROVED BY:

_____	_____
Dr. David B. Eggleston Committee Chair	Dr. Ruoying He
_____	_____
Dr. Astrid Schnetzer	Dr. David DeMaster

DEDICATION

This dissertation is dedicated to my mother, grandmothers, and all of the strong women who have shown me how to pursue life's passions as a leader with grace, poise, and a tremendous amount of grit. I also dedicate this dissertation to my husband, Dr. Ken Fincham, for supporting and encouraging me at every step.

BIOGRAPHY

Doreen McVeigh was born and raised in Barrington, Illinois a small town in the northwestern suburbs of Chicago. Several family trips to the mountains or beach usually resulted in her mother partaking in a few spirits, her father vomiting in reaction to his surroundings, and the three children having a grand time. Eager to participate in aquatic adventures, the three siblings joined the high school SCUBA club. Doreen became enthralled with marine life and the wonderful world that existed beneath the waves. Outside of work and on dry land, Doreen was an active horseback rider, thespian, and Irish dancer, which she continues to practice whenever possible.

Prior to her dissertation at North Carolina State University, Doreen attended Sweet Briar College in Virginia, where she majored in Biology. Sweet Briar offered the chance to explore scientific research on a variety of subjects, such as the cryptic sexual dioecy of the Tall Meadow Rue, *T. pubescens*, and the reproductive anatomy and physiology of the female walkingstick, *D. femorata*. In the quest to satisfy her thirst for knowledge and travel, Doreen studied 17th century Literature and History at the University of Oxford, Medieval History and 17th century art and architecture at the University of St. Andrews, and DNA methylation of the canine *IGF2/H19* genes at University College Dublin. Her liberal arts education taught Doreen the meaning of good scholarship, regardless of subject area, and the power to convey one's thoughts in a persuasive, coherent fashion. It is worth noting that until her third year of college, Doreen had not considered pursuing marine biology, and it was the fortuitous arrival of Dr. John Morrissey and his colony of chain catsharks that completely changed her path. With nearly 100 sharks in her care, Doreen learned elasmobranch husbandry and fell in love,

despite the fact that while cleaning the tanks she more than once got a mouthful of shark waste. Rest assured, she has since learned better siphon techniques.

Following graduation from Sweet Briar, Doreen started her master's degree at Hood College in Frederick, Maryland under the direction of Dr. Susan Carney and Dr. Drew Ferrier. Her time at Hood was transformational, as she learned how to lead a team of volunteers gathering data to better understand the population connectivity of the cownose ray, *Rhinoptera bonasus*. Her master's research taught her how to handle demanding fieldwork, raise awareness about the plight of stingrays, as well as isolate and sequence new mitochondrial genes. Stingrays will always have a special place in her heart, and she hopes to continue educating the public about these magnificent creatures for many years to come.

After completing her master's, Doreen enthusiastically embarked on the next adventure to start as a Ph.D. student at North Carolina State University in the Department of Marine, Earth, and Atmospheric Sciences. Her time conducting research at the university and becoming involved with the department has been one of the most rewarding and challenging experiences of a lifetime. In the lab, Doreen assisted on oyster projects in Pamlico Sound, enabling her to hone her abilities as a SCUBA diver and practical skills such as trailering and driving a boat. Outside of the lab, Doreen was actively involved with science education and communication through the North Carolina Museum of Natural Sciences and the Scientific Research Education Network (SciREN). As she reaches the end of her time as a Ph.D. student at NC State, Doreen will forever treasure the experiences and friends made over her four years in the Eggleston lab.

ACKNOWLEDGMENTS

Thank you to my mother, Wanda McVeigh, who raised and taught me to know your self worth and pursue happiness both professionally and personally. The support of my siblings, Andrew and Caitlin, and dearest friends, Aaron Wesley and Emma Bowers, made the difficult moments and periods of self-doubt bearable and I thank each and every one of you from the bottom of my heart. I'm so grateful to my husband, Dr. Ken Fincham, for his love and patience as I spent several weeks at sea with limited communication, and continue to enthusiastically explain the purpose of otoliths and organs I remove from his seafood dinners in nice restaurants. Thank you to my four-legged family members, particularly the kitties: Addie, Bee-Bee, Oliver, and Milo, and the dogs: Lilly, Feisianna, and Hope, who were always ready for hugs and companionship after a long day. No graduate experience is complete without a lab family, and I am so thankful for the friendship, guidance, and support of: Shannon Ricci, Seth Theuerkauf, Katelyn Theuerkauf, Jason Peters, Robert Dunn, Ashlee Lillis, Brandon Puckett, Pat Lyon, Olivia Caretti, and Kayelyn Simmons.

The faculty, staff, and graduate students in the Department of Marine, Earth, and Atmospheric Sciences (MEAS) have been tremendous over the years and made daily life in Jordan Hall one of joy. Thank you to Dr. Walt Robinson for serving as department head and maintaining such a welcoming and inclusive atmosphere for students who wanted to talk or share ideas. Many thanks to Dr. Gary Lackmann for being such a great Director of Graduate Programs and dedicating his time to support MEAS graduate students. Thank you to the administrative staff members who were always quick to answer emails and knew the answer to nearly every question: Laura Holland, Connie Hockaday, Beth Graf, Margo Hickman, SJ Curtis, Meredith Henry, and Marlu Bolton.

I am so grateful for the expertise and support by Dr. Dave Eggleston, my advisor and mentor, as we both took the plunge into deep-sea research. Thank you Dave for helping me undertake one of the most difficult tasks I have ever encountered, and for showing such kindness and support over the years. There were challenging moments for both of us with this research, but I'm thankful that we were in it together to face everything from deep-sea moorings to computer simulations, and even a newly discovered shipwreck! Working with Dave on both coastal and deep-sea research has helped me more fully appreciate the breadth and width of skills required to have in one's toolbox, and the importance of engaging in university life as a professional. This project would also not have been possible without the integration of both Dr. Eggleston's Marine Ecology Lab and Dr. Ruoying He's Ocean Observing and Modeling Group, and it has been a tremendous opportunity to work with both labs. In particular I'd like to acknowledge Dr. Austin Todd for the time and energy he has devoted to my project and the arduous task of teaching MATLAB and climatological modeling to a biologist. There's not enough money in the world to purchase all the beer I owe Austin for his help, so instead I offer my undying gratitude for your mentorship, patience, and friendship. *Vielen Dank für deine Hilfe den ganzen Weg von Deutschland*!

This project included a lot of fieldwork and time at sea working with fantastic scientists and crew over the years. Thank you to the crew of the *R/V Cape Hatteras, Pelican, Endeavor, Walton Smith*, and *Atlantis* for their professionalism and expertise while at sea. Many thanks to the engineering teams of *Alvin* and *Sentry* who worked tirelessly to help us achieve our science objectives over two cruises. Thank you to our partners on the SEEPC team from Duke University and the Oregon Institute of Marine Biology for making our time at sea so successful and enjoyable: Dr. Cindy Van Dover, Dr. Craig Young, Abbe La Bella,

Caitlin Plowman, Jamie Wagner, Amy Burgess, and many others. I'm grateful to the NCSU mooring and physical oceanography team, particularly Dr. Joseph Zambon for his leadership, humor, and friendship as we worked side-by-side on several cruises as the XBT drop team and CTD winch wenches.

I would also like to thank the many people who have helped shape my graduate experience outside of research, particularly the people at the North Carolina Museum of Natural Sciences (NCMNS), The Scientific Research and Education Network (SciREN), and the NC State Graduate School. Brian Malow and Katey Ahmann from NCMNS taught the Science Ambassador workshop for two years and provided me a place in the Daily Planet to share the fascinating science of deep-sea research with museum visitors. Thank you to the organizers and founders of SciREN for the chance to organize two years of SciREN Triangle events in partnership with the NCMNS that continues to teach hundreds of researchers how to develop lesson plans for K-12 classrooms. Thank you to the NC State Graduate School for providing many opportunities for education and outreach: 3MT, Graduate Research Symposium, and Graduate Student Day at the NC Legislature. It has been an honor to work with Dean Maureen Grasso and her group of talented associate deans and staff to highlight graduate research from NC State, and learn the strategies to become a successful leader of a university. Finally, my research would not have been possible without funding from the National Science Foundation, and I am very grateful for their financial support.

TABLE OF CONTENTS

LIST OF TABLES

Chapter 1

Chapter 2

Chapter 3

LIST OF FIGURES

Chapter 1

Chapter 2

DISSERTATION INTRODUCTION

Connectivity and spatial models of shallow water systems have made great progress in recent years, reaching finer scale measurements and better predicting capabilities (Cowen and Sponaugle 2009, Jones et al. 2009, Qian et al. 2014, Puckett et al. 2014). Furthermore, oceanographic models can now perform simulations to predict population connectivity subsequently verifiable by population genetics. Currently published articles do not directly couple hydrodynamic larval transport models with empirical data, which is an area crucial to understanding how oceanographic processes influence genetic structure of populations.

Studies of larval dispersal long considered larvae to be passive planktonic particles, completely subject to physical oceanographic processes, but in recent decades the roles of larval behavior in dispersal and settlement outcomes have become increasingly recognized (Levin 2006, Metaxas 2011). In marine systems, the exchange of dispersing larvae among subpopulations can drive the (i) dynamics of marine metapopulations, (ii) resilience of populations to exploitation, and (iii) success of management strategies such as no-take marine reserves (Cowan and Sponaugle 2009, Gaines et al. 2010, Puckett and Eggleston 2016). Several biophysical processes can drive dispersal and connectivity patterns, such as the location and timing of spawning relative to hydrodynamic features and the availability of suitable habitat (Sponaugle et al. 2002, Edwards et al. 2007, Ayata et al. 2010, Gilbert et al. 2010, Huret et al. 2010, Eggleston et al. 2010, Basterretxea et al. 2012, Pinsky et al. 2012). Processes occurring during the larval phases may also drive dispersal and connectivity. For example, larval behaviors alter the vertical distribution of larvae in the water column exposing larvae to different hydrodynamic conditions at different depths, thereby modifying

dispersal patterns (Sponaugle et al. 2002, Drew and Eggleston 2006, Paris et al. 2007, North et al. 2008, Butler et al. 2011). Moreover, the pelagic larval duration (PLD) may range from days to months, after which larvae must find suitable habitat and successfully settle (Levin, 2006, Young et al. 2012). Thus, spatiotemporal variation in population connectivity among subpopulations over ecological and evolutionary time scales can result from variations in the timing and location of spawning, hydrodynamic processes, larval behavior and mortality, and post-settlement processes such as emigration and mortality (Van Dover et al. 2002, Levin 2006, Mitarai et al. 2016).

For many marine benthic species, the planktonic larval stage allows the next generation to disperse and settle in new habitats over a variety of spatiotemporal scales. Population connectivity, the exchange of individuals among populations, can affect genetic composition, as well as the dynamics of local populations and communities (Cowen et al. 2007, Treml et al. 2012, Puckett et al. 2014). The length of time at which larvae can exist in the water column can greatly affect population connectivity, and varies by species from a few days to over a year (Thorson 1950, Wray and Raff 1991, Young et al. 1997, Le Pennec and Beninger 2000, Arellano and Young 2009). The wide range of larval behaviors and physical mechanisms together with their variability at multiple scales makes larval transport exceedingly difficult to measure (Pineda et al. 2007). Multiple sampling events while the larvae are in the water column can provide tremendous insight, however, the logistics of ship time, cost, and uncertainty of spawning events make direct observations difficult. Examining the effects of oceanographic events on transport is far more feasible in a modeling context,

where multi-year models can examine impacts of seasonal and inter-annual variability on the dispersal patterns of larvae to sites (Young et al. 2012, Qian et al. 2015). The ability to conduct meso-scale modeling increases our understanding and appreciation of the role morphological aspects can play in larval transport.

Therefore, the first objective of this dissertation was to address how does species-specific larval behavior and PLD influence the larval dispersal potential and population connectivity of three seep species: (1) the deep-sea polychaete, *Lamellibrachia luymesi*, (2) gastropod, *Bathynerita naticoidea*, and (3) crustacean, *Alvinocaris muricola*. Specifically, in Chapter 1 the dissertation compared species-specific biological parameters and particles subjected to advection and diffusion ("currents only") in the *US East* model across five sites in the Gulf of Mexico and South Atlantic Bight. In Chapter 2, the dissertation examined three possible behaviors and their effect on larval dispersal potential and population connectivity for the bivalve, *"Bathymodiolus" childressi*. Highly specific behavior parameters were programmed which reflected three behavior scenarios that have been observed by larvae caught in the Gulf of Mexico. Finally, in Chapter 3 the dissertation quantified potential connectivity for all four species (*L. luymesi*, *B. naticoidea*, *A. muricola*, and *"B." childressi*) using Lagrangian Particle Density Functions and connectivity matrices to evaluate the strength of potential population connectivity between five known methane seep sites.

REFERENCES

Arellano, S.M., and C.M. Young. 2009. Spawning, development, and the duration of larval life in a deep-sea cold-seep mussel. *Biol Bull* 216:149–162.

Ayata, S. D., P. Lazure, and E. Thiébaut. 2010. How does the connectivity between populations mediate range limits of marine invertebrates? A case study of larval dispersal between the Bay of Biscay and the English Channel (North-East Atlantic). *Prog Oceanog* 87(1):18-36.

Basterretxea, G., A. Jordi, I.A. Catalan, and A.N.A. SabatÉS. 2012. Model-based assessment of local-scale fish larval connectivity in a network of marine protected areas. *Fish Oceanog* 21(4):291-306.

Butler, M.J., C.B. Paris, J.S. Goldstein, H. Matsuda, and R.K. Cowen. 2011. Behavior constrains the dispersal of long-lived spiny lobster larvae. *Mar Ecol Prog Ser* 422:223-237.

Cowen, R.K. and S. Sponaugle. 2009. Larval dispersal and marine population connectivity. *Annu Rev Mar Sci* 1: 443-466.

Cowen, R.K., G. Gawarkiewicz, J. Pineda, S.R. Thorrold, and F.E. Werner. 2007. Population connectivity in marine systems. *Oceanog* 20(3):14-21.

Drew, A.C. and D.B. Eggleston. 2006. Currents, landscape structure, and recruitment success along a passive-active dispersal gradient. *Landsc Ecol* 21:917-913.

Edwards, K. P., J.A. Hare, F.E. Werner, and H. Seim. 2007. Using 2-dimensional dispersal kernels to identify the dominant influences on larval dispersal on continental shelves. *Mar Ecol Pro Ser* 352(77).

Eggleston, D.B., N.B. Reyns, L.L. Etherington, G.R. Plaia, and L. Xie. 2010. Tropical storm and environmental forcing on regional blue crab (*Callinectes sapidus*) settlement. *Fish. Oceanogr.* 19:89-106.

Gaines, S.D. C. White, M.H. Carr, and S.R. Palumbi. 2010. Designing marine reserve nerworks for both conservation and fisheries management. *Proc Natl Acad Sci USA* 107:18286-18293.

Gilbert, C. S., W.C. Gentleman, C.L. Johnson, C. DiBacco, J.M. Pringle, and C. Chen. 2010. Modelling dispersal of sea scallop (Placopecten magellanicus) larvae on Georges Bank: The influence of depth-distribution, planktonic duration and spawning seasonality. *Prog Oceanog* 87(1): 37-48.

Huret, M., P. Petitgas, and M. Woillez. 2010. Dispersal kernels and their drivers captured with a hydrodynamic model and spatial indices: a case study on anchovy (*Engralis enrasicolus*) early life stages in the Bay of Biscay. *Prog Oceanog* 87:6-17.

Jones, W. J. and R.C. Vrijenhoek. 2006. Evolutionary relationships within the "Bathymodiolus " childressi group. *Cah. Biol. Mar.* 47: 403–407.

LePennec, M. and P.G. Beninger. 1997. Aspects of the reproductive strategy of bivalves from reducing-ecosystem. *Cah Biol Mar* 38:132-133.

Levin, L. A. 2006. Recent progress in understanding larval dispersal: new directions and digressions. *Integr. Comp. Biol.* 46: 282-297.

Metaxas, A. 2011. Spatial patterns of larval abundance at hydrothermal vents on seamounts: evidence for recruitment limitation. *Mar. Ecol. Prog. Ser*, 437(10).

Mitarai, S., H. Watanabe, Y. Nakajima, A.F. Shchepetkin, and J.C. McWilliams. 2016. Quantifying dispersal from hydrothermal vent fields in the western Pacific Ocean. *PNAS* 113(11): 2976-2981.

North, E.W., Z. Schlag, R.R. Hood, M. Li, L. Zhong, T. Gross, and V.S. Kennedy. 2008.Vertical swimming behavior influences the dispersal of simulated oyster larvae in a coupled particle-tracking and hydrodynamic model of Chesapeake Bay. *Mar Ecol Prog Ser* 359:99-115.

Paris, C.B., L.M. Cherubin, and R.K. Cowen. 2007. Surfing, spinning, or diving from reef to reef: effects on population connectivity. *Mar Ecol Prog Ser* 347:285-300.

Pinsky, M. L., S.R. Palumbi, S. Andréfouët, and S.J. Purkis. 2012. Open and closed seascapes: where does habitat patchiness create populations with high fractions of self-recruitment? *Ecol App* 22(4):1257-1267.

Puckett, B.J., D.B. Eggleston, P.C. Kerr and R.A. Luettich Jr. 2014. Larval dispersal and population connectivity among a network of marine reserves. *Fish and Oceanogr 23*(4), 342-361.

Puckett, B. J. and D. B. Eggleston. 2016. Metapopulation dynamics guide marine reserve design: importance of connectivity, demographics, and stock enhancement. *Ecosphere* (in press).

Qian, H., Y. Li, R. He and D.B. Eggleston. 2015. Connectivity in the Intra-American Seas and implications for potential larval transport. *Coral Reefs*, 34(2):403-417.

Sponaugle, S., R.K. Cowen, A. Shanks, S.G. Morgan, J.M. Leis, J. Pineda, and J.L. Munro. 2002. Predicting self-recruitment in marine populations: biophysical correlates and mechanisms. *Bull Mar Sci* 70(Supplement 1): 341-375.

Thorson, G.L. 1950. Reproductive and larval ecology of marine bottom invertebrates. *Biol Rev* 1:1-45.

Treml, E.A., J.J. Roberts, Y. Chao, P.N. Halpin, H.P. Possingham, and C. Riginos. 2012. Reproductive output and duration of the pelagic larval stage determine seascape-wide connectivity of marine populations. *Integ Compar Biol* 52(4): 525-537.

Van Dover, C.L., C.R. German, K.G. Speer, L.M. Parson, and R.C. Vrijenhoek. 2002. Evolution and biogeography of deep-sea vent and seep invertebrates. *Science* 295(5558): 1253-1257.

Wray, G. A., and R. A. Raff. 1991. The evolution of developmental strategy in marine invertebrates. *Trends Ecol. Evol.* 6: 45–50.

Young, C.M., R. He, R.B. Emlet, Y. Li, H. Qian, S.M. Arellano, A.Van Gaest, K.C. Bennett, M. Wolf, T.I. Smart, and M.E. Rice. 2012. Dispersal of deep-sea larvae from Intra-American Seas: simulations of trajectories using ocean models. *Integ and Compar Biol* 52(4): 483-496.

Young, C. M., P. A. Tyler, and L. Fenaux. 1997. Potential for deep sea invasion by Mediterranean shallow water echinoids: pressure and temperature as stage-specific dispersal barriers. *Mar. Ecol. Progr. Ser.* 154: 197–209.

CHAPTER 1

LARVAL DISPERSAL AND POTENTIAL POPULATION CONNECTIVITY AMONG DEEP-SEA, HYDROCARBON SEEP INVERTEBRATES: INTERACTING EFFECTS OF BEHAVIOR AND SPAWNING LOCATION

ABSTRACT

The free-swimming larval stage of marine benthic invertebrates is a key life phase that promotes population connectivity. Benthic invertebrates of deep-sea methane seeps are widely distributed, however, how the biophysical factors impact and interact to drive dispersal of invertebrate larvae to disperse and encounter suitable habitat are not well known. This study uses a coupled biophysical model to predict spatiotemporal variability in population connectivity of deep-sea methane seep invertebrates in the Gulf of Mexico and U.S South Atlantic Bight, by quantifying potential larval particle dispersal and the likely processes driving this dispersal. Species-specific biological parameters, such as pelagic larval duration (PLD) and larval swimming behavior were assigned to particles simulating the deep-sea polychaete, *Lamellibrachia luymesi* (PLD = 21 days), gastropod, *Bathynerita naticoidea* (PLD = 90 days), and crustacean, *Alvinocaris muricola* (PLD = 186 days) that were allowed to disperse among five known methane seep sites. Particles with no programmed behavior were also released into the flow field to compare the effect of behavior on average dispersal distance and trajectories. Larval behavior, spawning location and species-specific PLDs strongly influenced particle distribution throughout the model domain. Average dispersal trajectories for particles exhibiting species-specific behavior varied 18 km to 854 km away from methane seep sites, extensively covering the Gulf of Mexico and South

Atlantic. This integrative approach of hydrodynamic modeling and simulated behavior advances our understanding of the factors regulating dispersal throughout the ocean, and the combined effects of oceanographic conditions and larval behavior on potential connectivity of five methane seep species in the Gulf of Mexico and Atlantic Ocean.

KEY WORDS

Bathynerita naticoidea, *Alvinocaris muricola*, *Lamellibrachia luysmesi*, biophysical model, larval dispersal, methane seep

INTRODUCTION

For many marine benthic species, the planktonic larval stage allows the next generation to disperse and settle in new habitats over a variety of spatiotemporal scales. Population connectivity, the exchange of individuals among populations, can affect genetic composition, as well as the dynamics of local populations and communities (Cowen et al. 2007, Treml et al. 2012, Puckett et al. 2014). The length of time at which larvae can exist in the water column, known as pelagic larval duration (PLD), can greatly affect population connectivity, and varies by species from a few days to over a year (Thorson 1950, Wray and Raff 1991, Young et al. 1997, Le Pennec and Beninger 2000, Arellano and Young 2009). Larval behavior can also influence both larval dispersal distance and the resulting biogeography. For example, vertical migration and horizontal swimming can have considerable influence on dispersal potential, as larvae capitalize on varying current speeds and directions in the water column to retain themselves within certain oceanographic features, or find suitable habitat (DeHaan and Sturges 2005, Sturges and Lugo-Fernandez 2005). While the study of how PLD and larval behavior influence dispersal is improving for many shallow-water species (e.g., Cowen et al. 2007, Cowen and Sponagule 2009, Puckett et al. 2014 and references therein), there is relatively little known regarding the importance of these factors on population connectivity in the deep-sea (Arellano et al. 2014, Young et al. 2012).

Larval dispersal via deep-sea ocean circulation is one of the major factors influencing the distribution and abundance, species diversity, and gene flow of deep-sea animals (Grassle 1989, Van Dover et al. 2002, Carney et al. 2006). While surface circulation patterns can be studied with the use of satellite observations, observations of deep currents are limited to data

generated from current meters positioned on deep-sea moorings, and deep ocean drifters. Deep ocean currents are generally 1-2 orders in magnitude slower than surface currents, and flow in opposite directions to surface currents (Sturges and Lugo-Fernandez2005). For example, in the Gulf of Mexico (GOM), the anticyclonic Loop Current dominates the upper-layer current flow with speeds of approximately 1 m s^{-1}, whereas the deep layer exhibits a cyclonic flow pattern with speeds of approximately 1-2 cm s^{-1} (DeHaan and Sturges 2005). Therefore, variation in deep-sea current velocities may result in potential larval dispersal patterns that are opposite of those predicted for larval dispersing in near-surface waters, and with potentially reduced population connectivity owing to relatively slow current speeds in the deep sea.

Methane seeps, also known as cold seeps, occur along continental margins where reduced methane and sulfide emerge from ocean sediment (Levin 2006). Methane seeps were fairly recently discovered (Paull et al. 1984), but have since been found throughout the world's oceans (MacDonald et al. 1994, Olu et al. 1996, Sibuet and Olu 1998, Egorov et al. 1999, Suess et al. 1999, Sahling et al. 2002, Van Dover et al. 2002). The exploration of methane activity off of the U.S. Atlantic Margin led to the discovery of more than 400 methane seeps (Skarke et al. 2014), which drastically increases scientific understanding of seep distribution and abundance patterns, as well as the implications for potentially high population connectivity among seep invertebrates.

Population connectivity and genetic structure in chemosynthetic ecosystems are of particular interest because of the obligate relationships between biomass-dominant species, particularly those that host autotrophic endosymbionts that help to metabolize the methane

gas that forms the basis of the food web. For example, in deep-sea hydrothermal vent systems effective dispersal mechanisms are based on (i) the rapid colonization of new vents by invertebrates following major eruptive events (Shank et al. 1998), (ii) evidence for cohort phenomena, whereby a vent is colonized by organisms of distinct age-classes over specific time events (Van Dover et al. 2002), and (iii) lack of evidence for population genetic structure on scales of <100 km for several vent species (e.g., Won et al. 2003, Hurtado et al. 2004). Less is known about population connectivity for hydrocarbon seep faunas (Levin 2005), however, the occurrence of amphi-Atlantic species complexes of mussels, shrimp, and other taxonomic groups (Olu-LeRoy et al. 2007, Cordes et al. 2007) suggests limited population connectivity in some cases, and spatially broad connectivity in others. For instance, for the deep-sea mussel *Bathymodiolus childressi*, molecular *mt*COI phylograms (Cordes et al. 2007) suggest contemporary gene flow and population connectivity within the Intra-American Seas (>1,000 km^2), which includes known deep-water seeps in the southeastern Caribbean, central and eastern GOM and along the Western Atlantic. Conversely, allozyme analysis of the deep-sea amphipod *Ventiella sulfuris* (Crustacea: Malacostraca Lysianassidae) shows strong isolation by distance (over an area of 1,200 km^2), likely due to the way in which it broods eggs (France et al. 1992, Virjenhoek 1997). Improved biophysical modeling techniques (Puckett et al. 2014, Qian et al. 2015) can predict potential larval dispersal and population connectivity among seep invertebrates with varying PLDs and larval behaviors and, thus, can help biological oceanographers predict how new populations are colonized and how present populations persist. These mechanisms can then

be tested with molecular tools that identify the spatial scales at which genetic differentiation occurs (Carney et al. 2006, Thaler et al. 2011).

Ocean circulation dynamics and dispersal potential of invertebrates in the deep sea are active areas of research, but are limited by a dearth of observations and empirical data on (i) larval distributions in the water column, (ii) larval behavior, and the (iii) timing and locations of spawning. This study assesses the influence of larval behavior and PLD, as well as spawning location and timing, on larval dispersal potential and population connectivity among methane seeps in the GOM and Western Atlantic Ocean. Three species of seep invertebrates with varying larval behaviors and PLDs are examined: (1) the deep-sea polychaete, *Lamellibrachia luymesi*, (2) the gastropod, *Bathynerita naticoidea*, and (3) the crustacean, *Alvinocaris muricola*.

MATERIALS AND METHODS

Climatological conditions were integrated (e.g., current fields and surface forcing) into a regional ocean modeling system, with current velocities subsequently driving a Lagrangian particle-tracking model that generated larval particle dispersal paths. These computer simulations compared the main and interactive effects of spawning location and larval dispersal behavior (versus without behavior), among three species of hydrocarbon seep-invertebrates with varying PLDs, on the following response variables: (1) general particle trajectories, (2) mean and (3) maximum dispersal distances.

Biophysical Model and Spatio-Temporal Scales

The *US East model* is a type of Regional Ocean Modeling System (ROMS) developed by the Ocean Observing and Modeling group at North Carolina State University (He et al. *in prep*). This model generates 3D current velocities under realistic climate conditions, such as wind speed, flow velocity, and temperature. The US East model domain (Fig.1) covers the entire Gulf of Mexico, U.S. South Atlantic, U.S. Mid-Atlantic and North Atlantic Bights, northwest Atlantic Ocean, as well as the Sargasso, Caribbean and Intra-American Seas. The grid spacing of *US East* is $1/12^{o}$ (7-10 km) and utilizes 36 terrain-following vertical levels with increased resolution towards the surface and ocean bottom.

Open boundary conditions, where model data flows freely into the eastern boundary of the model domain, are generated annually and derived from **HY**brid **C**oordinate **O**cean **M**odel (HYCOM) solutions. HYCOM is a global ocean model that assimilates satellite-observed sea surface temperature and height, and ARGOS measured temperature and salinity with daily predictions of circulation at 10 km spatial resolution (http://hycom.rsmas.miami.edu/dataserver). The HYCOM solutions from 2009-2014 are averaged annually to determine climatological monthly means for atmospheric and oceanographic conditions.

Surface atmospheric forcing used to drive the *US East* circulation model was derived from the National Center for Environmental Prediction (NCEP) reanalysis products (e.g. cloud cover) with a spatial grid spacing of 1.875^{o} and temporal resolution of six hours. Total cloud cover, precipitation, surface pressure, relative humidity, air temperature, surface wind, and net short-wave and long-wave radiations were used in a standard bulk formula (Fairall et

al. 2003) to derive wind stress and net surface heat flux which, in turn, were used to drive the ocean circulation model.

A five-year simulation of ocean currents was used for model spin-up of realistic ocean conditions, followed by a simulation period of particle trajectories. *USEast* was paired with a Lagrangian particle tracking model (see below) to track the position of larval particles released from five methane seep sites that are a part of a broader study of population connectivity among seep sites (*SEEPC* Collaborative Research Program; www.cmast.ncsu.edu/seepc): (1) Alaminos Canyon (26 21'17"N, 94 29'48" W), (2) Brine Pool (27 43'23"N, 91 16'30"W), (3) Florida Escarpment (26 1'48"N, 84 54'54"W, (4) Blake Ridge (32 29'45"N, 76 11'30"W), and (5) Cape Fear (32 58'45"N, 75 55'30"W) (Fig.1; Table 1). The seeps were chosen because they provide a means to study connectivity on spatial scales that match those at which vent systems are being studied (Hurtado et al. 2004) and include species that span large depth and geographic ranges and have diverse life-history characteristics.

Larval Behavior

Larval behaviors, such as (i) swimming speed, (ii) planktonic larval duration, and (iii) vertical distribution in the water column, were determined with a combination of published literature (Young et al. 1996, Van Gaest 2006, Arellano 2008, Young et al. 2012), shipboard observations of larvae, and zooplankton tows while at sea. For the purposes of clarification, behavior is defined as a particle actively moving or maintaining a presence at a particular

depth at an assigned swimming speed over the course of the particle's assigned PLD. The larval forms of *L. luymesi* and *B. naticoidea* were collected with MOCNESS (**M**ultiple **O**pening/**C**losing **N**et and **E**nvironmental **S**ensing **S**ystem) zooplankton tows from two seep sites during a research cruise (RV Atlantis AT26-15) by the authors in the Gulf of Mexico in 2014: Brine Pool (27^{o} 43.4 N 91^{o} 16.8 W) and GB648 (27^{o} 18.904 N, 92^{o} 22.800W). Based on larval morphology, it was estimated that the larvae were about halfway through their larval life (C. Young personal communication). Shipboard larval filming experiments were conducted as a joint project with Dr. Craig Young and his lab from the University of Oregon. Approximately 100 larvae were placed in cylindrical ~200 mL containers with filtered seawater, that were filled with ~180 mL of filtered seawater. The camera was able to accurately record larvae swimming in the container without larvae clinging to the container walls, bottom of the container, or larvae remaining only at the surface. All experiments took place in a dark, windowless cold room at 4^{o}C. The camera (Canon Rebel T3i) was positioned using a tripod to video record the swimming behavior of larvae in a single container. A single light source was used to provide just enough background light for the camera to focus on the larvae. The film was compiled into 30-second gifs in MATLAB and analyzed using ImageJ Particle Tracker plug-in (http://imagej.net/Particle_Tracker). Particle Tracker is a point tracking tool for the automated detection and tracking of particle trajectories as recorded by video. It makes it possible to visualize and analyze the detected particles and their trajectories by focusing on individual tracks and calculate distance traveled from the particle's original position. The Particle Tracker measured the starting and ending position of 30 larvae per video and calculated the number of body lengths traveled over five seconds. The values were

then averaged to determine mean upward swimming speed for each species. These mean values were then directly incorporated into the biophysical model to best represent the swimming speeds of these larvae. From the moment of release, larval particles were programmed to swim at a constant speed (0.2 cm s^{-1}), and particle density was held constant throughout the entire length of the PLD.

The adults of *L. luymesi* and *B. naticoidea* were collected using the Deep Submersible Vehicle (DSV) *Alvin* for morphological, genetic, and reproductive analysis. Adults were dissected and gametes obtained for spawning experiments. In a joint project between the University of Oregon and North Carolina State University, embryos from *L. luymesi* and *B. naticoidea* were cultured in filtered seawater maintained in 4^{o} C cold rooms. When approximately one-week old, both larval species were filmed in shipboard cold rooms for swimming speeds in the same manner described above. Swimming speeds were incorporated into the biophysical model to simulate the earliest swimming behavior of *L. luymesi* and *B. naticoidea*.

Estimating Planktonic Larval Duration

Planktonic larval durations (PLDs) used in our simulations were determined with a combination of published literature (Young et al. 2012, Arellano 2008, Van Gaest 2006, Young et al. 1996), personal observations, and zooplankton tows using a MOCNESS (**M**ultiple **O**pening/**C**losing **N**et and **E**nvironmental **S**ensing **S**ystem) while at sea. In many

cases, PLD was estimated by comparing larval size and known spawning dates of our study species. For example, the gastropod, *B. naticoidea* has an estimated PLD of four months, based on morphology of larvae obtained from MOCNESS tows, and has been found at thermocline depths of ~ 100m (Fig. 2; Young et al. 2012). The effects of pressure on spawning and larval survival or larval size does not appear to have any effect, as several studies have successfully reared larvae with very similar results and larvae have been collected in surface waters using MOCNESS (Arellano et al. 2014, Arellano and Young 2011, Young et al. 1996). The larvae of the polychaete, *L. luymesi*, cultured in the laboratory using filtered seawater at 7^{o}C have an estimated PLD of three weeks, and have been found at thermocline depths of 8^{o}C and 250 meters depth (Fig. 2; see methods in Young et al. 2012 and Arellano and Young 2009). Studies of metabolic rates for the chemosynthetic tubeworm, *L. luymesi* larvae also confirm a three-week, lecithotrophic larval period (Leong 1998). *L. luymesi* populations appear to be confined in the Gulf of Mexico due to their relatively short PLD (Young et al. 1996), which is why *L. luymesi* larval dispersal simulations were not released from Blake Ridge or Cape Fear seep sites in the South Atlantic Bight (see below). The deep-sea shrimp, *A. muricola* has an estimated PLD of six months, and disperses near the surface (~100 m to 0 m) (Fig. 2; Nye et al. 2013). In this case, PLD is based on the estimated PLD of other Alvinocarid species, however, this genus has several dispersal strategies, extended PLDs, and their dispersal depth is not yet fully known (Nye et al. 2013). Estimated PLDs and maximum dispersal depths used for the three species in the simulations is conservatively based yet directly observed by each of the three species. Alterations in behavior (i.e. growth, swimming speed, or PLD) due to temperature changes were not

accounted for in the following simulations. The author acknowledges that the calculations are limited and that better parameter estimates are needed, but unfortunately data is not available to incorporate into the model. While it is a limitation, the climatological model uses monthly averages, which reduces the chances of extreme changes in temperature having an effect on the dispersal potential of the larvae. Because of this, the distribution distance calculations are likely to be conservative estimates.

Particle-Tracking Model

The **L**agrangian **TRANS**port model (LTRANS) was adapted in this study to predict larval dispersal of individual particles with and without behavior. LTRANS is an offline particle-tracking model that predicts particle movement in three directions using advection, diffusion and behavior (North et al. 2006). LTRANS interpolates sea surface height, velocity, salinity, and temperature from grid locations, and utilizes a fourth-order Runge-Kutta scheme for particle advection. A random component is also added to particle motion to simulate subgrid-scale turbulent diffusion.

Particles were assigned characteristics of larval behavior, including (i) swimming speeds, (ii) vertical distribution in the water column, and (iii) PLD; detailed Fortran code related to programmed behavior can be found in Appendix 1. The dissertation used the 5-year ROMS circulation patterns described above to evaluate the spatial scales over which larvae may be dispersed. This resulted in simulating the effective geographic distances traveled among seep invertebrate larvae under spatiotemporally varying oceanographic conditions. Thus, our results predict potential variability in larval transport within the entire region. Successful dispersal also requires larvae (real or virtual) to encounter suitable

settlement habitat, which can be spatially isolated and often covers a small proportion of the area of potential dispersal. Therefore, depth, latitude, and longitude locations of seep sites were included as part of a broader study on population connectivity among seep sites in the *USEast* domain. For example, genetic and geochemical characterization of seep invertebrate populations is being conducted (C. Cunningham and C. Van Dover, Duke University, unpubl. data; B. Puckett and D. Eggleston, NC State University, unpubl. data; respectively) to test, in part, predictions of larval dispersal and connectivity generated from the present study. Putative settlement sites were divided into 7 km segments, thereby allowing for self-recruitment.

Each larval dispersal simulation included the release of 10 neutrally buoyant larval particles exhibiting constant swimming speeds every three hours from each of five seep sites, for a total of 30,000 particles per species simulation per site. In addition to the release of species-specific larval particles with their corresponding larval behaviors (see below), a total of 30,000 tracer particles, classified as currents only (i.e., no behavior), were used as a control for the behavioral simulations. These control tracer particles were subjected to advection and diffusion only. Subsequent particle tracks were analyzed using MATLAB (version 2014b) to determine the distance traveled by each particle over the course of their PLD.

Hypotheses and Statistical Analyses

Deep ocean currents are generally an order of magnitude slower than surface currents (Dickinson and Brown 1994). Therefore, I hypothesized that seep species whose larvae had a relatively long PLD and surface seeking larval behavior, would display the greatest average

and maximum potential distance travelled, irrespective of release site. Particle tracks were organized and compiled using Matlab (2014b) for several statistical analyses. I tested the main and interactive effects of (1) spawning site (i.e. seep locations), (2) particle behavior (active movement or passive drifting), and (3) PLD on two response variables: (i) mean dispersal distance, and (ii) maximum potential dispersal distance, with a multi-factor, three-way analysis of variance (ANOVA) model (Fig. 2). Multiple comparisons for significant main effects were identified with lower-level ANOVA models (including standard error) and Tukey's multiple comparisons test. Maximum potential dispersal was estimated as the top 5% of dispersal distances within a given set of average distances. For example, particle distances were sorted in descending order and the top five percent, or 1,500 particle distances from 30,000, were then used to calculate the average maximum distance for each simulation.

RESULTS

General Particle Trajectories

A total of 30,000 particles were released per simulation per site (10 particles released every three hours) for a total of 360,000 particles in the Gulf of Mexico, and 180,000 particles in the Western Atlantic. Dispersal trajectories varied greatly according to whether or not particles exhibited behavior, as well as their PLD. While there was variation in average dispersal distance, the overall trend was consistent, with the greatest dispersal observed for *A. muricola* (PLD: 196 days) with surface seeking behavior, followed by *B. naticoidea* (PLD: 90 days) dispersing at thermocline depth, and *L. luymesi* (PLD: 21 days), which dispersed at thermocline depth (Figs 3-7). Dispersal trajectories also varied greatly according to release

site. For example, particles with and without behavior released from Alaminos Canyon in the eastern GOM had the lowest average and average max dispersal distances of the five release sites (compare Fig. 3 with Figs. 4-7). Particles released from Brine Pool in the Northern-central area of the GOM dispersed throughout the east and west areas of the GOM (Fig. 4), whereas particles released from Florida Escarpment connected with the Loop Current and spread to the South-Atlantic Bight (Fig. 5). Particles released from the Cape Fear Diapir and Blake Ridge in the South Atlantic Bight dispersed south with the Deep Western Boundary Current, as well as north into the Mid-Atlantic Bight (Fig. 6 & 7).

How Does Species-Specific Behavior Affect Average Dispersal Distance?

Lamellibrachia luymesi

Mean distance travelled by particles simulating *L. luymesi* larval particles (21 PLD at approximately 200 m depth) varied significantly according release site and behavior (with vs without) (two-way ANOVA; $F = 3900$, $df = 2, 85{,}677$, $p<0.0001$). Mean dispersal was 4- to 28-times greater with behavior than without (Fig. 8). For particles exhibiting behavior, mean distance travelled was significantly higher when released from Florida Escarpment (Fig. 5; 274 km $\pm$0.82), followed by Brine Pool (Fig. 4; 213 km $\pm$0.82), and Alaminos Canyon (Fig. 3; 171 km $\pm$0.82). Average dispersal distances for particles without behavior were greatest when released from Florida Escarpment (Fig. 5; 274 km $\pm$0.82), followed by Brine Pool (Fig. 4; 75 km $\pm$0.82), and Alaminos Canyon (Fig. 3; 6 km $\pm$0.09). Particles with no behavior dispersed along the depth contours of the western GOM and towards the middle of the GOM, as well as partway around the edge of Florida (Fig. 5), yet were not able to

successfully disperse into the Western Atlantic. Average dispersal distances varied significantly among all three Gulf of Mexico sites (Tukey's test; $p<0.0001$). Conversely, mean distance traveled by particles without behavior was significantly higher when released from Brine Pool, than either Alaminos Canyon or Florida Escarpment (Figs. 3, 4, and 5; Tukey's Multiple Comparison test). It is important to note that there remains uncertainty around the Standard Error values when analyzing the statistical results from model simulations. The values are statistically valid, but are only as accurate as the model parameters (e.g. current speeds); thus, uncertainties only reflect different dispersal trajectories based on the assumption of accurate current regimes.

Bathynerita naticoidea

Mean distance travelled by particles simulating *B. naticoidea* (90 PLD at approximately 200 m depth) varied significantly depending on release site and behavior (with vs without) (two-way ANOVA; $F = 1800$, $df = 4, 142{,}795$, $p<0.0001$). Mean dispersal was 18-85-times greater with behavior than without (Fig. 10). For particles exhibiting behavior, mean distance travelled was significantly higher when released from Florida Escarpment (Fig. 4; 670 km $\pm$1.27), followed by Blake Ridge (Fig. 6; 287 km $\pm$1.27), Cape Fear (Fig. 7; 286 km $\pm$1.27), Brine Pool (Fig. 4; 241 km $\pm$0.15), and Alaminos Canyon (Fig. 3; 268 km $\pm$1.27, Tukey's Multiple Comparison test). Overall particles dispersed throughout the south and east of the GOM, Florida Strait, and South Atlantic Bight. Average dispersal distances varied significantly among Alaminos Canyon, Brine Pool, and Florida Escarpment sites (Tukey's

test; $p<0.0001$), however, there were no differences in average dispersal distance between Blake Ridge and Cape Fear ($p = 0.9948$).

Alvinocaris muricola

Mean distance travelled by particles simulating *A. muricola* (PLD = 186 days and dispersing near-surface from 0-100m depth) varied significantly with release site and behavior (with vs without) (two-way ANOVA; $F = 2200$, $df = 4, 142{,}795$, $p<0.0001$). For particles exhibiting behavior, mean distance travelled was significantly higher when released from Alaminos Canyon (Fig. 3; 854 km $\pm$2.53), followed by Brine Pool (Fig. 4; 846 km $\pm$1.27), Florida Escarpment (Fig. 5; 757 km $\pm$1.27), Blake Ridge (Fig. 6; 616 km $\pm$1.27), and Cape Fear (Fig. 7; 612 km $\pm$1.27) (Fig. 8). Average dispersal distances varied among Alaminos Canyon, Brine Pool, and Florida Escarpment sites (Tukey's test; $p<0.0001$), however, there were no differences in average dispersal distance between Blake Ridge and Cape Fear ($p = 0.7657$). Average dispersal distances varied significantly across all sites ($p < 0.0001$) for particles with no behavior. Overall particles dispersed widely throughout the GOM, Florida Strait, as well as the South- and Mid-Atlantic Bights, with mean dispersal 13-75 times greater with behavior than without (Fig. 11).

How Does Species-Specific Behavior Affect Average Maximum Dispersal Distance?

21-Day PLD

The average maximum distance (AMD) compares the top five percent of larval particles to determine the predicted maximum dispersal distance for each species, and varied

significantly with release site and behavior (two-way ANOVA; F = 27000, df = 2, 1481, p<0.0001). The AMD for particles with *L. luymesi* behavior (Fig. 9) had significantly higher dispersal distances at Florida Escarpment (571 km ±0.54), followed by Brine Pool (439 km ±0.54), and Alaminos Canyon (403 km ±0.54). The least square means adjusted with Tukey showed statistically significant AMD differences between all three sites (p < 0.0001). The AMD for 21-day PLD with currents only particles released from Brine Pool (109 km ±0.12) was higher than those released from Florida Escarpment (81 km ±0.12), followed by Alaminos Canyon (21 km ±0.12). AMD varied significantly among Alaminos Canyon, Brine Pool, and Florida Escarpment sites (Fig. 9; Tukey's test; p<0.0001).

90-Day PLD

The AMD for particles with *B. naticoidea* behavior (Fig. 10) varied significantly with release site and behavior (with vs without) (two-way ANOVA; F = 2000, df = 4, 7135, p<0.0001), and had significantly higher dispersal distances at Florida Escarpment (1232 km ±5.1), followed by Blake Ridge (844 km ±5.1), Brine Pool (811 km ±5.1), Cape Fear (758 km ±5.1), and Alaminos Canyon (614 km ±5.1). Average maximum dispersal distances varied among all sites (Tukey's test; p<0.0001). The AMD for currents only particles dispersing for 90-days had the highest dispersal at Brine Pool (297 km ±0.12), followed by Florida Escarpment 237 km (±0.12), Cape Fear (116 km ±0.12), Alaminos Canyon was 110 km (±0.20), and Blake Ridge (106 km ±0.12). AMD varied among all sites (Fig. 10; Tukey's test; p<0.0001).

186-Day PLD

The AMD for particles with *A. muricola* behavior (Fig.11) varied significantly with release site and behavior (two-way ANOVA; $F = 36000$, $df = 4, 7135$, $p<0.0001$), and had the highest level of dispersal at Alaminos Canyon (2181 km $\pm$2.26), followed by Brine Pool (1648 km $\pm$2.26), Florida Escarpment (1354 km $\pm$2.26), Cape Fear (1181 km $\pm$2.26), and Blake Ridge (1155 km $\pm$2.26). Currents only particles had significantly higher dispersal distances at Brine Pool (500 km $\pm$0.26), followed by Florida Escarpment (320 km $\pm$0.26), Cape Fear (215 km $\pm$0.26), Blake Ridge (201 km $\pm$0.26), and Alaminos Canyon (129 km $\pm$0.26). Average maximum dispersal distances varied among all sites (Fig. 11; Tukey's test; $p<0.0001$).

DISCUSSION

Since their discovery, deep-sea chemosynthetic ecosystems have been key systems within which to test the generality of paradigms developed for shallow-water species. This study explored the roles of larval behavior, pelagic larval duration, and putative spawning locations on potential population connectivity of hydrocarbon seep invertebrates. The goal was to assess the dispersal trajectories of the deep-sea polychaete, *Lamellibrachia luymesi*, gastropod, *Bathynerita naticoidea*, and crustacean, *Alvinocaris muricola* among seep-sites in the Gulf of Mexico and Western Atlantic Ocean using a coupled biophysical model. Generally, the results highlight the importance of incorporating larval behavior into computer simulations, as this can have a tremendous impact on dispersal trajectories. Particles dispersed widely throughout the GOM, Florida Strait, as well as the South- and Mid-Atlantic

Bights, with mean dispersal distances being 13-75 times greater with behavior than without. For example, average larval dispersal distance for *A. muricola* released from Alaminos Canyon was 854 km (±2.53), whereas with currents only was 38 km (±0.28). Adding varying larval behavior and PLDs to the particle-tracking model dramatically changed the average distance and average maximum dispersal distances, thereby highlighting the need to incorporate species-specific simulations, even if the full larval history of a particular species is unknown. Our trajectory results show that particles do encounter other seep sites in our spatial domain, however that does not assume that there is a strong enough connection to influence population dynamics or genetic structure. Further analysis is needed to quantify the level of connectivity between each of the seeps sites in our study, as well as the level of self-recruitment, to calculate the strength of each species' connectivity across in the model domain. Unfortunately, genetic population patterns for any of the three species remains unexplored, but future genetic work could be guided by the results of the dispersal pattern from these species-specific simulations.

Very few studies have attempted to model larval dispersal in the deep sea, and most have been limited by the availability of reliable estimates of biological parameters, including planktonic larval duration and larval behavior (Cowen and Sponaugule 2009, Young et al. 2012, Hilario et al. 2015 and references therein, Mitarai et al. 2016). Hilario et al. (2015) reviewed the application of biophysical models in the study of larval dispersal and population connectivity, with the majority of models not incorporating any biological behavior (e.g., PLD and vertical migration). The present study highlights how incorporating biological traits greatly influences larval dispersal trajectories and distances travelled, and why more

biologically accurate simulations are necessary. A similar experiment conducted by Young et al. (2012) released particles from various coordinates within 80 km of a site where adults were known to be abundant. Particles were not programmed with vertical migration behavior, and particle distances were compared between depths above and below the thermocline (Young et al. 2012). Our current study builds upon the work by Young et al. (2012) by incorporating more biological parameters, such as species-specific larval swimming speeds and vertical placement in the water column, in addition to releasing particles from known methane seep sites. MOCNESS data collected during SEEPC cruises combined with film experiments of larvae swimming at sea provide direct evidence of the larvae present at particular depths and the rate at which they swim to maintain themselves at depth. While data is limited to the movement and behavior of the three species in this study, plankton tow results indicate that the larvae are found in the upper 200 m of the water column. Similar to our study, Young et al. (2012) found that dispersal potential is strongly related to PLD, as well as the effect of release site on dispersal direction. The dispersal potential for hydrothermal vent particles in the Pacific Ocean was assessed by Mitarai et al. (2016) with a variety of PLDs but did not include other biological parameters (e.g. larval swimming speeds and vertical distributions). Their model results show high connectivity within hydrothermal vent basins without clear directionality to particle dispersal patterns; however, basin-to-basin dispersal appears more infrequent with strong directionality associated with the major currents. This may also be a result on geological or physical boundaries that alter the current flow throughout the region and limit connectivity, with sporadic events such as weather events exerting enough of a force on surface current patterns. Integration of biological

parameters into the model by Mitarai et al. (2016) will likely enhance the accuracy of predictions concerning larval dispersal and population connectivity among invertebrates inhabiting hydrothermal vent systems.

Current Dynamics

Shallow water larvae exhibit many similarities to deep-sea larvae, with dispersal strongly linked to current dynamics, larval behavior, and PLD. In contrast to deep currents, surface currents are subject to interactions of cross-shelf water flow, as well as coastal topography, tidal forces, and wind (Gawarkiewicz et al. 2007). The high level of variability within coastal environments makes it difficult to accurately model all of the fine scale properties driving observed dispersal, particularly across larger scales from near shore to offshore environments (Werner et al. 2007). While deep-sea dispersal must also address issues related to the scale of dispersal, cross-shelf dynamics is unique to shallow water systems. Larvae from shallow water environments can also exhibit high levels of retention due to coastal bathymetry and topography, which can create areas of reduced flow and sea floor friction found in coastal and estuarine regions. Similarly, eddies in coastal environments may also enhance the retention of shallow-water larvae, which has been observed in the GOM and WAM for deep-sea larval dispersal. Therefore, the physical features of coastal areas, in concert with coastal circulation, strongly influence the potential larval dispersal distance for shallow water species by likely minimizing dispersal distance and increase retention of larvae from their natal site.

Coastal processes strongly affect larval transport and dispersal distance, but it is essential to incorporate biological behavior with the physical environment to fully understand the interaction of these factors on connectivity. For example, research has extensively incorporated population genetics, larval behavior, geography and biophysical modeling to study the connectivity of corals and develop Marine Protected Areas (MPAs; Jones et al. 2009). Similar to many deep sea invertebrates, there is wide variation in coral behavior from brooding larvae to broadcast spawning to observed changes in larval development that alters PLD further complicates the ability to understand connectivity patterns in reefs. Yet for both fish and corals found in reefs, many studies have found that there is a high degree (>50%) of self-recruitment based on results from otolith chemistry, larval tagging, parentage analysis, biophysical modeling (Jones et al. 2009 and references therein). The results of this study indicate that the average dispersal distance for larval particles with behavior can be as large as 1,100 km, which is far greater than observed dispersal distances for shallow water species; yet it is important to determine the effects of long distance dispersal on potential population connectivity. While high levels of self-recruitment suggest that local populations are self-sustained, more research is required to understand the dynamics larval retention and connectivity in fish and coral reefs (Botsford et al. 2009). Shallow water populations are subjected to stress from environmental degradation and harvest, and while pressure is currently limited for deep-sea communities, anthropogenic activities such as bottom trawling, oil extraction, and mining may compromise the health and stability of deep-sea ecosystems.

Caveats

Numerical Modeling and Physical Oceanographic Conditions

The benefit of using a climatological hydrodynamic model is to predict general dispersal patterns of larval particles under average atmospheric and oceanic conditions, as well as to better understand what factors may be important in driving variation in dispersal and potential population connectivity. Climatological models use average atmospheric and oceanographic conditions to predict average dispersal trajectories of larval particles, and with rigorous testing it is safe to assume that the average conditions in the model reflect the general seasonal current patterns. Thus, the dispersal paths from this study are considered approximations of actual dispersal trajectories of seep larvae under variable oceanographic conditions. While the average oceanographic conditions in the model are relatively accurate based on previous validation studies (R. He et al. in prep), there are inherent uncertainties in biophysical models, such as the resolution of water flow features (e.g. eddies and flow rates), and the biological characteristics that larvae may utilize to alter their dispersal potential path (swimming behavior, larval buoyancy, ontogenetic vertical migration, etc.). For example, the inter-annual variability in hindcast models exhibit features such as meandering currents over the course of a model year, variable eddy shedding, and greater fluctuations in sea surface temperature. Climatological models, however, represent a powerful tool to examine the relative importance of larval behavior and PLD on average and maximum dispersal distances, as well as from different spawning sites that, in turn, can help to refine model parameters for more accurate predictions in future studies of this nature. The climatological model is also limited by a grid scale of 7-10 km, and does not have the resolution to explore

the fine scale movements of the particles. This somewhat coarse spatial resolution is a necessary trade-off for the immense spatial domain in this study (over 1,000,000 km^2). The increase in physical ocean circulation modeling capabilities in recent years has made it much easier to understand how oceanographic features affect the potential dispersal paths and distances of larvae from their natal site. Further research of methane seep larvae throughout the Gulf of Mexico and Western Atlantic using coupled biophysical models should focus on increased model resolution scale and a thorough comparison of hindcast and climatological results to determine which physical model most accurately represents larval particle dispersal. While climatological models assess dispersal patterns in average atmospheric and oceanic conditions, hindcast models integrate known input from past events into the domain. For example, hindcast models show that seasonal and inter-annual variability in circulation patterns can have strong effects on particle dispersal distance (Qian et al. 2014). Hindcast modeling results can also address what parameters are required of physical models to better understand how far larval particles travel, and what factors may control the dispersal trajectory variability seen with different species' larval phase.

Currently, models are limited by assumptions that increase the resolution of current velocity, eddy resolution, and upwelling strength. Moreover, computing power is not yet strong enough to completely reproduce fine-scale field conditions, such as bathymetric features and eddies. Many aspects of oceanographic models have become more accurate (Todd et al. 2014), and more research is necessary to validate and test the resolution of currents, eddies, upwelling and directional flow of water in the model domain. While models are not designed to simulate every aspect of observed conditions, our dispersal results and the

results of others (Kinlan et al. 2005, Young et al. 2012, Puckett et al. 2014,) emphasize the predictive strength of biophysical models on larval retention and dispersal. Additionally, increased understanding of basic biology and larval behavior will improve the accuracy of simulated larval dispersal. Due to limitations on the basic biology of deep-sea species, certain assumptions about dispersal behavior and PLD are likely to be conservative. In each of the species' simulations, the dispersal depth and PLD were depths were the majority of larvae have been found from several MOCNESS tows, yet there were some larvae (for example, *B. naticoidea*) captured at less than 100 m depth. It is also not known if the larvae undergo diel vertical migration (DVM) while dispersing at depth, which may also alter their dispersal distance. Therefore, average PLDs and dispersal depths were used in the simulations to avoid overestimating dispersal.

Biological Conditions

Limited direct observations of spawning events have found huge variation in the number of eggs released, with some species releasing only 200 eggs per individual, and others over 200,000 per individual (Tyler and Young 1999). While egg production is distinct from the successful development of larvae, assumptions related to deep-sea fecundity are focused on total number of eggs for most species; hence, it was necessary to make best estimates in this study. Additionally, the number of larvae will be correlated to the area of the seep and the number of fauna per unit area, as well as number of larvae released per individual species. It has been estimated that *L. luymesi* has a maximum measured fecundity of 60,000 eggs per individual. There is tremendous variation in the density of tubeworms with large

aggregations estimated in the tens of thousands, which could mean up to 1.02 x 10^9 eggs released per meter per year. Yet, what isn't known is the age at which adults become reproductively mature, and how many of the eggs are spawned per day (C. Young *personal communication*). In contrast, *B. naticoidea* maximum fecundity has been estimated at 2,000,000 eggs being released per meter during a synchronous hatching event at the Brine Pool seep over a single spawning event. The actual density of adult invertebrates at each seep site was not included in this study, and instead focused on the larval dispersal phase. Therefore, the number of particles released in the simulations may be an underestimate of larvae produced from a single spawning event from a seep community, yet it still provides statistically valid insight into the dispersal of particles released from a known seep site for in depth analysis of potential connectivity.

It is also very computationally expensive to release large quantities of particles for LTRANS to track over the course of a simulation at every three-hour time step, which was taken into consideration during the experimental design of the simulation runs. For example, tracking 30,000 particles (10 particles every three hours) released from a site takes approximately 28 hours to compute, where as it would take more than 170 hours to perform a simulation with 200,000, and 1,700 hours to track 2,000,000 particles released into the flow field. With the current limitations in computing, it is not yet possible to simulate a spawning event from a dense seep community, and future work should mimic as best as possible the number of larvae created by dense seep communities with the use of high performance computers. Methods for assessing larval behavior are limited to direct observation, laboratory

rearing experiments, and larval identification from plankton and MOCNESS tows. North et al. (2006) parameterized the swimming behaviors of two species of oyster, *C. virginica* and *C. ariakensis*, based on lab experiments and found that differences in swimming behavior had profound effects on dispersal distance in the Chesapeake Bay. In contrast, swimming behavior of oyster larvae in the relatively shallow, wind-driven Pamlico Sound estuary, North Carolina had relatively minor effects on potential larval dispersal and population connectivity compared to the roles of the location and timing of spawning (Puckett et al. 2014). Larval fish and coral simulations (James et al. 2002, Jones 2009, Qian 2015) have also investigated the role of behavioral parameters in simulations and its role in the connectivity, retention, and dispersal patterns of larvae across the Caribbean and Western Atlantic Margin. While it is an assumption to have the same swimming speed over the course of the PLD, the data gathered from the shipboard filming experiments provided a means to incorporate species-specific data into the model. The limited data available for larval swimming speeds is compounded by the difficulty in maintaining deep-sea larval cultures over the course of their development, as well as catching larvae at different stages of growth in MOCNESS plankton tows. Quantifying species-specific, larval swimming parameters remains a challenging task for deep-sea invertebrates.

Future Research

Further study should also focus on the integration of genetic and geochemical findings alongside the model's results to determine model accuracy of larval particle dispersal. Estimates of gene flow strength may infer dispersal paths of larvae (Thaler et al. 2011), the

frequency of genetic connectivity of chemosynthetic communities (Van Dover et al. 2002, Wanatabe et al. 2005), and the degree to which the genetic estimates agree with the model output (Galindo et al. 2010). DNA analysis from samples collected over the course of several SEEPC research cruises is currently being analyzed by colleagues at Duke, and results will soon provide a method to assess the model's predictions against empirical data. Geochemical tracer analysis is an alternative approach to genetic techniques when quantifying larval connectivity of invertebrate populations. Environmental factors such as temperature, salinity and trace metal concentrations create a fingerprint of conditions that remain on the larval shell throughout the PLD, which can then be used to characterize connectivity over regional (>35 km) scales (Kroll et al. 2016).

In summary, I have demonstrated an approach to understand the response of species-specific larval dispersal in a climatological, hydrodynamic domain. Biological parameters such as PLD, swimming speed, and vertical distribution of particles can disperse virtual larvae over hundreds of kilometers from known methane seep sites throughout the Gulf of Mexico and Western Atlantic Margin. Obtaining values of the relevant physiological and behavioral parameters of larvae that can be integrated into biophysical models should continue to take high priority in the study of deep-sea invertebrates and predictions of population connectivity. This study has shown the significance of integrating species-specific larval behavioral parameters in order to more accurately study the effects of behavior on particle dispersal potential in the Gulf of Mexico and Western Atlantic Margin.

ACKNOWLEDGEMENTS

We are grateful to the following for their time and support of rearing of larvae while at sea: C. Young, C. Plowman, K. Meyer, and L. Genio. Special thanks to the crews of the *R/V Cape Hatteras, Pelican, Endeavor,* and *Atlantis* for their expertise while at sea, as well as the engineering teams of *Alvin* and *Sentry*. We are also grateful to A. Todd and S. Ricci for their technical support with this project. The funding for this project was provided by NSF OCE-1031050.

REFERENCES

Adams, D.K., and L.S. Mullineaux. 2008. Supply of gastropod larvae to hydrothermal vents reflects transport from local larval sources. *Limnol and Oceanog* 53(5): 1945-1955.

Arellano, S.M., A.L. Van Gaest, S.B. Johnson, R.C. Vrijenhoek, and C.M. Young. 2014. Larvae from deep-sea methane seeps disperse in surface waters. *Proc R Soc B* 281: 20133276.

Arellano, S. and C. M. Young. 2009. Spawning, development, and the duration of larval life in a deep-sea cold-seep mussel. *Biol. Bull.* 216(2): 149-162.

Botsford, L.W. J.W. White, M.A. Coffroth, C.B. Paris, S. Plines, T.L. Shearer, S.R. Thorrold, G.P. Jones. 2009. Connectivity and resilience of coral reef metapopulations in marine protected areas: matching empirical efforts to predictive needs. *Coral Reefs* 28: 327-337.

Carney, S.L., M.I. Formica, H. Divatia, K. Nelson, C.R. Fisher, and S.W. Schaeffer. 2006. Population structure of the mussel *"Bathymodiolus" childressi* from Gulf of Mexico hydrocarbon seeps. *Deep-Sea Res I* 53: 1061-1072.

Cowen, R.K. and S. Sponaugle. 2009. Larval dispersal and marine population connectivity. *Marine Science* 1.

Cowen, R.K., G. Gawarkiewicz, J. Pineda, S.R. Thorrold, and F.E. Werner. 2007. Population connectivity in marine systems. *Oceanog* 20(3):14-21.

Cowen, R.K., C.B. Paris, and A. Srinivasan. 2006. Scaling connectivity in marine populations. *Sci* 311: 522-527.

Cordes, E. E., S. Carney, S. Hourdez, R.S. Carney, J.M. Brooks, and C.R. Fisher. 2007. Cold seeps of the deep Gulf of Mexico: community structure and biogeographic comparisons to Atlantic equatorial belt seep communities. *Deep Sea Research Part I: Oceanographic Research Papers* 54(4): 637-653.

DeHaan C.J. and W. Sturges. 2005. Deep cyclonic circulation in the Gulf of Mexico. *J Phys Oceanog* 35: 1801-1812.

Dickson, R.R. and J. Brown.1994. The production of North Atlantic Deep Water: sources, rates, and pathways. *Journal of Geophysical Research: Oceans* 99(C6):12319-12341.

Egorov, A.V., K. Crane, P.R. Vogt, A.N. Rozhkov, and P.P. Shirshov. 1999. Gas hydrates that outcrop on the sea floor: stability models. *Geo-Marine Letters* 19(1-2): 68-75.

Epifanio, C.E., G. Perovich, A.I. Dittel, and S.C. Cary. 1999. Development and behavior of megalopa larvae and juveniles of the hydrothermal vent crab *Bythograea thermydron*. *Mar Ecol Prog Ser* 185: 147-154.

Fairall, C. W., E.F. Bradley, J.E. Hare, A.A. Grachev, and J.B. Edson. 2003. Bulk parameterization of air-sea fluxes: Updates and verification for the COARE algorithm. *J of Clim*, 16(4), 571-591.

France, S.C., R.R. Hessler, and R.C. Vrijenhoek. 1992. Genetic differentiation between spatially-disjunct populations of the deep-sea, hydrothermal vent-endemic amphipod *Ventiella sulfuris*. *Mar Biol* 114: 551-559.

Galindo, H.M., A.S. Pfeiffer-Herbert, M.A. McManus, Y. Chao, F. Chai, and S.R. Palumbi. 2010. Seascape genetics along a steep cline: using genetic patterns to test predictions of marine larval dispersal. *Molec Ecol* 19: 3692-3707.

Gawarkiewicz, G.G., S.G. Monismith, and J. Largier. 2007. Observing larval transport processes affecting population connectivity: progress and challenges. *Oceanog* 20(3): 40-53.

Gilg, M.R. and T.J. Hilbish. 2003. The geography of marine larval dispersal: coupling genetics with fine-scale physical oceanography. *Ecol* 84(11): 2989-2998.

Grassle, J.F. 1989. Species diversity in deep-sea communities. *Trends in Ecology & Evolution* 4(1): 12-15.

Hilario, A. A. Metaxas, S. M. Gaudron, K.L. Howell, A. Mercier, N. C. Mestre, R. E. Ross, A.M. Thurnherr, and C. Young. 2015. Estimating dispersal distance in the deep sea: challenges and applications to marine reserves. *Front Mar Sci* 2(6): 1-14.

Hurtado, L.A., R.A. Lutz, and R.C. Vrijenhoek. 2004. Distinct patterns of genetic differentiation among annelids of eastern Pacific hydrothermal vents. *Molecular ecology* 13(9): 2603-2615.

James, M.K., P.R. Armsworth, L.B. Mason, and L. Bode. 2002. The structure of reef fish metapopulations: modelling larval dispersal and retention patterns. *Proceedings of the Royal Society of London B: Biological Sciences* 269(1505): 2079-2086.

Jones, G. P., Almany, G. R., Russ, G. R., Sale, P. F., Steneck, R. S., Van Oppen, M. J. H., & Willis, B. L. 2009. Larval retention and connectivity among populations of corals and reef fishes: history, advances and challenges. *Coral Reefs, 28*(2): 307-325.

Kinlan, B.P., S.D. Gaines, S.E. Lester. 2005. Propagule dispersal and scales of marine community process. *Diversity Distrib* 11: 139-148.

Kroll, I.R., A.K. Poray, B.J. Puckett, D.B. Eggleston, F. J. Fodrie. 2016. Environmental effects on elemental signatures in eastern oyster *Crassostrea virginica* shells: using geochemical tagging to assess population connectivity. *Mar Ecol Prog Ser* 543: 173-186.

Levin, L.A. 2006. Recent progress in understanding larval dispersal: new directions and digressions. *Integ and Compar Biol* 46(3): 282-297.

Leong, PKK. 1998. Metabolic importance of Naþ, Kþ -ATPase activity during early development of marine invertebrates [dissertation]. [California]: University of Southern California.

Le Pennec, M., and P. G. Beninger. 2000. Reproductive characteristics and strategies of reducing-system bivalves. *Comp. Biochem. Physiol. A Mol. Integr. Physiol.* 126: 1–16.

MacDonald, I.R., N.L. Guinasso Jr., R. Sassen, J.M. Brooks, L. Lee, and K.T. Scott. 1994. Gas hydrate that breaches the sea floor on the continental slope of the Gulf of Mexico. *Geol* 22: 699-702.

Mitarai, S., H. Watanabe, Y. Nakajima, A.F. Shchepetkin, and J.C. McWilliams. 2016. Quantifying dispersal from hydrothermal vent fields in the western Pacific Ocean. *PNAS* 113(11): 2976-2981.

North, E.W., Z. Schlag, R.R. Hood, M. Li, L. Zhong, T. Gross, and V.S. Kennedy. 2006. Vertical swimming behavior influences the dispersal of simulated oyster larvae in a coupled particle-tracking and hydrodynamic model of Chesapeake Bay. *Mar Ecol Prog Ser* 359: 99

Nye, V., J.T. Copley, and P.A. Tyler. 2013. Spatial variation in the population structure and reproductive biology of *Rimicaris hybisae* (Caridea: Alvinocarididae) at hydrothermal vents on the mid-cayman spreading centre. *Plos One* 8(3): 1:15.

Olu, K., M. Sibuet, F. Harmegnies, J.P. Foucher, and A. Medioni. 1996. Spatial distribution of diverse cold seep communities living on various diapiric structures of the souther Barbados prism. *Progress in Oceanog* 38: 347-376.

Olu-LeRoy, K, R. von Cosel, S. Hourdez, S.L. Carney, and D. Jollivet. 2007. Amphi-Atlantic cold-seep Bathymodiolus species complexes across the equatorial belt. *Deep-Sea Res I* 54:1890-911.

Paull, CK, B. Hecker, R. Commeau, R.P. Freeman-Lynde, C. Neumann, W.P. Corso, S. Golubic, J.E. Hook, E. Sikes, and J. Curray. 1984. Biological communities at the Florida Escarpment resemble hydrothermal vent taxa. *Sci* 226: 965-967.

Puckett, B.J., D.B. Eggleston, P.C. Kerr and R.A. Luettich Jr. 2014. Larval dispersal and population connectivity among a network of marine reserves. *Fish and Oceanogr 23*(4), 342-361.

Qian, H., Y. Li, R. He, and D.B. Eggleston. 2015. Connectivity in the Intra-American seas and implications for potential larval transport. *Coral Reefs* 34(2), 403-417.

Sahling, H., D. Rickert, R.W. Lee, P. Linke, and E. Suess. 2002. Macrofaunal community structure and sulfide flux at gas hydrate deposits from the Cascadia convergent margin, NE Pacific. *Mar Ecol Prog Ser* 231: 121-138.

Schlag, Z. R., and E. W. North. 2012. Lagrangian TRANSport (LTRANS) v.2 model User's Guide. Technical Report of the University of Maryland Center for Environmental Science Horn Point Laboratory. Cambridge, MD. 183 p.

Shank, T.M., D.J. Fornari, K.L. Von Damm, M.D. Lilley, R.M. Haymon and R.A. Lutz. 1998. Temporal and spatial patterns of biological community development at nascent deep-sea hydrothermal vents (9 50′ N, East Pacific Rise). *Deep Sea Research Part II: Topical Studies in Oceanography* 45(1): 465-515.

Sibuet, M. and K. Olu. 1998. Biogeography, biodiversity and fluid dependence of deep-sea cold-seep communities at active and passive margins. *Deep-Sea Res II* 45:517-567.

Siegel, D.A., B.P. Kinlan, B. Gaylord, and S.D. Gaines. 2003. Lagrangian descriptions of marine larval dispersion. *Mar Ecol Prog Ser* 260: 83-96.

Skarke, A., C. Ruppel, M. Kodis, D. Brothers and E. Lobecker. 2014. Widespread methane leakage from the sea floor on the northern US Atlantic margin. *Nature Geoscience*, 7(9): 657-661.

Sturges, W., and A. Lugo-Fernandez. 2005. Circulation in the Gulf of Mexico: Observations and Models. American Geophysical Union ISBN: 9780875904269

Suess, E. M.E. Torres, G. Bohrmann, R.W. Collier, J. Greinert, P. Linke, G. Rehder, A. Trehu, K. Wallmann, G. Winckler, and E. Zuleger. 1999. Gas hydrate destabilization: enhanced dewatering benthic material turnover and large methane plumes at the Cascadia convergent margin. *Earth and Planetary Sci Letters* 170: 1-15.

Thaler, A.D., K. Zelnio, W. Saleu, T.F. Schultz, J. Carlsson, C. Cunningham, R.C. Vrijenhoek, and C.L. Van Dover. 2011. The spatial scale of genetic subdivision in populations of *Ifremeria nautilei*, a hydrothermal vent gastropod from the southwest Pacific. *BMC Evol Biol* 11(372): 1-12.

Thorson, G. L. 1950. Reproductive and larval ecology of marine bottom invertebrates. *Biol. Rev.* 1**:** 1-46.

Todd, A.C., S.L. Morey, and E.P. Chassignet. 2014. Circulation and cross-shelf transport in the Florida Big Bend. *J of Mar Res* 72(6) 445-475.

Treml, E.A., J.J. Roberts, Y. Chao, P.N. Halpin, H.P. Possingham, and C. Riginos. 2012. Reproductive output and duration of the pelagic larval stage determine seascape-wide connectivity of marine populations. *Integ Compar Biol* 52(4): 525-537.

Van Dover, C.L., C.R. German, K.G. Speer, L.M. Parson, and R.C. Vrijenhoek. 2002. Evolution and biogeography of deep-sea vent and seep invertebrates. *Science* 295(5558): 1253-1257.

Van Gaest and A. Lea. 2006. Ecology and early life history of Bathynerita naticoidea: evidence for long-distance larval dispersal of a cold seep gastropod.

Virjenhoek, R.C. 1997. Gene flow and genetic diversity in naturally fragmented metapopulations of deep-sea hydrothermal vent animals. *J Hered* 88(4): 285-293.

Wanatabe, H., S. Tsuchida, K. Fujikura, H. Yamamoto, F. Inagaki, M. Kyo, and S.Kojima. 2005. Population history associated with hydrothermal vent activity inferred from genetic structure of neoverrucid barnacles around Japan. *Mar Ecol Prog Ser* 288: 233-240.

Won, Y., C.R. Young, R.A. Lutz, and R.C. Vrijenhoek. 2003. Dispersal barriers and isolation among deep-sea mussel populations (Mytilidae: Bathymodiolus) from eastern Pacific hydrothermal vents. *Molecular Ecology* 12(1):169-184.

Wray, G. A., and R. A. Raff. 1991. The evolution of developmental strategy in marine invertebrates. *Trends Ecol. Evol.* 6: 45–50.

Young, C.M., P.A. Tyler, and J.D. Gage. 1996 (a). Vertical distribution correlates with pressure tolerances of early embryos in the deep-sea asteroid Plutonaster bifrons. *Journal of the Marine Biological Association of the United Kingdom* 76(3): 749-757.

Young, C.M., M.G. Devin, W. Jaeckle, S.U.K Ekaratne, S.B. George. 1996 (b). The potential for ontogenetic vertical migration by larvae of bathyal echinoderms. *Oceanol Acta* 19: 263-271.

Young, C. M., P. A. Tyler, and L. Fenaux. 1997. Potential for deep sea invasion by Mediterranean shallow water echinoids: pressure and temperature as stage-specific dispersal barriers. *Mar. Ecol. Progr. Ser.* 154: 197–209.

Young, C.M. 2003. Reproduction, Development and life-history traits. Ecosystems of the World ed. P.A. Tyler. Volume 28: 381-426

Young, C.M., R. He, R.B. Emlet, Y. Li, H. Qian, S.M. Arellano, A.Van Gaest, K.C. Bennett, M. Wolf, T.I. Smart, and M.E. Rice. 2012. Dispersal of deep-sea larvae from Intra-American Seas: simulations of trajectories using ocean models. *Integ and Compar Biol* 52(4): 483-496.

TABLE

Table 1. Methane seep sites in the Gulf of Mexico and U.S. Western Atlantic Ocean.

Site Name	Site Latitude (N)	Site Longitude (W)	Site Depth (m)
Alaminos Canyon	26 21'17"	94 29'48"	1300
Florida Escarpment	26 1'48"	84 54'54"	3300
Brine Pool	27 43'23"	91 16' 30"	660
Blake Ridge	32 29'45"	76 11'30"	2150
Cape Fear	32 58'45"	75 55'30"	2500

FIGURES

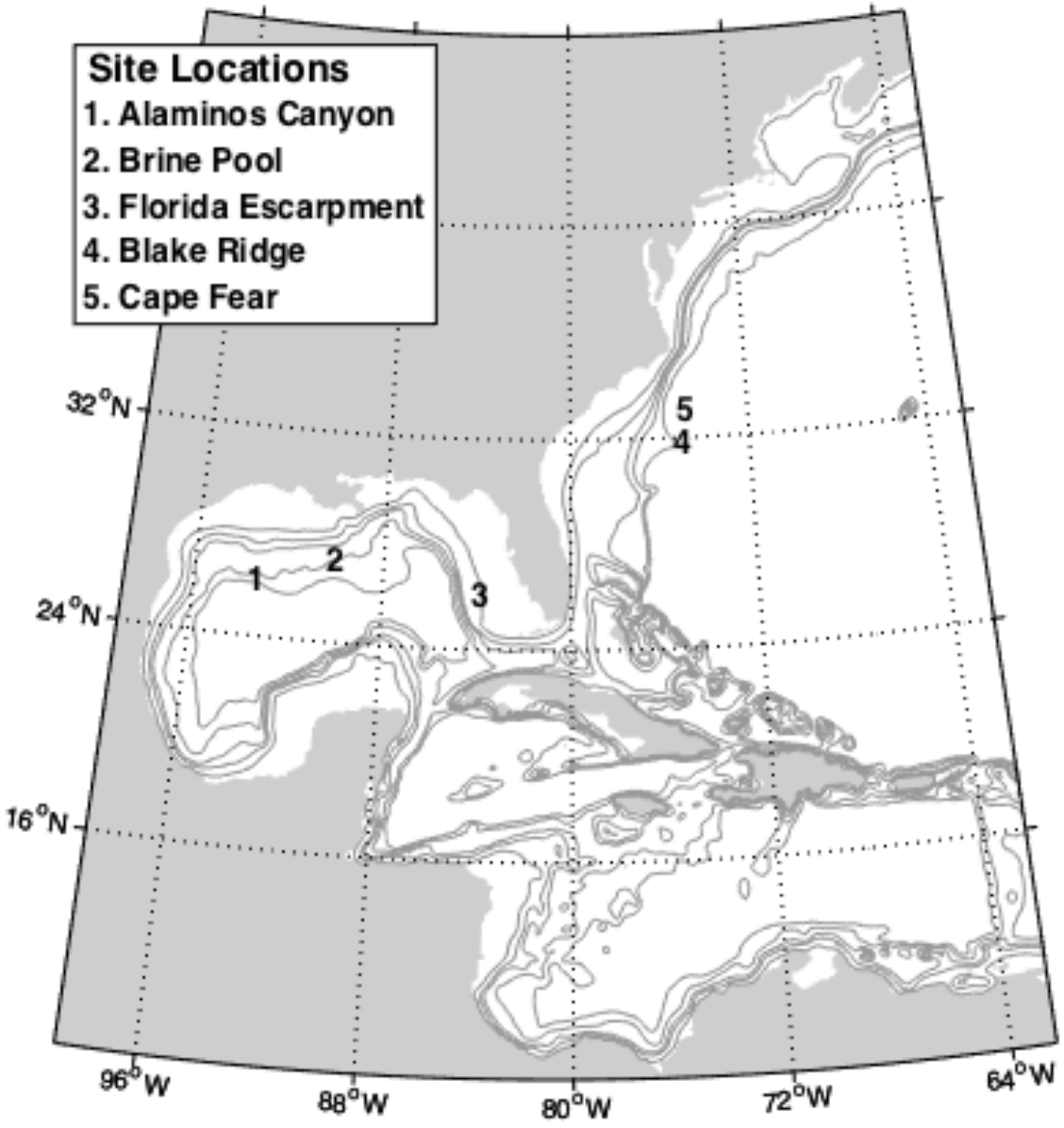

Figure 1. Spatial domain of *USEast* circulation model. Methane seep study sites are plotted on the model domain to match latitude, longitude, and depth of the actual locations: Alaminos Canyon, Brine Pool, Florida Escarpment, Blake Ridge, and Cape Fear.

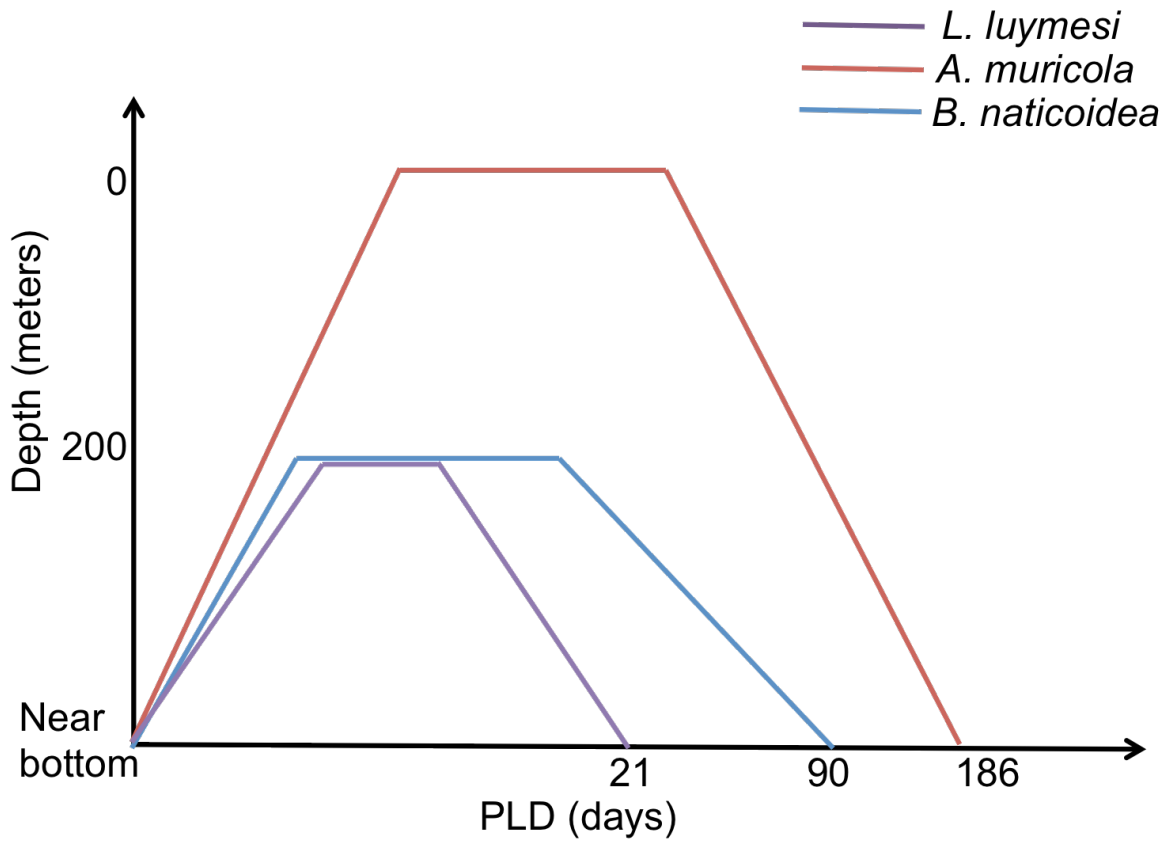

Figure 2. Schematic diagram of programmed species-specific behavior. Particles of *B. naticoidea* and *L. luymesi* dispersed at thermocline over the duration of their PLD, while *A. muricola* dispersed at the surface. All particles were programmed to arrive on sea floor and settle by the end of their specific PLD.

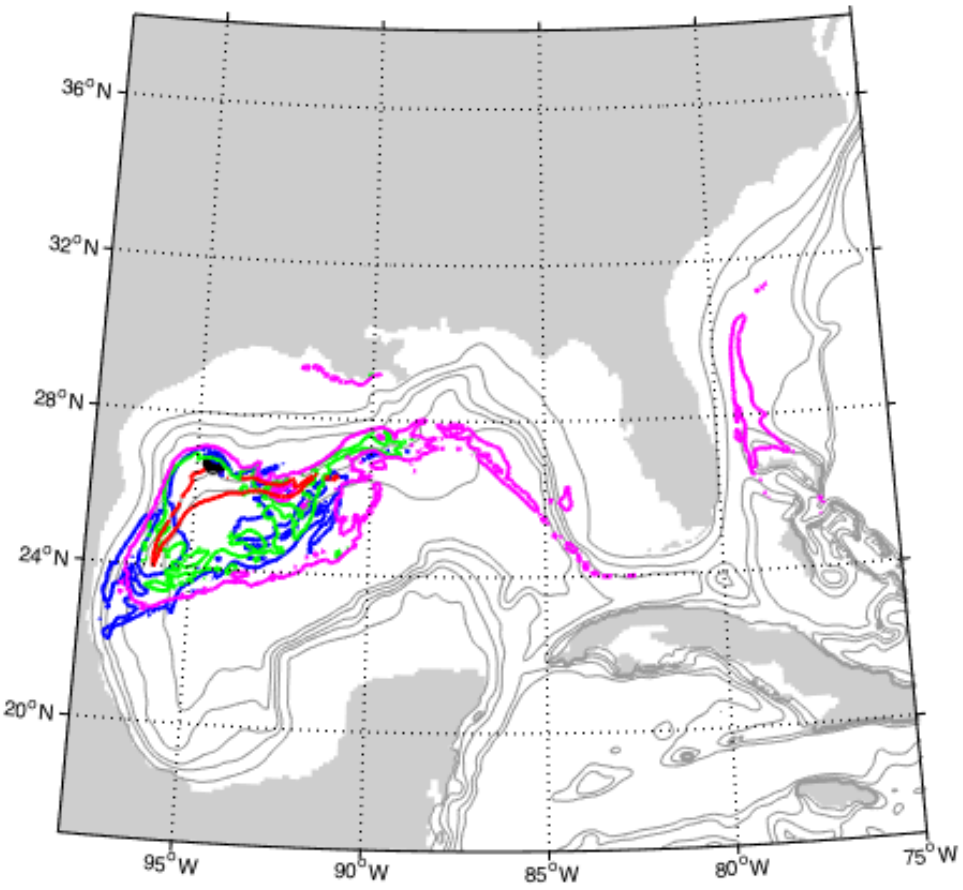

Figure 3. Particle trajectories released from Alaminos Canyon in the Gulf of Mexico. The black dot indicates the release site; dispersal paths of *B. naticoidea* are blue, *L. luymesi* are green, *A. muricola* are magenta, and Currents only are in red.

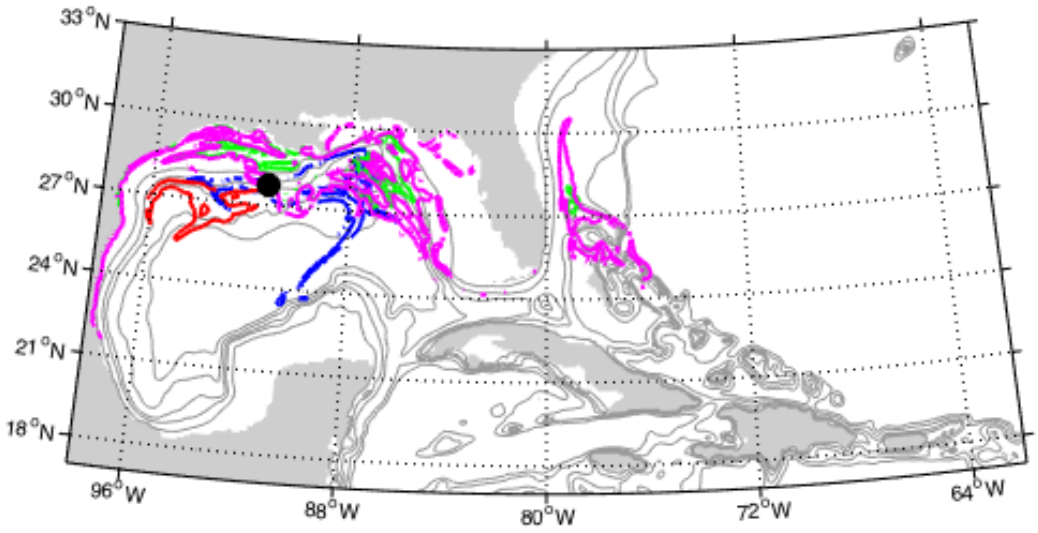

Figure 4. Particle trajectories released from Brine Pool in the Gulf of Mexico The black dot indicates the release site; dispersal paths of *B. naticoidea* are blue, *L. luymesi* are green, *A. muricola* are magenta, and Currents only are in red.

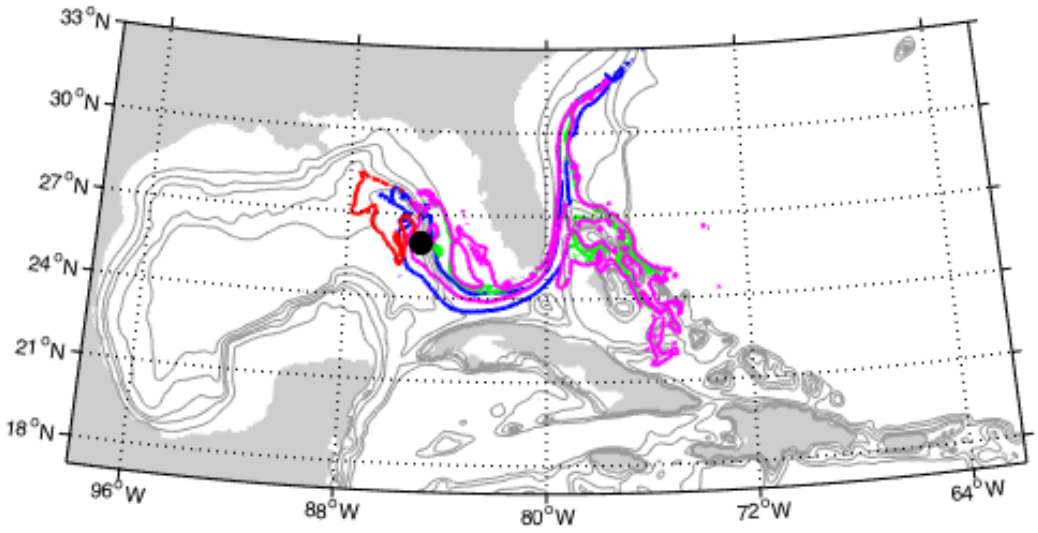

Figure 5. Particle trajectories released from Florida Escarpment in the Gulf of Mexico The black dot indicates the release site; dispersal paths of *B. naticoidea* are blue, *L. luymesi* are green, *A. muricola* are magenta, and Currents only are in red.

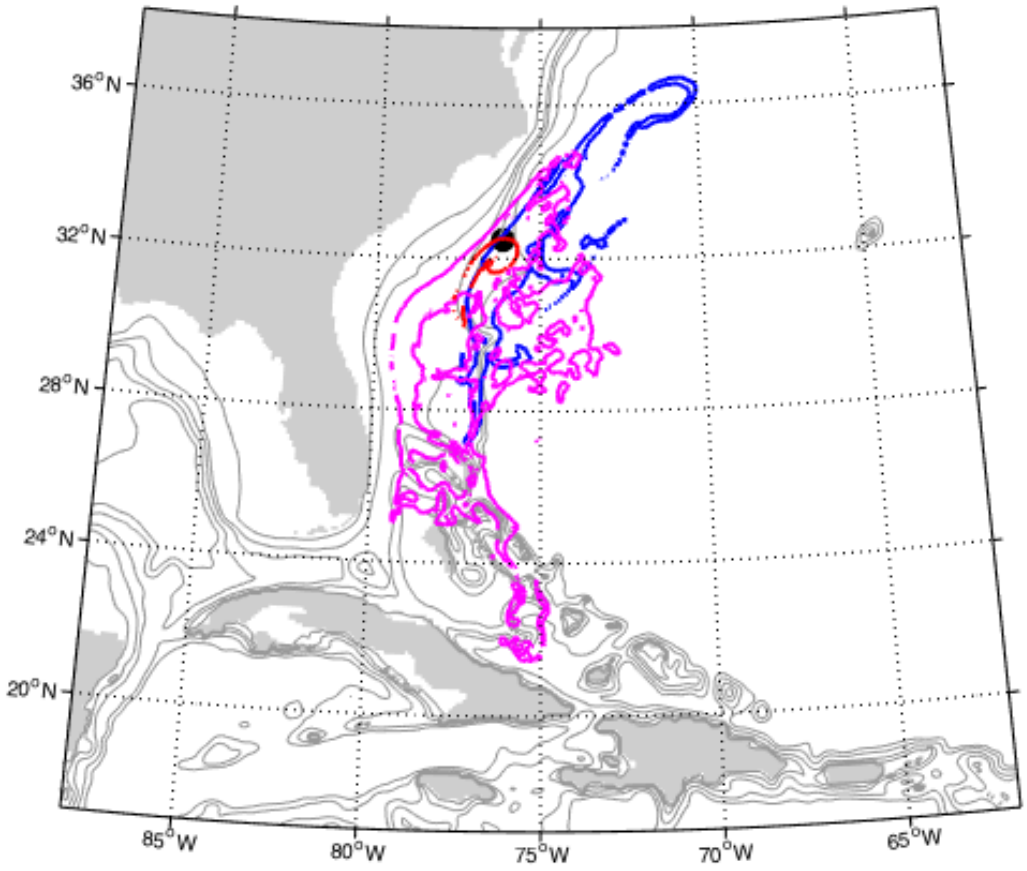

Figure 6. Particle trajectories released from Blake Ridge in the South Atlantic Bight. The black dot indicates the release site; dispersal paths of *B. naticoidea* are blue, *A. muricola* are magenta, and Currents only are in red.

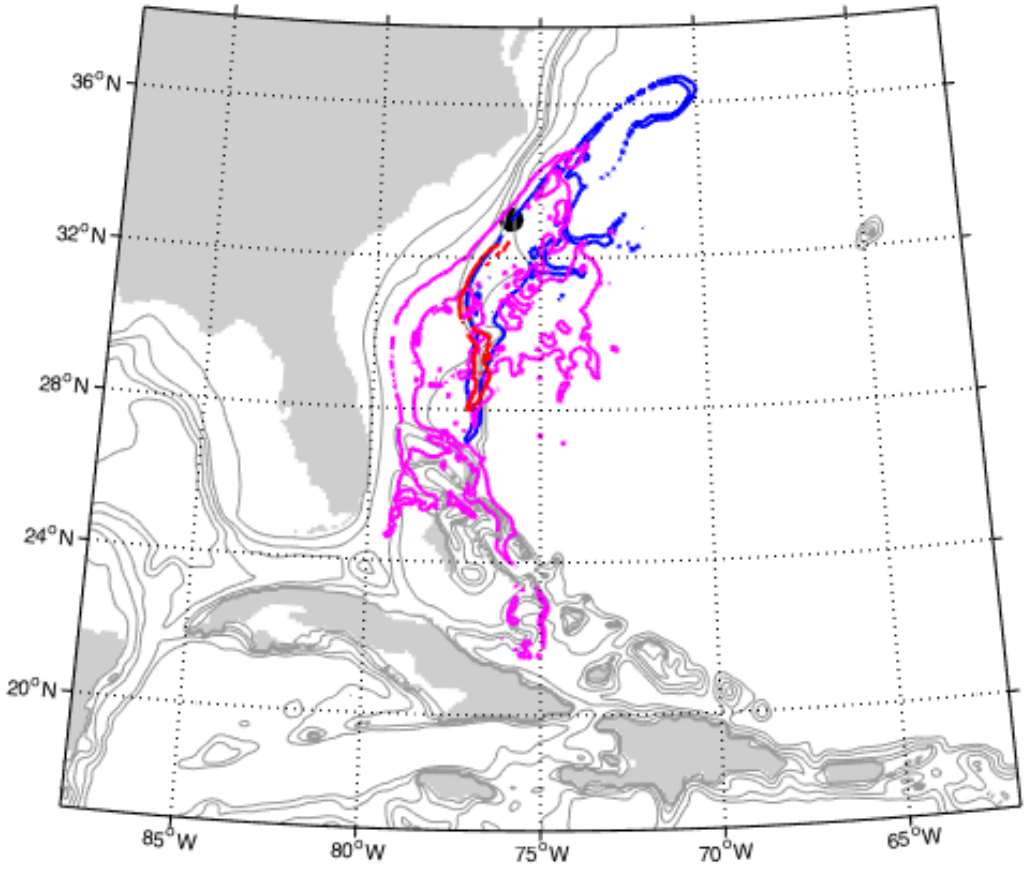

Figure 7. Particle trajectories released from Cape Fear Diaper in the South Atlantic Bight. The black dot indicates the release site; dispersal paths of *B. naticoidea* are blue, *A. muricola* are magenta, and Currents only are in red.

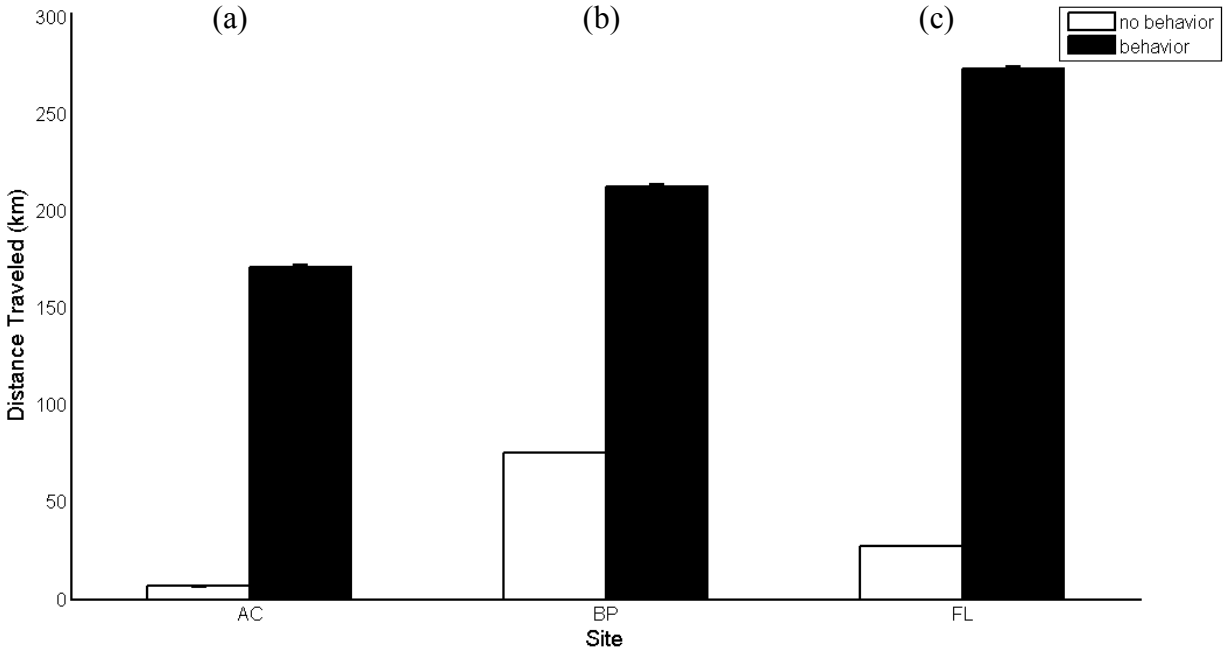

Figure 8. Effects of (i) particle release site and (ii) larval behavior (with vs without) on mean (+SE) distance travelled (km) by the polychaete worm *Lamellibrachia luymesi* over a 21-Day PLD. AC = Alaminos Canyon, BP = Brine Pool, and FL = Florida Escarpment.

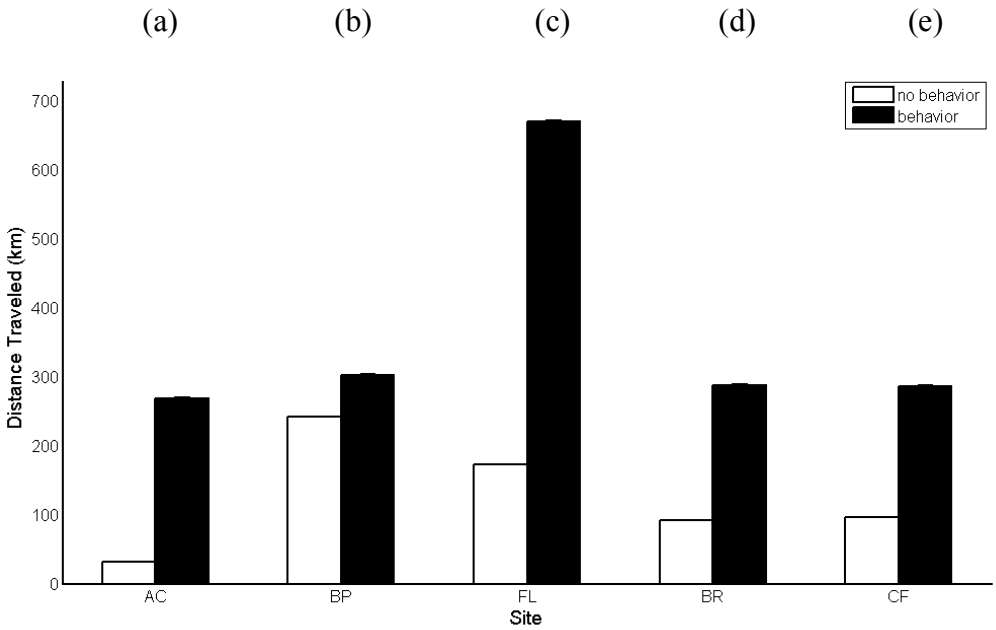

Figure 9. Effects of (i) particle release site and (ii) larval behavior (with vs without) on mean (+SE) distance travelled (km) by the gastropod *Bathynerita naticoidea* over a 90-Day PLD. AC = Alaminos Canyon, BP = Brine Pool, FL = Florida Escarpment, BR = Blake Ridge, and CF = Cape Fear Diaper.

(a) (b) (c) (d) (e)

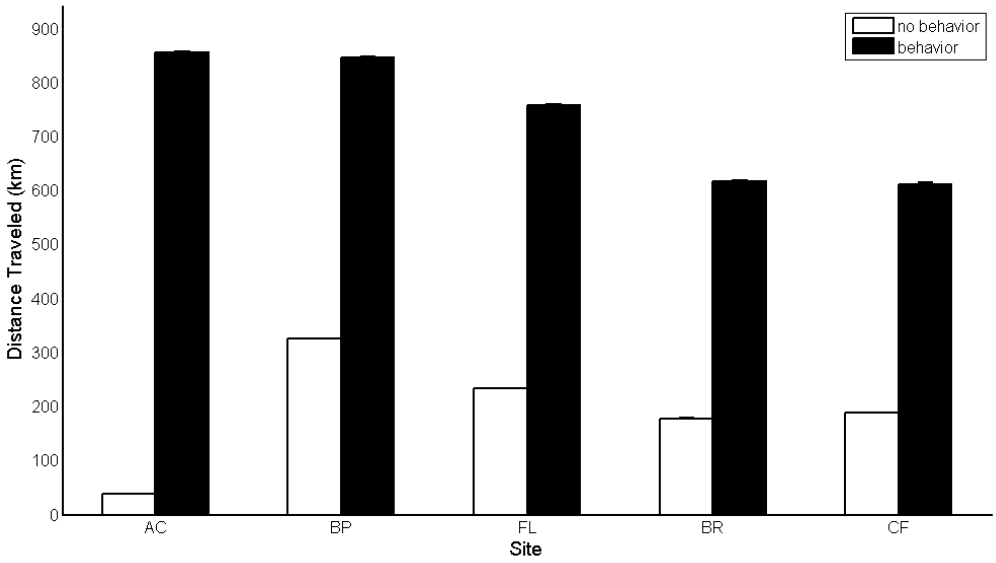

Figure 10. Effects of (i) particle release site and (ii) larval behavior (with vs without) on mean (+SE) distance travelled (km) by the shrimp *Alvinocaris muricola* over a 90-Day PLD. AC = Alaminos Canyon, BP = Brine Pool, FL = Florida Escarpment, BR = Blake Ridge, and CF = Cape Fear Diaper.

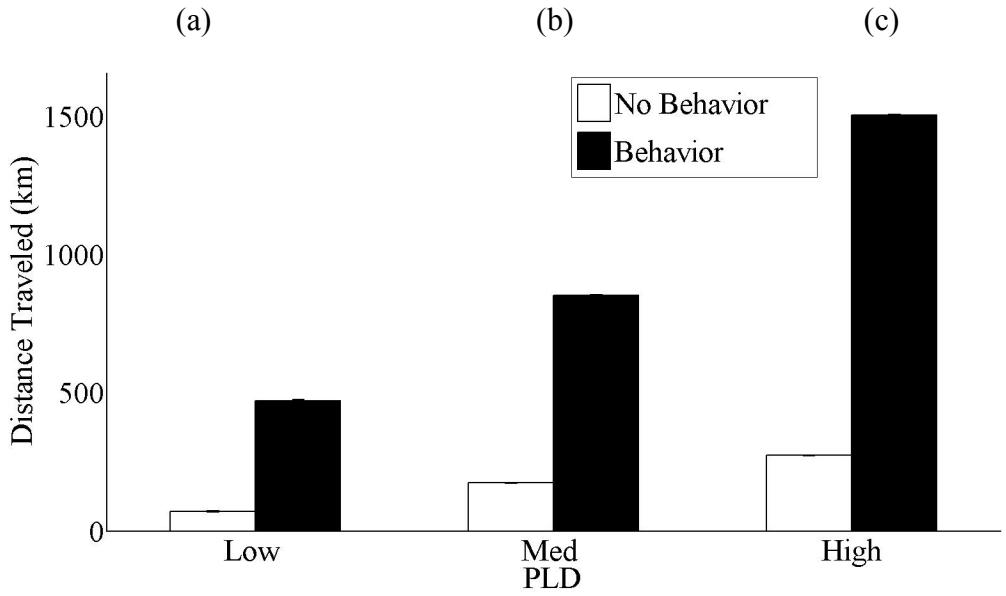

Figure 11. Effects of (i) PLD and (ii) larval behavior (with vs without) on mean (+SE) maximum distance (top 5% of simulations) travelled (km) for all methane seep sites. Low = 21 day PLD characteristic of the polychaete worm *Lamellibrachia luymesi*, Med = 90 day PLD characteristic of the gastropod, *Bathynerita naticoidea*, and High = 186 PLD characteristic of the crustacean, *Alvinocaris muricola*.

CHAPTER 2

VARIATION IN LARVAL BEHAVIOR ALTERS POTENTIAL LARVAL DISPERSAL AND POPULATION CONNECTIVITY OF A DEEP-SEA BIVALVE

ABSTRACT

A major goal in marine ecology is describing patterns of larval dispersal and population connectivity, as well as their underlying mechanisms. Numerous studies across a range of relatively shallow (<100 m) ecosystems have examined the relative importance of larval behavior and spawning location on larval dispersal and population connectivity—deep-sea chemosynthetic communities present an opportunity to test if paradigms generated from shallow ecosystems apply in the deep sea. A biophysical model was used to explore potential larval dispersal and population connectivity of the deep-sea mussel, "*Bathymodiolus" childressi*, among three methane seep sites in the Gulf of Mexico. Three possible larval dispersal strategies (simulations) were evaluated: (1) Protracted spawning period followed by demersal drift of larvae with a PLD of 395 days, (2) Discrete spawning and variable larval vertical distribution with 100 m dispersal, and (3) Discrete spawning and variable larval vertical distribution with near-surface dispersal. Average dispersal trajectories for particles varied 16 km to 1488 km away from methane seep sites, extensively covering the Gulf of Mexico and South Atlantic. Despite deep-sea currents that are an order of magnitude slower than surface currents, the relatively long PLD of *"B." childressi*, coupled with surface-seeking larval behavior, facilitate long-distance dispersal that potentially connects methane seep populations throughout the Gulf of Mexico and US Western Atlantic. Overall, larval behavior had a significant effect on mean dispersal distance ($p<0.0001$). Particles with

Simulation 3 behavior had the greatest dispersal distance (1173 km ±2.00), followed by Simulation 2 (921 km ±2.00), and Simulation 1 behavior (237 km ±1.43). This integrative method of highly detailed simulated larval behavior, coupled with hydrodynamic modeling, provides information on (1) the spatiotemporal scales of potential population connectivity of invertebrates that inhabit deep-sea chemosynthetic ecosystems, as well as (2) the relative importance of spawning location and larval behavior on potential population connectivity.

KEYWORDS

"Bathymodiolus" childressi, biophysical model, larval dispersal, methane seep, Gulf of Mexico

INTRODUCTION

In marine systems, the exchange of dispersing larvae among subpopulations can drive the (i) dynamics of marine metapopulations, (ii) resilience of populations to exploitation, and (iii) success of management strategies such as no-take marine reserves (Cowan and Sponaugle 2009, Gaines et al. 2010, Puckett and Eggleston 2016). Several biophysical processes can drive dispersal and connectivity patterns, such as the location and timing of spawning relative to hydrodynamic features and the availability of suitable habitat (Young 1987, Sponaugle et al. 2002, Edwards et al. 2007, Ayata et al. 2010, Gilbert et al. 2010, Huret et al. 2010, Eggleston et al. 2010, Basterretxea et al. 2012, Pinsky et al. 2012). Distribution mechanisms occurring during the larval phases may also drive dispersal and connectivity. For example, larval behaviors alter the vertical distribution of larvae in the water column exposing larvae to different hydrodynamic conditions at different depths, thereby modifying dispersal patterns (Sponaugle et al. 2002, Drew and Eggleston 2006, Paris et al. 2007, North et al. 2008, Butler et al. 2011). Moreover, the Pelagic Larval Duration (PLD) may range from days to months, after which larvae must find suitable habitat and successfully settle (Levin, 2006, Young et al. 2012). Thus, spatiotemporal variation in population connectivity among subpopulations over ecological and evolutionary time scales can result from variation in the timing and location of spawning, hydrodynamic processes, larval behavior and mortality, and post-settlement processes such as emigration and mortality (Van Dover et al. 2002, Levin 2006, Mitarai et al. 2016).

While the importance of larval dispersal and its influence on connectivity has been explored for over a century in relatively shallow ecosystems (Wallace 1876, Scheltema 1971,

Scheltema 1986, Caley et al. 1996), the recent discovery of deep-sea hydrothermal vent (Corliss and Ballard 1977) and methane seep invertebrate communities (Paull 1984) has provided novel ecological communities within which to test paradigms of larval dispersal and population connectivity generated from shallow ecosystems (Glig and Hilbish 2003, Baums et al. 2005, Levin 2006, Hedgecock et al. 2007). For example, the patchy nature of these deep-sea ecosystems, combined with deep ocean currents that are generally an order of magnitude slower than surface currents, suggests that population connectivity may be limited compared to shallow marine ecosystems (Messias et al. 1999, Arhan et al. 2003). Conversely, recent observations suggest that deep-sea, methane seep invertebrates are broadly distributed across ocean basins due, in part, to the long-distance dispersal potential of the larvae (Gaines et al. 2007, Arellano et al. 2014). For example, 12% of all known methane seep fauna are found on both the eastern and western sides of the Atlantic Ocean (Olu et al. 2010, Arellano et al. 2014).

A major challenge in studying dispersal of deep-sea organisms is the availability of biological data for both adult and larval stages. Although recent observations of larval behavior and knowledge of reproductive biology of adults in both the field and laboratory have improved, it remains very difficult to study free-floating larvae throughout various stages of the PLD (Young et al. 2012, Arellano and Young 2014). Given the relatively sparse information on larval biology and spawning dynamics of deep-sea organisms, biophysical modeling was used to explore potential larval dispersal and population connectivity of the deep-sea mussel, *"Bathymodiolus" childressi*, a species where information on larval

behavior and spawning periodicity is more readily available via the literature and from observations made during this study.

"Bathymodiolus" childressi Biology

Mytilid mussels are found in deep-sea reducing habitats in the subfamily Bathymodiolinae (Gustafson et al. 1998), and the genus *Bathymodiolus* consists of species that are found in hydrothermal vents and methane seeps. *Bathymodiolus* species contain chemosynthetic bacterial endosymbionts in their gills, which serve as their primary energy source (Childress et al. 1986), but supplement their diet by filter feeding (Pile and Young 1999). *"Bathymodiolus" childressi* is found throughout the Gulf of Mexico and Western Atlantic and at depths from 200 m to more than 3,000 m (Gustafson et al. 1998, Tyler et al. 2000, Carney et al. 2006, and *personal observations*). Molecular phylogeny analysis of *"B." childressi* indicates uncertainty about its taxonomic status, and so followed the recommendation of Jones et al. (2006) and used quotation marks around the genus name. Population genetic analysis by Carney et al. (2006) found no genetic differentiation between "*B." childressi* populations from the shallowest (~200 m) and deepest (>2,500 m) sites; however, there are genetic similarities across large geographic distances, which may indicate widespread dispersal. The broad distribution of "*B." childressi* indicates periods of moderate connectivity through the dispersal of the mussel larvae at both contemporary and evolutionary time scales, but the manner in which larvae disperse to reach sites of varying distances remains unverified (Young et al. 2012, Arellano et al. 2014).

It is also unknown if gametogenesis of "*Bathymodiolus" childressi* occurs throughout the year as some observations in the Gulf of Mexico suggest spawning may be synchronous and periodic (Tyler et al. 1996, Young *personal observation*). The developmental method for "*B." childressi* larvae is not known, but has been inferred by examining basic characteristics such as its small egg size and planktotrophic larval feeding strategy, which suggests a relatively long PLD (Thorson 1950, Ockelmann 1965). A relatively long PLD has been observed in other "*Bathymodiolus"* species (Berg 1985, Hessler et al. 1988, LePennec and Beninger 1997, Colaco et al. 2006).

Previous studies initially indicated that bathymodiolin mussel larvae disperse demersally and do not have the energetic capability to migrate towards surface waters (Lutz et al. 1984, Turner et al. 1985). Observations and collections of larvae at hydrothermal vents and methane seeps also suggested that the majority of species occur near the sea floor (Kim et al. 1998, Mullineaux et al. 2005). However, Arellano et al. (2014) identified "*B." childressi* larvae in the upper 100 m of the water column while conducting MOCNESS tows over the Brine Pool site in the northern Gulf of Mexico (650 m; 27 43'23"N, 91 16'30"W), and found that larvae do have the energetic capability to migrate into the euphotic zone. Larvae were also found throughout different depths of the water column from the MOCNESS tows at similar developmental stages and size, making it difficult to understand the primary dispersal depth for "*B." childressi*. While estimated larval size ranges for bathymodiolin mussels exist (Young et al. 1999, Arellano et al. 2014), the timing of spawning and larval development rates are unknown. The larval forms of "*B." childressi* are believed to have a PLD of at least one year, but actual larval duration is undetermined.

In this study, larval behavior for *"B." childressi,* such as (i) spawning date, (ii) swimming speed, (iii) planktonic larval duration, and (iv) vertical distribution in the water column were estimated through a combination of shipboard experiments, MOCNESS tows, and results from previous studies (Arellano 2008, Young et al. 2012, Arellano et al. 2014). The "*B." childressi* larvae at similar stages of development have been found at varying ocean depths in the Atlantic, which may indicate variation on dispersal techniques. Therefore, the purpose of this study was to analyze the effects of three observed larval behaviors on potential larval dispersal and population connectivity among seep sites.

MATERIALS AND METHODS

A climatological, hydrodynamic model was coupled with a Lagrangian, particle-tracking model to predict dispersal paths for three possible larval behavioral scenarios for the deep-sea bivalve, *"B." childressi* released from three spawning sites in the Gulf of Mexico. The output was used to compare the main and interactive effects of the three spawning locations and three different larval dispersal behaviors for *"B." childressi* on the following response variables: (1) general particle trajectories, as well as (2) mean versus (3) maximum dispersal distances.

Biophysical Model and Spatio-Temporal Scales

The *US East*, hydrodynamic model domain (Fig.1) covers the entire Gulf of Mexico, U.S. South Atlantic, U.S. Mid-Atlantic and North Atlantic Bights, northwest Atlantic Ocean, as well as the Sargasso, Caribbean and Intra-American Seas. *US East* is a type of Regional

Ocean Modeling System (ROMS) that generates 3D current velocities under realistic climate conditions, and was developed by the Ocean Observing and Modeling group at North Carolina State University (He et al. *in prep*). The grid spacing of *US East* is 7-10 km and utilizes 36 terrain-following vertical levels with increased resolution towards the surface and ocean bottom layers.

The atmospheric and oceanic conditions for the *USEast* model were optimized with two model data sets: HYCOM and ARGOS. The **HY**brid **C**oordinate **O**cean **M**odel (HYCOM) is a global ocean model that assimilates satellite-observed sea surface temperature and height, as well as ARGOS- measured temperature and salinity to generate daily predictions of ocean circulation at 10 km spatial resolution (http://hycom.rsmas.miami.edu/dataserver). HYCOM model solutions from 2009-2014 were averaged annually to determine climatological monthly means for atmospheric and oceanographic conditions, which, in turn, generated the open boundary conditions across which model data flowed freely into the eastern boundary of the *US East* domain.

Surface atmospheric forcing used to drive the *US East* circulation model was derived from the **N**ational **C**enter for **E**nvironmental **P**rediction (NCEP) reanalysis products (e.g. cloud cover), with a spatial grid of 1.875^{o} and temporal resolution of six hours. Total cloud cover, precipitation, surface pressure, relative humidity, air temperature, surface wind, and net short-wave and long-wave radiations were used in a standard bulk formula (Fairall et al. 2003) to derive wind stress and net surface heat flux which, in turn, were used to drive the ocean circulation model.

A five-year simulation of ocean currents was used for model spin-up of realistic ocean conditions, followed by simulation period of particle trajectories. *USEast* was paired with a Lagrangian particle tracking model (see below) to track the position of larval particles released from three methane seep sites in the GoM that are a part of a broader study of population connectivity of invertebrates among seep sites (*SEEPC* Collaborative Research Program; www.cmast.ncsu.edu/seepc): (1) Alaminos Canyon (26 21'17"N, 94 29'48" W), (2) Brine Pool (27 43'23"N, 91 16'30"W), and (3) Florida Escarpment (26 1'48"N, 84 54'54"W (Fig.1). The seeps were chosen because they provide a means to study connectivity on spatial scales that match those at which vent systems are being studied (Hurtado et al. 2004) and include species that span large depth and geographic ranges and have diverse life-history characteristics.

Particle-Tracking Model

The **L**agrangian **TRANS**port model (LTRANS) is an offline, particle-tracking model that predicts particle movement in three directions using advection, diffusion and behavior (North et al. 2006). LTRANS interpolates sea surface height, water velocity, salinity, and temperature from grid locations, and utilizes a fourth-order Runge-Kutta scheme for particle advection.

Particles were assigned characteristics of *"B." childressi* larval behavior, including (i) swimming speeds, (ii) vertical distribution in the water column, and (iii) PLD. I used the circulation patterns described above to evaluate the spatial scales over which *"B." childressi* larvae may be dispersed under spatiotemporally varying oceanographic conditions. Thus, our

results predict potential variability in larval transport within the entire region under three observed behavioral scenarios. Successful dispersal also requires larvae (real or virtual) to encounter suitable methane-seep settlement habitats, which can be spatially isolated and often cover a small proportion of the area of potential dispersal. Therefore, I included the depth, latitude, and longitude locations of discrete seep sites that are the target of our broader study on population connectivity among seep sites in the *US East* domain. Genetic and geochemical characterization of *"B." childressi* populations is being conducted (C. Young and S. Arellano, unpubl. data, C. Cunningham and C. Van Dover, Duke University, unpubl. data; B. Puckett and D. Eggleston, NC State University, unpubl. data) to test some of the predictions of larval dispersal and connectivity generated from the present study. Putative settlement sites were divided into 7 km segments, thereby allowing for self-recruitment.

Larval Behavior and Dispersal Simulation Scenarios for "B." childressi

PLDs used in our simulations were determined using the best available information from a combination of published literature (Young et al. 1996, Van Gaest 2006, Arellano 2008, Young et al. 2012), personal observations, and zooplankton tows during the field investigation. Larval behaviors, such as: (i) swimming speed, (ii) PLD, and (iii) vertical distribution, were determined with a combination of published literature (Arellano 2008, Young et al. 2012) and MOCNESS (**M**ultiple **O**pening/**C**losing **N**et and **E**nvironmental **S**ensing **S**ystem) zooplankton tows as part of the field study. The larval forms of *"B." childressi* were collected with MOCNESS tows over several years (1995-2014) at two sites in the Gulf of Mexico, Brine Pool (27^{o} 43.4 N 91^{o} 16.8 W) and Bush Hill (27^{o} 47N, 92^{o} 30W

(C. Young *personal communication,* Arellano et al. 2014, Arellano and Young 2011, Arellano and Young 2009, Arellano 2008, Tyler et al. 2006, Eckelbarger and Young 1999), with subsequent ship-based behavioral observations incorporated into this study.

Based on these data, three possible larval dispersal strategies (simulations) were evaluated: (1) protracted spawning period followed by demersal drift of larvae with a PLD of 395 days, (2) discrete spawning and variable larval vertical distribution with near surface dispersal, and (3) discrete spawning and variable larval vertical distribution with near-surface dispersal. It is important to re-emphasize that the actual timing of spawning and larval vertical distribution of *"B." childressi* is unknown, and the present study explores whether or not there are major differences in dispersal metrics and potential population connectivity among the three putative spawning and larval dispersal scenarios.

(1). Protracted spawning and demersal drift. -- The first simulation included the release of 10 larval particles every three hours from the seep sites, for a total of 30,000 particles per simulation per site over the course of a year. The particles were programmed with demersal drift behavior, which meant all particles stayed within three meters of the sea floor throughout the 395-day PLD (Fig. 2). While the actual fecundity of *"B." childressi* has not yet been quantified, the number of particles released in the simulations is likely an underestimate of larvae produced from a single spawning event from a dense seep community, but provides statistically valid insight into the dispersal of particles released from a known seep site.

(2). Discrete spawning and variable larval vertical distribution with near surface dispersal. -- In the second simulation, 20 particles were released every hour for a total of 14,880 particles released over the period of a week in Mid-October. This change in the amount of particles released over a specific time period correlates with direct observations of spawning at Brine Pool and Bush Hill methane seep sites in the GoM (C. Young *personal observation*). The behavioral assignments for the larval particles released in Mid-October are extremely specific to match very precise observations of *"B." childressi* larvae over the course of their larval life (*personal observation* and C. Young *personal observation*). Particles were programmed to exhibit no behavior the first two days, followed by weak upward swimming behavior at 0.02 cm s^{-1} from day three to ten. On the tenth day, swimming speed increased to 0.2 cm s^{-1} until particles reached 100 m. Particles dispersed at near surface (<100 m) for 175 days, and programmed to swim down to the sea floor at 0.2 cm s^{-1} to arrive on bottom by 185th day of their PLD. Due to the variation in site depth, up to 10 days were programmed to allow particles enough time to reach the sea floor; therefore, there is some variation in the number of days particles drift near bottom over the course of their PLD. Particles then drifted within three meters above bottom until the end of the 395-PLD (Fig. 2). The number of particles released in Simulations 2 and 3 provide statistically sound understanding into the dispersal patterns of particles with each behavior type.

(3). Discrete spawning and variable larval vertical distribution with near-surface dispersal. -- In the third simulation, the programmed spawning occurred in the same manner as described in Simulation 2. Particles exhibited no behavior the first two days, followed by weak upward swimming behavior at 0.02 cm s^{-1} from day three to ten. On the tenth day,

swimming speed increased to 0.2 cm s^{-1} until particles reached near the surface (<100 m). There, particles dispersed in surface waters for approximately 385 days, and started swimming down to the sea floor at 0.2 cm s^{-1} in order arrive on bottom by the end of the 395-PLD (Fig. 2).

Hypotheses and Statistical Analyses

Deep ocean currents are generally an order of magnitude slower than surface currents (Dickinson and Brown 1994). Therefore, it is hypothesized that *"B." childressi* with surface seeking larval behavior would display the greatest average and maximum potential distance travelled, irrespective of release site. In additional to examining general particle trajectories among the various spawning sites and larval dispersal behaviors, particle tracks were organized and compiled using Matlab software (2014b) for several statistical analyses. The main and interactive effects of (1) spawning site (3 sites) and (2) particle behavior (3 behavioral simulations) were tested on two response variables: (i) mean dispersal distance and (ii) maximum potential dispersal distance, with a multi-factor, three-way analysis of variance (ANOVA) model. Multiple comparisons for significant main effects were identified with lower-level ANOVA models and Tukey's multiple comparisons test. Maximum potential dispersal was estimated as the top 5% of dispersal distances within a given set of average distances. For example, particle distances were sorted in descending order and the top five percent, or 1,500 particle distances from Simulation 1 and 744 particle distances from simulations two and three were then used to calculate the average maximum distance.

RESULTS

General Particle Trajectories

A total of 30,000 particles were released (10 particles released every three hours), for larval dispersal scenario 1, and 14,880 particles released in simulations two and three (20 particles released hour) for a total of 179,280 particles that were tracked in the Gulf of Mexico over a 395-day PLD. Dispersal trajectories varied greatly according to site and behavior for each of the three simulations. While there was variation in average dispersal distance, the overall trend was consistent, with the greatest dispersal observed for Simulation 3 involving surface seeking behavior by *"B." childressi*, followed by Simulation 2 with larvae dispersing at the surface for 175 days followed by 215 days drifting three meters above bottom, and Simulation 1 in which larvae dispersed three meters above bottom throughout its 395-day PLD (Figs 3-5). Dispersal trajectories also varied greatly according to release site. For example, particles released from Alaminos Canyon in the eastern GOM had the lowest average and average maximum dispersal distances of the three release sites (compare Fig. 3 with Figs. 4-5). Particles released from Brine Pool in the Northern-central area of the GOM dispersed throughout the eastern areas of the GOM and South-Atlantic Bight (Fig. 4), whereas particles released from Florida Escarpment connected with the Loop Current and spread to the South-Atlantic Bight (Fig. 5).

"B." childressi Simulation 1

The mean distance travelled by particles (demersal drift three meters above bottom throughout the 395-PLD) varied significantly according to release site (one-way ANOVA; $F = 815{,}985$, $df = 2, 85{,}679$, $p < 0.0001$). For example, mean distance travelled was higher when

released from Brine Pool (Fig. 4; 432 km ±0.23), followed by Florida Escarpment (Fig. 5; 262 km ±0.23), and Alaminos Canyon (Fig. 3; 16 km ±0.23), (Tukey's test; $p<0.0001$). In general, particles with demersal drift behavior did not disperse widely throughout the GOM, and instead followed the bathymetric contour of the GOM with an easterly spread (Figs. 3-5).

"B." childressi Simulation 2

Mean distance travelled by particles (near surface drift for 175 days followed by 215 days drifting three meters above bottom) also varied significantly with release site (one-way ANOVA; $F = 38{,}752$, $df = 2, 44{,}639$, $p<0.0001$). Generally, mean distance travelled was higher when released from Florida Escarpment (Fig. 5; 1248 km ±2.61), followed by Brine Pool (Fig. 4; 1187 km ±2.61), and Alaminos Canyon (Fig. 3; 328 km ±2.61) (Tukey's test; $p<0.0001$). Overall, particles with surface drift followed by demersal drift behavior dispersed widely throughout the GOM and South-Atlantic Bight.

"B." childressi Simulation 3

Mean distance travelled by particles (near surface drift for 385 days) also varied significantly with release site (one-way ANOVA; $F = 3718$, $df = 2, 44{,}639$, $p<0.0001$). Mean distance was significantly higher when released from Brine Pool (Fig. 4; 1488 km ±4.47), followed by Florida Escarpment (Fig. 5; 1016 km ±4.47), followed by and Alaminos Canyon (Fig. 3; 1016 km ±4.47) (Tukey's test; $p<0.0001$). Particles with surface drift followed by demersal drift behavior also dispersed widely throughout the GOM and South and Mid-Atlantic Bight.

Effects of Behavior on Larval Dispersal

The distances for all particles were grouped by behavior to analyze the mean dispersal distance across all sites. For example, all particles with Simulation 1 behavior were sorted in order to identify overall mean distance with that particular behavior. The results were then compared to the mean distances for simulations two and three. The type of behavior had a significant effect on mean dispersal distance (ANOVA; $F = 86{,}316$, $df = 2, 174{,}959$, $p<0.0001$). The Least Square Means showed statistically significant differences between all three behaviors ($p < 0.0001$). The average distance varied among all three behavior simulations (Fig. 7; Tukey's test; $p<0.0001$). The particles with Simulation 3 behavior had the greatest dispersal distance (near surface drift; Fig. 7; 1173 km $\pm$2.00), followed by Simulation 2 (near surface drift for 175 days followed by ~215 days drifting demersally three meters above bottom; Fig. 7; 921 km $\pm$2.00), and Simulation 1 behavior (demersal drift; Fig. 7; 237 km $\pm$1.43).

The average maximum distance (AMD) for each *"B." childressi* behavior simulation (Fig.8) varied with site and behavior (two-way ANOVA; $F = 29359$, $df = 2, 8747$, $p<0.0001$), with the highest level of dispersal from Simulation 3 (1875 km $\pm$5.69), followed by Simulation 2 (1454 km $\pm$5.86), and Simulation 1 (305 km $\pm$4.10). Average maximum dispersal distances varied significantly among all sites (Fig. 8; Tukey's test; $p<0.0001$) and behaviors (Fig. 9; Tukey's test; $p<0.0001$).

DISCUSSION

The study of deep-sea larvae and their dispersal to spatially isolated habitats remains one of the most challenging aspects of deep-sea science. This study used a coupled biophysical model to explore the roles of three observed larval behaviors and spawning locations on potential larval dispersal and population connectivity for the mussel, "*Bathymodiolus" childressi.* In general, *"B." childressi* particles dispersed widely throughout the GOM, Florida Strait, as well as the South- and Mid-Atlantic Bights, while mean dispersal distances were much greater when larvae dispersed in the euphotic zone than at relatively deep (>600 m) depths. For example, mean dispersal for "*B." childressi* Simulation 1 (bottom following) was 237 km, whereas mean dispersal distances in simulations two (near surface and bottom following) and three (near surface) were 921 km and 1173 km, respectively. Our results show that particles do encounter other seep sites in the *US East Model* spatial domain, however; this result that does not prove that there is a strong enough connection to influence population dynamics or genetic structure. To calculate the connection strength across the model domain, further analysis is needed to quantify the level of connectivity at both contemporary and evolutionary time scales between each of the seeps sites in our study system, as well as the level of self-recruitment.

Simulating larval dispersal for deep-sea organisms is limited due to the lack of biological data, which complicates the reliability of available estimates (Cowen and Sponaugule 2009, Young et al. 2012, Hilario et al. 2015 and references therein, Mitarai et al. 2016). A previous bioenergetics model study by Arellano (2008) on larval "*B." childressi* assessed the potential of swimming to the surface, and concluded that larvae were

energetically capable of swimming from ~660 m to the surface in ~ 10 days. Although our biophysical model was based on data personally collected from shipboard experiments (observed data), over 98% of modeled particles reached surface water depths in approximately 10 days (modeled data), which is consistent with Arellano's (2008) findings. While population genetic data is not yet available from the adults collected from seep sites, results will be soon be available to verify the model observations and provide further insight into the connectivity of *"B." childressi* in the GOM.

Population genetic analysis of "*B." childressi* mitochondrial genes and nuclear markers show no distinction between nine methane seep populations in the Gulf of Mexico over spatial scales ranging from the Gulf of Mexico to the Western Atlantic, and at depths from 200 m to more than 3,000 m (Carney et al. 2006). While other deep-sea species have depth related distribution (e.g., *Escarpia laminata* and *Lamellibrachia luymesi*) in the Gulf of Mexico (Rex 1981, Pequegnat et al. 1990, France and Kocher 1996, Chase et al. 1998, MacDonald et al. 2003, Cordes et al. 2007), bathymodiolins are found across biogeographic areas of different depths (Van Dover et al. 1996; Desbruye`res et al. 2000).

Other bathymodiolin species have similarly extensive depth ranges, which suggest that it may be a characteristic of the genus (O'Mullan et al. 2001). Ongoing population genetic studies "*B." childressi* from *SEEPC* colleagues indicate widespread mixing and connectivity throughout the Gulf of Mexico, although tests are still in progress (J. Wagner, Duke University, *personal communication*). This genetic information suggests *"B." childressi* larvae may use some form of near surface dispersal tactics to disperse throughout the GOM.

Few studies have modeled larval dispersal behavior in the deep sea, with the greatest limitations in understanding due to dependable biological estimates (Cowen and Sponaugule 2009, Young et al. 2012, Hilario et al. 2015 and references therein, Mitarai et al. 2016). Hilario et al. (2015) reviewed the application of biophysical models in the study of larval dispersal and population connectivity in the deep sea, and found the majority of models did not incorporate any behavior (e.g., PLD and vertical migration). In one of the few studies that incorporated behavior, Young et al. (2012) released larval particles from randomly chosen coordinates within 80 km of a seep sites in the Intra-American Seas, where adult *"B." childressi* were known to be abundant, but were not programmed with vertical migration behavior. Young et al. (2012) found *"B." childressi* particles dispersed widely throughout the GOM and South Atlantic Bight. Our current study builds upon the work by Young et al. (2012) by incorporating very specific biological parameters, such as larval swimming speeds and vertical distribution scenarios over the duration of *"B." childressi* PLD, as well as releasing particles from known methane seep sites. I found that mean dispersal distances were greater than those found by Young et al. (2012).

Caveats

Coupled biophysical models can be valuable tools to study the general dispersal patterns of larval particles, and better understand how behavior drives variation in dispersal and potential population connectivity. The dispersal paths and mean distances from the three possible behavior scenarios examined in this study are considered the best approximations to date of actual dispersal trajectories of *"B." childressi* larvae under variable atmospheric and oceanographic conditions. The biological uncertainties remain exist with regards to larval

dispersal depth, behavior, and PLD, which is why this study specifically focused on the part of larval behavior, and the array of directly observed behaviors of larvae caught in plankton tows (Table 1). Working with limited and conflicting data provided an opportunity to explore the array of behaviors tested, and extensively study the effect of those behavior parameters on potential dispersal. Eddies and currents do have a seasonal component in the model domain, which results in eddies circulating in the western area of the GOM basin during the October spawning season, which may influence the observed dispersal patterns via Loop Current meandering and eddy shedding. Although the seasonal atmospheric conditions consisted of monthly averages within the climatological model, the model domain is a convenient way to examine behavior on average dispersal distances from different sites in the GOM. The climatological model is limited by grid scale of 7-10 km, and without grid nesting it is not possible to understand the fine scale movements of particles in the domain. This somewhat coarse spatial resolution is a necessary trade-off for the immense spatial domain in this study (over 1,000,000 km^2). The increase in physical ocean circulation modeling capabilities in recent years has made it easier to understand how oceanographic features affect the potential dispersal paths and distances of larvae from their natal site.

The highly detailed larval particle behavior simulations presented are some of the most complex performed to date for a deep-sea bivalve. Nevertheless, there are certain assumptions that had to be made. It was assumed that *"B." childressi* particles swim vertically and at a constant rate from days 2-10 at 0.02 cm s^{-1}, and then at 0.2 cm s^{-1} for the remainder of their PLD. Little is known about their swimming behavior, nor how the larvae respond to light, pressure, and temperature over the course of their PLD. Previous laboratory

observations (Arellano 2008) show that *"B." childressi* larvae do increase vertical swimming velocity with an increase in temperature (7 to 15^{o}C), and while it was beyond the scope of this study to manipulate swimming particle behavior in response to temperature, the particles swimming speeds were adjusted throughout the larval life to best match empirical data. Particles were programmed to exhibit no behavior the first two days, followed by weak upward swimming behavior at 0.02 cm s^{-1} from day three to ten. On the tenth day, swimming speed increased to 0.2 cm s^{-1} until particles reached 100 m. Moreover, larval cultures of "*B." childressi* in laboratory experiments were distributed throughout the container, and did not swim unidirectionally upward, rather the larvae "meandered" (Arellano 2008, C. Young *personal communication*, *personal observation*).

Future Research

Future work should incorporate energetics and respiration data into larval dispersal simulations, as well as diel vertical migration patterns, to determine their relative effects on dispersal potential. Further research of *"B." childressi* larval dispersal throughout the Gulf of Mexico should focus on increasing the spatial scale of resolution to explore the effects of small-scale oceanographic features on large-scale dispersal patterns. The climatological model in the present study used the monthly mean conditions throughout the domain, whereas hindcast model conditions may show how inter-annual variability might impact seasonal larval dispersal patterns. The seasonal nature of "*B." childressi* spawning may have a strong impact on potential dispersal, and further studies should compare mean dispersal distances among all four seasons to determine if seasonal differences in spawning influence the dispersal and potential connectivity for larval particles with a 13-month PLD.

Currently, models are limited by assumptions that increase the resolution of current velocity, eddy resolution, and upwelling strength, due to the lack of available observed data by moorings, acoustic current meters, and CTDs. Moreover, computing power is not yet strong enough to completely reproduce fine-scale field conditions, such as bathymetric features and eddies. Many aspects of oceanographic models have become more accurate over time via the integration of temperature, river flow, and flow velocity (Todd et al. 2014), yet more research is necessary to validate and test the resolution of currents, eddies, upwelling and directional flow of water in the model domain. While models are not designed to simulate every aspect of observed conditions, our dispersal results and the results of others (Kinlan et al. 2005, Young et al. 2012, Puckett et al. 2014, 2016) emphasize the predictive strength of biophysical models on larval retention and dispersal. Moreover, increased understanding of basic biology and larval behavior of *"B." childressi* will improve the accuracy of simulated larval dispersal.

In summary, biological parameters of *"B." childressi* larvae such as swimming speed at particular points over a larval particle's PLD, and the amount of time spent in near surface waters, had a significant effect on the dispersal of larval particles throughout the Gulf of Mexico and U.S South Atlantic. These results suggest that obtaining values of the relevant physiological and behavioral parameters of deep-sea larvae that can be integrated into biophysical models should continue to take high priority in the study of deep-sea invertebrates and predictions of population connectivity.

ACKNOWLEDGEMENTS

We are especially grateful for the support and expertise of C. Young for insight into *"B." childressi* larval behavior and biology. Thank you to the crew of the *R/V Atlantis*, *Alvin*, and *Sentry* for collecting adults and larvae at sea. Funding for this project was provided by NSF OCE-1031050.

REFERENCES

Arellano, S.M., A.L. Van Gaest, S.B. Johnson, R.C. Vrijenhoek, and C.M. Young. 2014. Larvae from deep-sea methane seeps disperse in surface waters. *Proc R Soc B* 281 (1786): 20133276.

Arellano, S.M., and C.M. Young. 2011. Temperature and salinity tolerances of embryos and larvae of the deep-sea mytilid mussel "Bathymodiolus" childressi. *Mar Biol* 158(11), 2481-2493.

Arellano, S.M., and C.M. Young. 2009. Spawning, development, and the duration of larval life in a deep-sea cold-seep mussel. *Biol Bull* 216:149–162.

Arellano, S.M. 2008. Embryology, larval ecology, and recruitment of *"Bathymodiolus" childressi*, a cold seep mussel from the Gulf of Mexico. Dissertation University of Oregon.

Arhan M., H. Mercier, Y. Park. 2003. On the deep-water circulation of the eastern South Atlantic Ocean. *Deep-Sea Research Part I* 50:889-916.

Ayata, S. D., P. Lazure, and E. Thiébaut. 2010. How does the connectivity between populations mediate range limits of marine invertebrates? A case study of larval dispersal between the Bay of Biscay and the English Channel (North-East Atlantic). *Prog Oceanog* 87(1):18-36.

Baums, I.B., W. W. Miller, and M. Hellberg. 2005. Regionally isolated populations of an imperiled Caribbean coral, Acropora palmata. *Molec Ecol* 14:1377-1390.

Basterretxea, G., A. Jordi, I.A. Catalan, and A.N.A. SabatÉS. 2012. Model-based assessment of local-scale fish larval connectivity in a network of marine protected areas. *Fish Oceanog* 21(4):291-306.

Berg, C.J. Jr. 1985. Reproductive strategies of mollusks from abyssal hydrothermal vent communities. *Biol Soc Wash Bull* 6: 185-197.

Butler, M.J., C.B. Paris, J.S. Goldstein, H. Matsuda, and R.K. Cowen. 2011. Behavior constrains the dispersal of long-lived spiny lobster larvae. *Mar Ecol Prog Ser* 422:223-237.

Caley, M.J., M.H. Carr, M.A. Hixon, T.P. Hughes, G.P. Jones, and B.A. Menge. 1996. Recruitment and the local dynamics of open marine populations. *Annual review of ecology and systematics* 27: 477-500.

Carney, S.L., M.I. Formica, H. Divatia, K. Nelson, C.R. Fisher, S.W. Schaeffer. 2006. Population structure of the mussel *"Bathymodiolus" childressi* from Gulf of Mexico hydrocarbon seeps. *Deep Sea Res I* 53: 1061-1072

Childress, J. J., C.R. Fisher, J. M. Brooks, M. C. Kennicutt II, R. R. Bidigare, and A. E. Anderson.

1986. A methanotrophic marine molluscan (Bivalvia, Mytilidae) symbiosis: mussels fueled by gas. *Science* 233: 1306-1308.

Colaco, A. I. Martins, M. Laranjo, L. Pires, C. Leal, C. Prieto, V. Costa, H. Lopes, D. Rosa, P.R. Dando, and R. Serrao-Santos. 2006. Annual spawning of the hydrothermal vent mussel, *Bathymodiolus azoricus*, under controlled aquarium conditions at atmospheric pressure. *J Exp Mar Biol Ecol* 333:166-171.

Corliss, J. B., and R. D. Ballard. 1977. Oases of life in the cold abyss. *NatI. Geogr. Mag.* 152: 441-453.

Cowen, R.K., G. Gawarkiewicz, J. Pineda, S.R. Thorrold, and F.E. Werner. 2007. Population connectivity in marine systems. *Oceanog* 20(3):14-21.

Cowen, R.K. and S. Sponaugle. 2009. Larval dispersal and marine population connectivity. *Annu Rev Mar Sci* 1: 443-466.

Craddock, C. W.R. Hoeh, R.G. Gustafson, R.A. Lutz, J. Hasimoto, R.C. Vrijenhoek. 1995a. Evolutionary relationships among deep-sea mytilids (Bivalvia: Mytilidae) from hydrothermal vents and cold-water methane/sulfide seeps. *Mar Biol* 121: 477-485.

Craddock, C.W., W.R. Hoeh, R.A. Lutz, R.C. Vrijenhoek. 1995b. Extensive gene flow among Mytilid (*Bathymodiolus thermophilus*) populations from hydrothermal vents of the eastern Pacific. *Mar Biol* 124137-146.

Drew, A.C. and D.B. Eggleston. 2006. Currents, landscape structure, and recruitment success along a passive-active dispersal gradient. *Landsc Ecol* 21:917-913.

Eckelbarger, K.J. and C.M. Young.1999. Ultrastructure of gametogenesis in a chemosynthetic mytilid bivalve (Bathymodiolus childressi) from bathyal, methane seep environment (northern Gulf of Mexico). Mar Biol 135:635-646.

Edwards, K. P., J.A. Hare, F.E. Werner, and H. Seim. 2007. Using 2-dimensional dispersal kernels to identify the dominant influences on larval dispersal on continental shelves. *Mar Ecol Pro Ser* 352(77).

Eggleston, D.B., N.B. Reyns, L.L. Etherington, G.R. Plaia, and L. Xie. 2010. Tropical storm and environmental forcing on regional blue crab (*Callinectes sapidus*) settlement. *Fish. Oceanogr.* 19:89-106.

Fairall, C. W., E.F. Bradley, J.E. Hare, A.A. Grachev, and J.B. Edson. 2003. Bulk parameterization of air-sea fluxes: Updates and verification for the COARE algorithm. *J of Clim*, 16(4), 571-591.

Gaines, S.D., B. Gaylord, L.R. Gerber, A. Hastings, B.P. Kinlan. 2007. Connecting places: The ecological consequences of dispersal in the sea. *Oceanog* 20: 90-99.

Gaines, S.D. C. White, M.H. Carr, and S.R. Palumbi. 2010. Designing marine reserve nerworks for both conservation and fisheries management. *Proc Natl Acad Sci USA* 107:18286-18293.

Gawarkiewicz, G.G., S.G. Monismith, and J. Largier. 2007. Observing larval transport processes affecting population connectivity: progress and challenges. *Oceanog* 20(3): 40-53.

Gilbert, C. S., W.C. Gentleman, C.L. Johnson, C. DiBacco, J.M. Pringle, and C. Chen. 2010. Modelling dispersal of sea scallop (Placopecten magellanicus) larvae on Georges Bank: The influence of depth-distribution, planktonic duration and spawning seasonality. *Prog Oceanog* 87(1): 37-48.

Gilg, M. R. and T. J. Hilbish. 2003. The geography of marine larval dispersal: coupling genetics with fine- scale physical oceanography. *Ecol* 84: 2989–2998.

Gustafson, R.G., R.D. Turner, R.A. Lutz, R.C. Vrijenhoek. 1998. A new genus and five species of mussels (Bivalvia Mytilidae) from deep-sea sulfide/hydrocarbon seeps in the Gulf of Mexico. *Malacologia* 40: 63-112.

Hedgecock, D., P. H. Barber, S. Edwards. 2007. Genetic approaches to measuring connectivity. *Oceanog* 20: 70-79.

Hessler, R.R., W.M. Smithy, M.A. Boudrias, C.H. Keller, R.A. Lutz, and J.J. Childress. 1988. Temporal change in megafauna at the Rose Garden hydrothermal vent (Galapagos Rift; eastern tropical Pacific). *Deep Sea Res* 35: 1677-1709.

Huret, M., P. Petitgas, and M. Woillez. 2010. Dispersal kernels and their drivers captured with a hydrodynamic model and spatial indices: a case study on anchovy (*Engralis enrasicolus*) early life stages in the Bay of Biscay. *Prog Oceanog* 87:6-17.

Jollivet, D, T. Comtet, P. Chevaldonne, S. Hourdez. 1998. Unexpected relationship between dispersal strategies and speciation within the association *Bathymodiolus* (Bivalvia)—*Branchipolynoe* (Polychaeta) inferred from the rDNA neutral ITS2 marker. *Cah. Biol. Mar* 39: 359-362.

Jones, W. J. and R.C. Vrijenhoek. 2006. Evolutionary relationships within the "Bathymodiolus " childressi group. *Cah. Biol. Mar.* 47: 403–407.

Karl, S., S. Schutz, D. Desbruyeres, R.A. Lutz, R.C. Vrijenhoek. 1996. Molecular analysis of gene flow in the hydrothermal vent clam *Calyptogena magnifica*. *Molec Mar Biol and Biotech* 5: 193: 202.

Kim SL, Mullineaux LS. 1998. Distribution and near- bottom transport of larvae and other plankton at hydrothermal vents. Deep Sea Res. II 24, 423 – 440.

LePennec, M. and P.G. Beninger. 1997. Aspects of the reproductive strategy of bivalves from reducing-ecosystem. *Cah Biol Mar* 38:132-133.

Levin, L. A. 2006. Recent progress in understanding larval dispersal: new directions and digressions. *Integr. Comp. Biol.* 46: 282-297.

Lutz R.A., Jablonski D, Turner RD. 1984. Larval dispersal at deep-sea hydrothermal vents. Science 226: 1451 – 1454. (doi:10.1126/science.226.4681.1451)

Macavoy, S.E., R.S. Carney, E. Morgan, S.A. Macko. 2008. Stable isotope variation among the mussel *Bathymodiolus childressi* and associated heterotrophic fauna at four cold-seep communities in the Gulf of Mexico. *J Shellf Res* 27(1): 147-151.

Messias, M. J., C. Andrie, L. Memery, and H. Mercier. 1999. Tracing the North Atlantic Deep Water through the Romanche and Chain fracture zones with chlorofluoromethanes. *Deep Sea Research Part I* 46: 1247-1278.

Mitarai, S., H. Watanabe, Y. Nakajima, A.F. Shchepetkin, and J.C. McWilliams. 2016. Quantifying dispersal from hydrothermal vent fields in the western Pacific Ocean. *PNAS* 113(11): 2976-2981.

Mullineaux LS, Mills SW, Sweetman AK, Beaudreau AH, Metaxas A, Hunt HL. 2005. Vertical, lateral and temporal structure in larval distributions at hydrothermal vents. Mar. Ecol. Prog. Ser. 293, 1 – 16. (doi:10.3354/ meps293001).

North, E.W., Z. Schlag, R.R. Hood, M. Li, L. Zhong, T. Gross, and V.S. Kennedy. 2008.Vertical swimming behavior influences the dispersal of simulated oyster larvae in a coupled particle-tracking and hydrodynamic model of Chesapeake Bay. *Mar Ecol Prog Ser* 359:99-115.

North, E.W., Z. Schlag, R.R. Hood, M. Li, L. Zhong, T. Gross, and V.S. Kennedy. 2006. Vertical swimming behavior influences the dispersal of simulated oyster larvae in a coupled particle-tracking and hydrodynamic model of Chesapeake Bay. *Mar Ecol Prog Ser* 359: 99.

Ockelmann, K. W. 1965. Developmental types in marine bivalves and their distribution along the Atlantic coast of Europe. Pp. 25-35 in *Proceedings of the First European Malacology Congress* 1962, Cox, L.R., and J.P. Peake, eds. Malacological Society of London, London.

Okubo, A., and S.A. Levin. 2002. *Diffusion and Ecological Problems* (2nd ed.), Springer Verlag, p 488.

Olu K, Cordes EE, Fisher CR, Brooks JM, Sibuet M, Desbruye`res D. 2010. Biogeography and potential exchanges among the Atlantic Equatorial belt cold-seep faunas. PLoS ONE 5, e11967. (doi:10. 1371/journal.pone.0011967.t003)

Olu-Le Roy K, Cosel RV, Hourdez S, Carney SL, 7. Jollivet D. 2007. Amphi-Atlantic cold-seep Bathymodiolus species complexes across the equatorial belt. Deep-Sea Res. I 54, 1890 – 1911. (doi:10.1016/j.dsr.2007.07.004

O'Mullan, G.D., P.A.Y. Maas, R.A. Lutz, R.C. Vrijenhoek. 2001. A hybrid zone between hydrothermal vent mussels (Bivalvia: Mytilidae) from the Mid-Atlantic Ridge. *Molec Ecol* 10: 2819-2831.

Paris, C.B., L.M. Cherubin, and R.K. Cowen. 2007. Surfing, spinning, or diving from reef to reef: effects on population connectivity. *Mar Ecol Prog Ser* 347:285-300.

Paull, CK, B. Hecker, R. Commeau, R.P. Freeman-Lynde, C. Neumann, W.P. Corso, S. Golubic, J.E. Hook, E. Sikes, and J. Curray. 1984. Biological communities at the Florida Escarpment resemble hydrothermal vent taxa. *Sci* 226: 965-967.

Pile, A.J. and C.M. Young. 1999. Plankton availability and retention efficiencies of cold-seep symbiotic mussels. *Limnol Oceanogr* 44:1833-1839.

Pinsky, M. L., S.R. Palumbi, S. Andréfouët, and S.J. Purkis. 2012. Open and closed seascapes: where does habitat patchiness create populations with high fractions of self-recruitment? *Ecol App* 22(4):1257-1267.

Puckett, B.J., D.B. Eggleston, P.C. Kerr and R.A. Luettich Jr. 2014. Larval dispersal and population connectivity among a network of marine reserves. *Fish and Oceanogr 23*(4), 342-361.

Puckett, B. J. and D. B. Eggleston. 2016. Metapopulation dynamics guide marine reserve design: importance of connectivity, demographics, and stock enhancement. *Ecosphere* (in press).

Schlag, Z. R., and E. W. North. 2012. Lagrangian TRANSport (LTRANS) v.2 model User's Guide. Technical Report of the University of Maryland Center for Environmental Science Horn Point Laboratory. Cambridge, MD. 183 p.

Scheltema, R.S.1971. Larval dispersal as a means of genetic exchange between geographically separated populations of shallow-water benthic marine gastropods. B*iological Bulletin*, 140(2): 284-322.

Scheltema, R.S. 1986. On dispersal and planktonic larvae of benthic invertebrates: an eclectic overview and summary of problems. *Bull. Mar. Sci.* 39(2): 290-322.

Sponagule, S. R.K. Cowen, and A.L. Shanks. 2002. Predicting self-recruitment in marine

populations: biophysical correlates and mechanisms. *Bull Mar Sci* 70: 341-275.

Sponaugle, S., R.K. Cowen, A. Shanks, S.G. Morgan, J.M. Leis, J. Pineda, and J.L. Munro. 2002. Predicting self-recruitment in marine populations: biophysical correlates and mechanisms. *Bull Mar Sci* 70(Supplement 1): 341-375.

Thorson, G.L. 1950. Reproductive and larval ecology of marine bottom invertebrates. *Biol Rev* 1:1-45.

Turner RD, Lutz RA, Jablonski D. 1985 Modes of Molluscan larval development at the deep-sea hydrothermal vents. Bull. Biol. Soc. Wash. 6, 167 – 184.

Tyler, P. C.M. Young. 1999. Reproduction and dispersal at vents and cold seeps. *Jour Mar Biol Assoc UK* 79: 193-208.

Tyler, P.A., C.M. Young and A. Clarke. 2000. Embryonic pressure and temperature tolerances in an antarctic echinoid: potential for deep-sea invasion. Mar Ecol Prog Ser

Tyler, P., C. M. Young, E. Dolan, S. M. Arellano, S. D. Brooke, and M. Baker. 2006. Gametogenic periodicity in the chemosynthetic cold-seep mussel *"Bathymodiolus" childressi. Mar. Biol.* 150 (5): 829-840.

Van Dover, C.L., C.R. German, K.G. Speer, L.M. Parson, and R.C. Vrijenhoek. 2002. Evolution and biogeography of deep-sea vent and seep invertebrates. *Science* 295(5558): 1253-1257.

Van Gaest and A. Lea. 2006. Ecology and early life history of Bathynerita naticoidea: evidence for long-distance larval dispersal of a cold seep gastropod.

Wallace, A.R. 1876. The geographical distribution of animals, Volume 1. Harpers New York, pp 503.

Won, Y. C.M. Young, R.A Lutz, R.C. Vrijenhoek. 2003. Dispersal barriers and isolation among deep-sea mussel populations (Mytilidae: *Bathymodiolus*) from eastern Pacific hydrothermal vents. *Molec Ecol* 12: 169-184.

Young, C.M., R. He, R.B. Emlet, Y. Li, H. Qian, S.M. Arellano, A.Van Gaest, K.C. Bennett, M. Wolf, T.I. Smart, and M.E. Rice. 2012. Dispersal of deep-sea larvae from Intra-American Seas: simulations of trajectories using ocean models. *Integ and Compar Biol* 52(4): 483-496.

Young, C.M., S.U.K. Ekaratne, and J.L. Cameron 1998. Thermal tolerances of embryos and planktotrophic larvae of Archaeopneustes hystrix (Spatangoidea) and Stylocidaris lineata (Cidaroidea), bathyal echinoids from the Bahamian Slope. *J of Exper Mar Biol and Ecol* 223:65-76.

Young, C.M. 1987. The novelty of supply side ecology. *Science* 235: 415-416.

TABLE

Table 1. Uncertainties with regards to behavior, dispersal depth, and PLD of *"B." childressi*.

Simulation	Spawning Date	Behavior	Modeled PLD	Possible PLD
Simulation 1	Year round	Demersal Drift	395	1185
Simulation 2	October (observed)	Mixed (Near Surface/Demersal)	395	1185
Simulation 3	October (observed)	Near Surface	395	1185

FIGURES

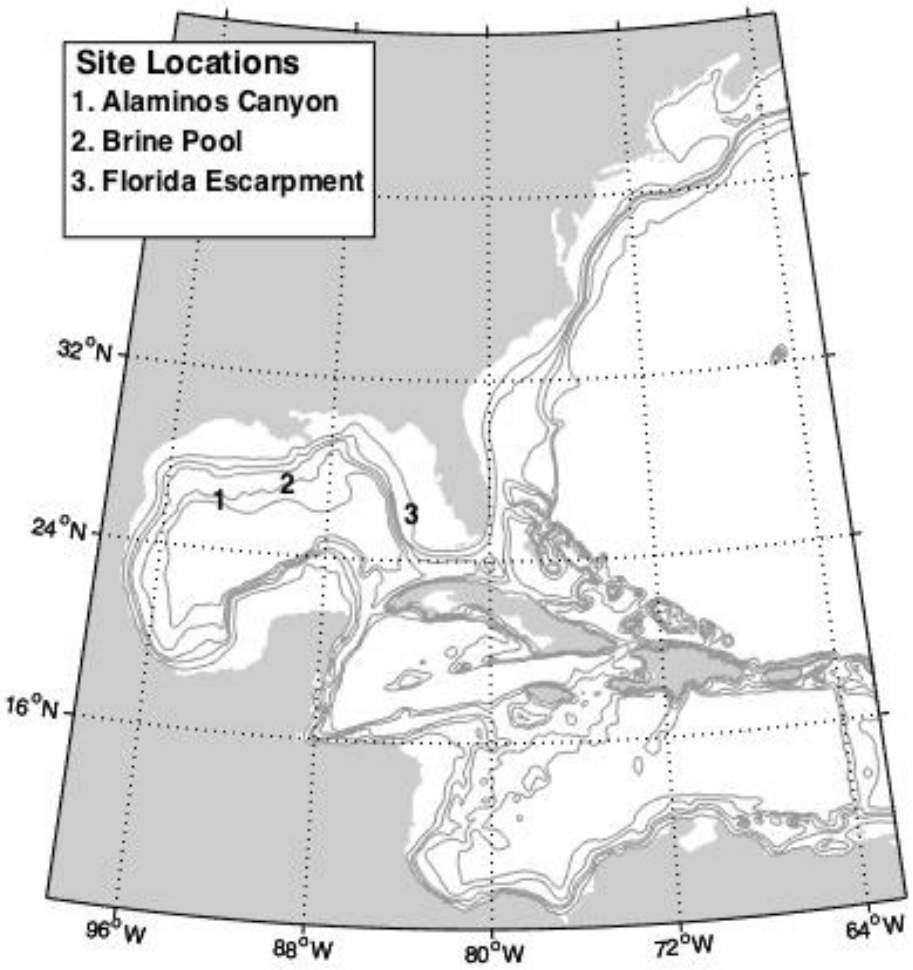

Figure 1. Spatial domain of *USEast* circulation model. Methane seep study sites are plotted on the model domain to match latitude, longitude, and depth of the actual locations: Alaminos Canyon (26 21'17"N, 94 29'48" W, 1300 m), Brine Pool (27 43'23"N, 91 16'30"W, 660 m), and Florida Escarpment 26 1'48"N, 84 54'54"W, 3500 m).

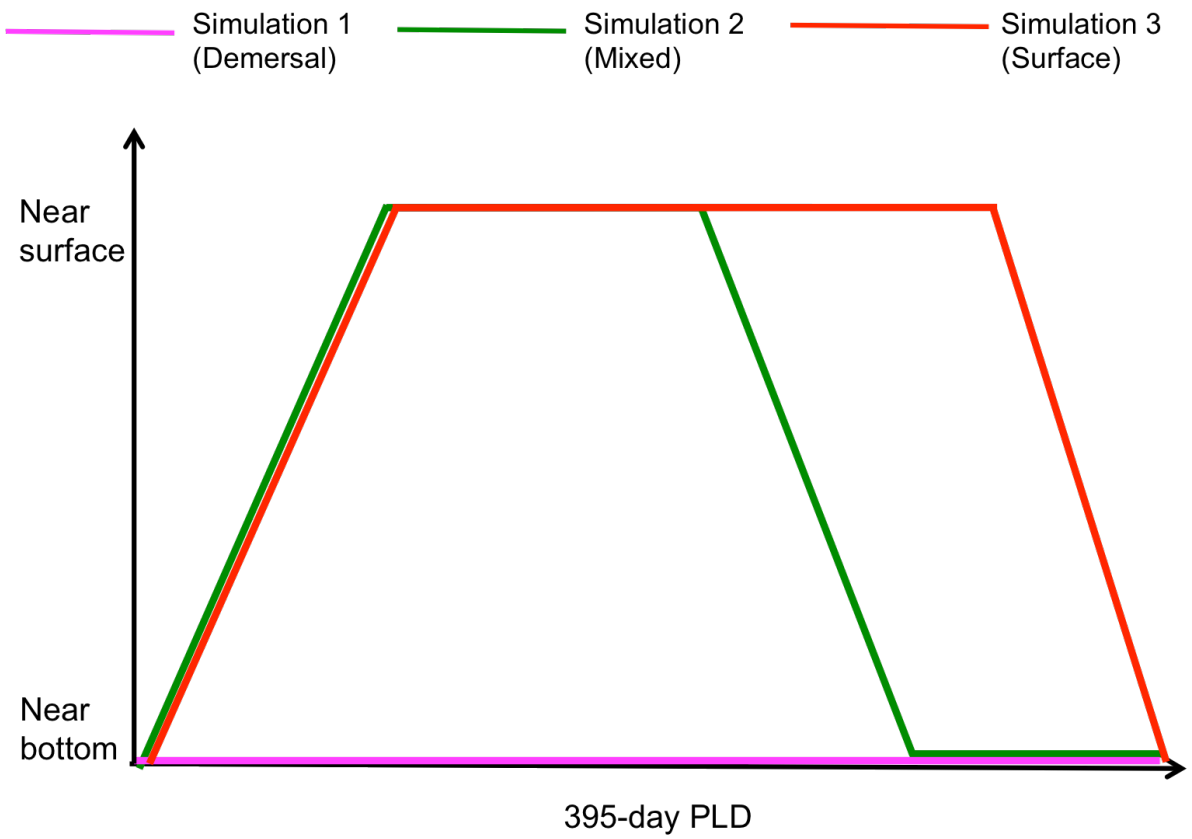

Figure 2. Schematic diagram of specific larval behavior simulations for *"B." childressi*. Simulation 1: larvae disperse near bottom for 395 days. Simulation 2: larvae disperse 175 days at the surface followed by 215 days of demersal drift. Simulation 3: larvae disperse for 395 days at the surface. All particles were programmed to arrive on the sea floor and settle by the end of their specific behavioral simulation.

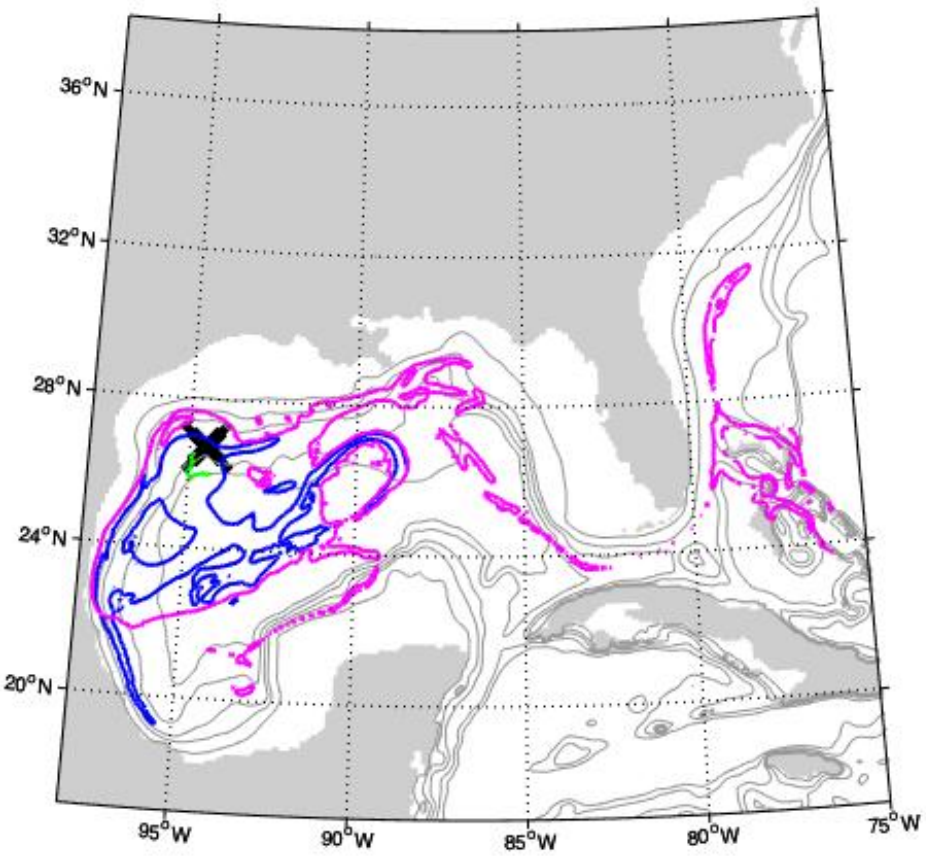

Figure 3. Particle trajectories released from Alaminos Canyon in the Gulf of Mexico. The "X" indicates the release site; dispersal paths of *"B." childressi* Simulation 1 are in green, *"B." childressi* Simulation 2 are blue, and *"B." childressi* Simulation 3 are magenta.

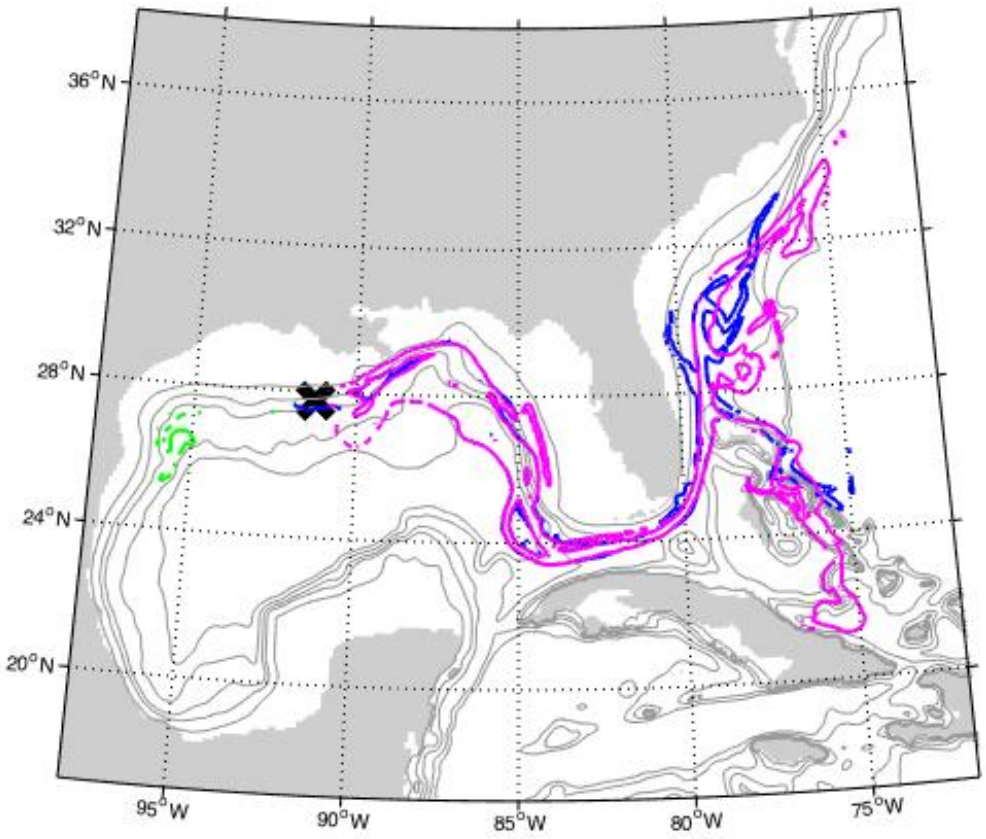

Figure 4. Particle trajectories released from Brine Pool in the Gulf of Mexico. The "X" indicates the release site; dispersal paths of *"B." childressi* Simulation 1 are in green, *"B." childressi* Simulation 2 are blue, and *"B." childressi* Simulation 3 are magenta.

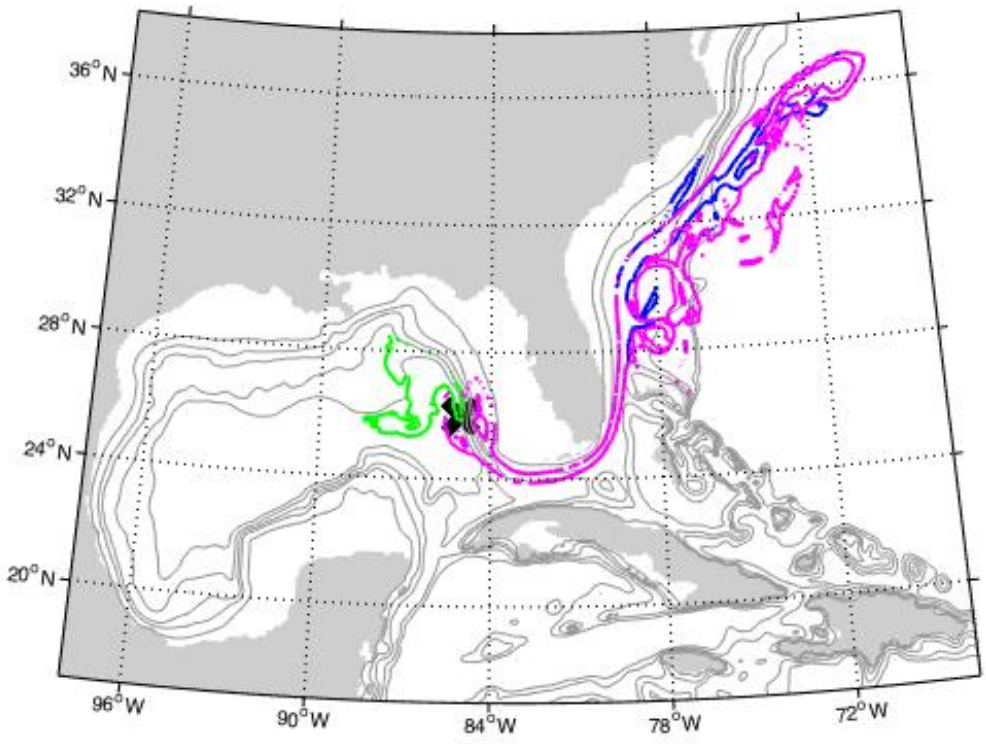

Figure 5. Particle trajectories released from Florida Escarpment in the Gulf of Mexico. The "X" indicates the release site; dispersal paths of *"B." childressi* Simulation 1 are in green, *"B." childressi* Simulation 2 are blue, and *"B." childressi* Simulation 3 are magenta.

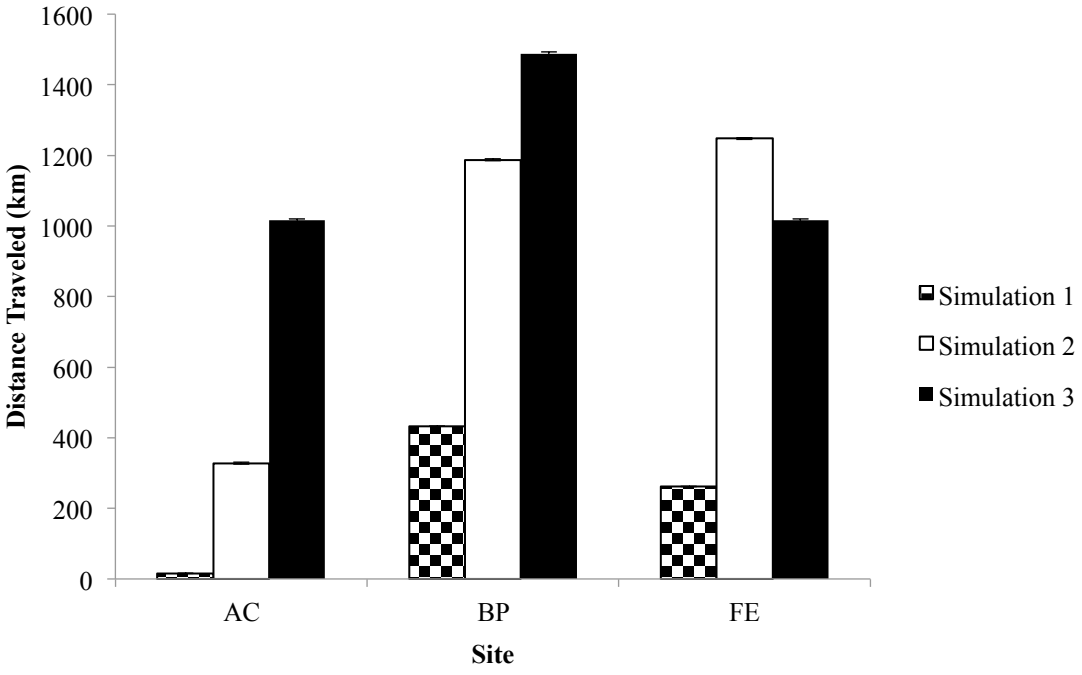

Figure 6. Effects of (i) particle release site and (ii) larval behavior (demersal drift, surface to demersal drift, and surface drift) on mean (+SE) distance travelled (km) by *"Bathymodiolus" childressi* over 395-day PLD. AC = Alaminos Canyon, BP = Brine Pool, and FL = Florida Escarpment. Simulation 1: larvae disperse near bottom for 395 days. Simulation 2: larvae disperse 175 days at the surface followed by 215 days of demersal drift. Simulation 3: larvae disperse the surface.

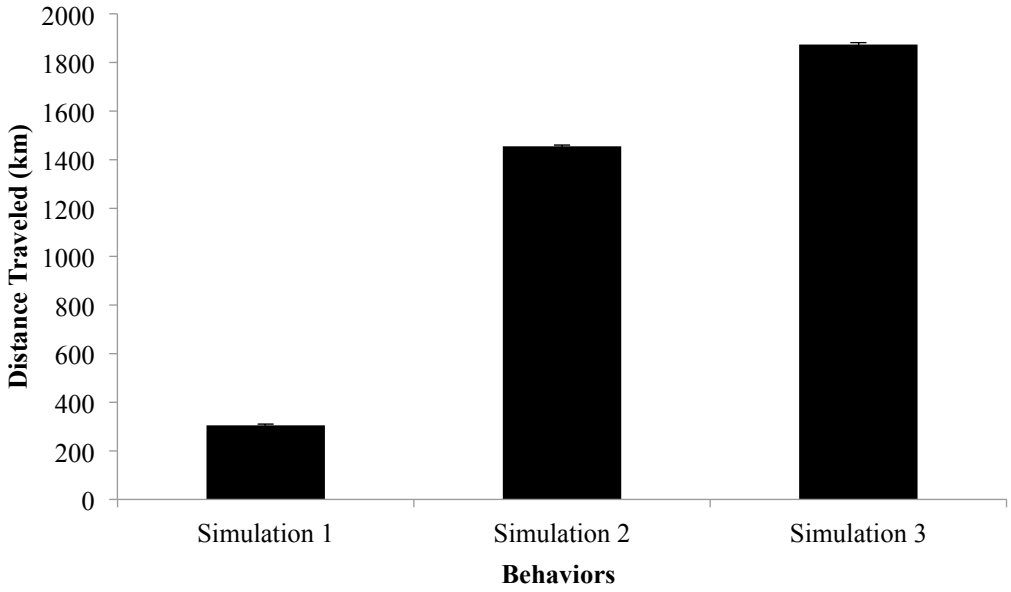

Figure 7. Effects of larval behavior (demersal drift, surface to demersal drift, and surface drift) on mean (+SE) distance travelled (km) by *"Bathymodiolus" childressi* over 395-day PLD. Simulation 1: larvae disperse near bottom for 395 days. Simulation 2: larvae disperse 175 days at the surface followed by 215 days of demersal drift. Simulation 3: larvae disperse near the surface.

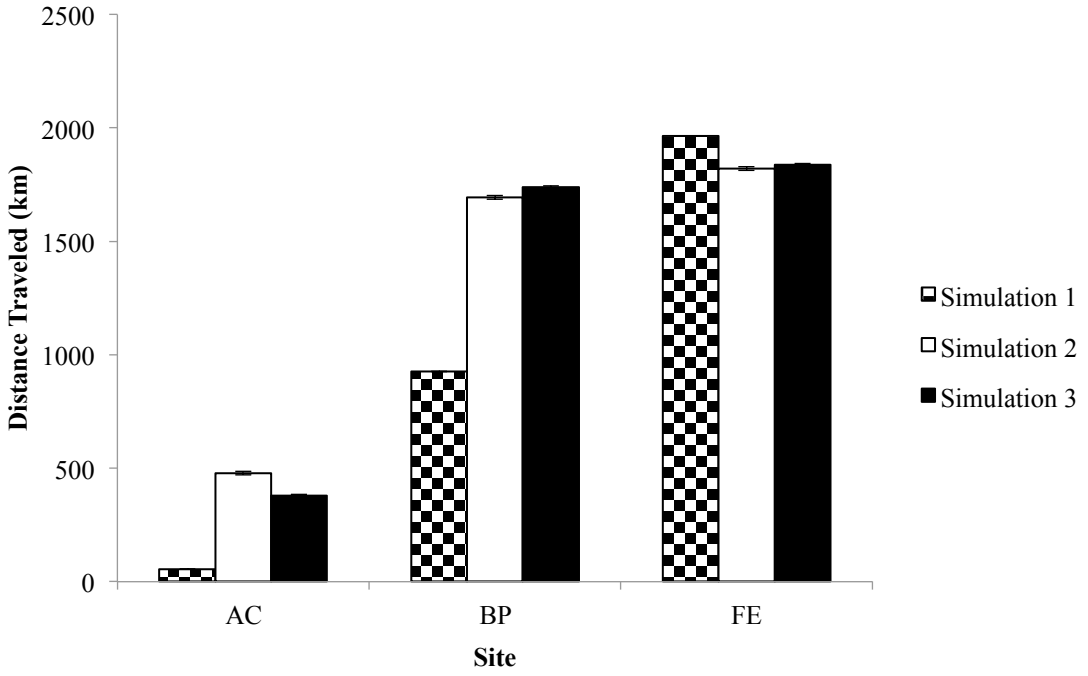

Figure 8. Effects of (i) particle release site and (ii) larval behavior (demersal drift, surface to demersal drift, and surface drift) on average maximum (+SE) distance travelled (km) by *"Bathymodiolus" childressi* over 395-day PLD. AC = Alaminos Canyon, BP = Brine Pool, and FL = Florida Escarpment. Simulation 1: larvae disperse near bottom for 395 days. Simulation 2: larvae disperse 175 days at the surface followed by 215 days of demersal drift. Simulation 3: larvae disperse near the surface.

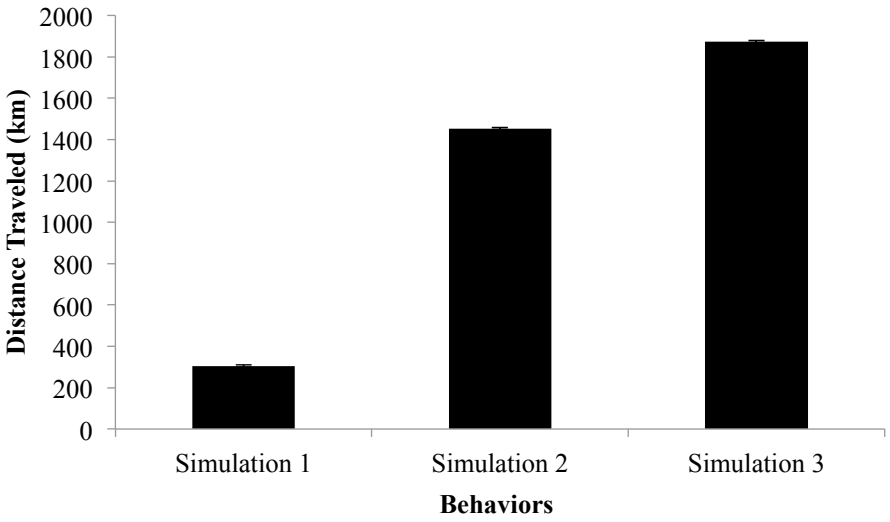

Figure 9. Effects of larval behavior for *"Bathymodiolus" childressi* on average maximum distance traveled. Behavior 1 (dermersal drift), behavior 2 (surface to demersal drift) and behavior 3 (surface drift) on average maximum (+SE) distance travelled (km) by *"Bathymodiolus" childressi* over 395-day PLD.

CHAPTER 3

RELATVE STRENGTH OF LARVAL DISPERSAL PATHWAYS AND POPULATION CONNECTIVITY AMONG DEEP-SEA METHANE SEEP INVERTEBRATES

ABSTRACT

This study assessed the influence of larval behavior and pelagic larval duration (PLD), as well as spawning location in the Gulf of Mexico and Western Atlantic, on the relative strength of larval dispersal and population connectivity among four species of methane seep invertebrates: (1) the deep-sea polychaete, *Lamellibrachia luymesi*, (2) gastropod, *Bathynerita naticoidea*, and (3) crustacean, *Alvinocaris muricola*, and (4) the mollusk *"Bathymodiolus" childressi*. There were marked differences in the strength of larval dispersal pathways, as demonstrated by Lagrangian Particle Density Functions (LPDFs) among the different species and release sites, with a majority of larval particles remaining near their natal site. The LPDF trajectories of particles released from the northern Gulf of Mexico with surface seeking "*B." childressi* behavior (Simulation 3) readily dispersed throughout the eastern GOM and into the US Western Atlantic. Conversely, *L. luymesi* and "*B." childressi* (Simulation1) demersal drifting particles were spatially constrained to the northern and western GOM, with no connection to the Western Atlantic. The majority of *A. muricola* and *B. naticoidea* particles released from Blake Ridge and Cape Fear in the South Atlantic dispersed south of the release sites along the shelf-break depth contour to the Caribbean. Patterns of population connectivity varied greatly among species, with the greatest amount of connectivity for *B. naticoidea* and *A. muricola*, and the least amount of

connectivity exhibited by surface-seeking *"B." childressi* and *L. luymesi*. Generally, the connectivity matrices indicate that species with broad dispersal will have relatively low connectivity than those with more limited dispersal. Despite the extensive dispersal of particles, there was no other degree of connectivity. These results are the first known attempt to integrate empirical observations of invertebrate seep larvae into a biophysical model to assess dominant dispersal pathways and population connectivity. The findings highlight the importance of larval behavior and spawning location on the spatial scales of dispersal and population connectivity.

KEYWORDS

Biophysical model, population connectivity, larval dispersal, methane seep

INTRODUCTION

Larval dispersal can be a fundamental driver of population dynamics and biogeography in marine systems (Palumbi 2004, Treml et al. 2012, Lester et al. 2007, Botsford et al. 2009, and Kough and Paris 2015). Population connectivity, the exchange of individuals among populations, can affect genetic composition, as well as the dynamics of local populations and communities (Cowen et al. 2007, Cowen and Sponagule 2009, Treml et al. 2012, Puckett et al. 2014). Depending upon a particular species' life history characteristics, the scale of larval dispersal can range from a few meters over a pelagic larval duration (PLD) of a few days, to thousands of kilometers over a PLD of several months (Kinlan and Gaines 2003). Spatiotemporal variation in the strength of connectivity among subpopulations in a metapopulation can be relatively high. For instance, metapopulation dynamics driven by subpopulation-scale demographic rates such as growth and spawning output, or driven by larval connectivity among subpopulations (Puckett and Eggleston 2016 and references therein).

Methane seeps and hydrothermal vents are distributed globally, but population connectivity among these chemosynthetic communities by benthic invertebrates is poorly understood (Metaxas 2011). Many of these populations rely on a dispersive larval phase to maintain populations. Studies of hydrothermal vent communities show that new vent habitats are colonized by non-local larval sources after catastrophic eruptions (Tunnicliffe et al. 1997, Mullineaux et al. 2010), yet are maintained by local larval sources during periods between eruptions (Metaxas 2004, Adams and Mullineaux 2008). The extent of larval

retention and dispersal are influenced by larval behavior, as well as local and regional hydrodynamics (Marsh et al. 2001, Metaxas 2004, McGillicuddy et al. 2010).

Deep-sea, chemosynthetic communities are unique compared to shallow-water ecosystems because of their global, yet patchy distribution, as well as the nutritional dependence of many of the sessile invertebrates that form these communities on methanogenic bacteria as an energy source (Childress et al. 1986, Pile and Young 1999). Previous studies on hydrothermal vents have determined that effective dispersal is dependent on factors such as the rapid colonization of new vents by invertebrates following major eruptive events (Shank et al. 1998), as evident in cohorts of distinct age-classes (Van Dover et al. 2002). Moreover, the occurrence of seep species of mollusks, crustaceans, and other taxonomic groups across the Atlantic Ocean suggest broad connectivity (Olu-LeRoy et al. 2007, Cordes et al. 2007). Molecular *mt*COI phylograms for the deep-sea mussel *"Bathymodiolus" childressi*, suggest contemporary gene flow and population connectivity across known deep-water seeps in the southeastern Caribbean, central and eastern Gulf of Mexico and along the Western Atlantic (Cordes et al. 2007). In contrast, the deep-sea amphipod *Ventiella sulfuris* shows strong allozyme isolation at spatial scales of a few hundred meters, likely due to the way in which it broods eggs and has a limited PLD (France et al. 1992, Virjenhoek 1997).

It is difficult to directly observe deep-sea larvae because they are relatively small and difficult to track in the water column throughout their PLD in the water column. Therefore, biophysical modeling techniques can be useful ways to help biological oceanographers predict the strength of larval dispersal and population connectivity (Puckett et al. 2014, Qian

et al. 2015), pending subsequent validation via molecular or geochemical techniques (Carney et al. 2006, Thaler et al. 2011, Kroll et al. 2016).

Larval behavior and dispersal physiology are key factors controlling population connectivity. Behavior such as vertical migration, dispersal depth, and PLD strongly influence the strength and spatial scales of population connectivity over time (Paris and Cowen 2004, Puckett et al. 2014). Initially it was believed that deep-sea larvae dispersed only in deep currents, however, recent studies suggest that deep-sea larvae of both hydrothermal vents and methane seeps disperse in near-surface waters (Young et al. 2012, Arellano et al. 2014).

It is critical to understand the population connectivity of deep-sea methane seep larvae to gain insight into the dominant transport mechanisms in the region. The Gulf of Mexico (GOM) is a semi-closed sea in the western Atlantic Ocean and hydrodynamically connects to the Western Atlantic via the Gulf Stream. The dominant near-surface currents include the Yucatan Current, which then becomes the Loop Current in the GOM, and finally forms the Florida Current and Gulf Stream as it flows at speeds of 2 m s^{-1} out of the GOM (Oey 2005). This circulation pattern is an integral part of the western boundary current in the North Atlantic Subtropical Gyre, as it transports water, heat, salt and nutrients throughout the region. In contrast, the deep-sea currents exhibit cyclonic flow, with deep current water flowing south from the Western Atlantic in a counter clockwise fashion at a rate of 5-10 cm s^{-1} (Oey 2012). Near surface in the GOM is more variable with the Loop Current reaching depths up to 900 m in some areas in the eastern GOM and frequently changing flow patterns and variable current speeds of 0.2 m s^{-1} (Weatherly et al. 2005).

Population connectivity of invertebrates in the deep sea is limited by a dearth of observations and empirical data on: (i) larval distributions in the water column, (ii) larval behavior, and the (iii) timing and locations of spawning. The purpose of this study is to assess the influence of larval behavior and PLD, as well as spawning location and timing, on the dominant pathways and potential connectivity among methane seeps in the GOM and Western Atlantic Ocean. Four species of seep invertebrates with varying larval behaviors and PLDs are examined: (1) the deep-sea polychaete, *Lamellibrachia luymesi*, (2) gastropod, *Bathynerita naticoidea*, and (3) crustacean, *Alvinocaris muricola*, and (4) the mollusk *"Bathymodiolus" childressi*.

MATERIALS AND METHODS

The relative strengths of larval dispersal pathways and sub-population connectivity among four species of methane seep invertebrates, across five methane seep sites spanning the Gulf of Mexico, Caribbean and US Western Atlantic, were characterized with a biophysical model. Statistically comprehensive Lagrangian probability density functions (LPDF, Mitarai et al. 2009) and connectivity matrices were used to characterize the dominant dispersal pathways, sources, and destinations of particles in the *USEast* hydrodynamic model domain.

Model Setup

The *USEast* climatological model was developed by the Ocean Observing and Modeling Group at North Carolina State University (R. He et al. *under review*) and covers the entire Gulf of Mexico, U.S. South Atlantic, Mid-Atlantic and North Atlantic Bights, northwest Atlantic Ocean, as well as the Sargasso, and Caribbean Seas (Fig. 1). The Hybrid Coordinate Ocean Model (HYCOM) specified initial and open boundary conditions of

satellite observed SST, salinity, and daily circulation patterns at 10 km spatial resolution (http://hycom.rsmas.miami.edu/dataserver). The National Center for Environmental Prediction (NCEP) provided the surface atmospheric data, which has a spatial and temporal resolution of 1.875^{o} and 6 hours, and used to drive the *USEast* model. The ocean circulation model was driven by factors such as: total cloud cover, precipitation, surface pressure, relative humidity, air temperature, surface wind, and net shortwave and long-wave radiations (Fairall et al. 2003) to derive wind stress and net surface heat flux. *USEast* was coupled with a Lagrangian particle tracking model (LTRANS) to track the position of larval particles released from five methane seep sites that are a part of a broader study of population connectivity among seep sites (*SEEPC* Collaborative Research Program <www.cmast.ncsu.edu/seepc>): (1) Alaminos Canyon (26 21'17"N, 94 29'48" W), (2) Brine Pool (27 43'23"N, 91 16'30"W), (3) Florida Escarpment (26 1'48"N, 84 54'54"W, (4) Blake Ridge (32 29'45"N, 76 11'30"W), and (5) Cape Fear Diapir (32 58'45"N, 75 55'30"W) (Fig. 1). The seeps were chosen because they provide a means to study connectivity on spatial scales that match those at which vent systems are being studied (Hurtado et al. 2004) and include species that span large depth and geographic ranges and have diverse life-history characteristics.

Particle–tracking, LPDFs, and Connectivity Matrices

The **L**agrangian **TRANS**port model (LTRANS) is an offline particle-tracking model with a fourth-order Runge-Kutta tracking scheme for particle advection (North et al. 2006). LTRANS was used to quantify the LPDFs (see description below) and connectivity matrices

for four invertebrate species, each with their own larval behavior characteristics of (i) swimming speeds, (ii) vertical distribution in the water column, and (iii) PLD: *Lamellibrachia luymesi*, *Bathynerita naticoidea*, *Alvinocaris muricola*, and *"Bathymodiolus" childressi*. The larval particle simulations for *L. luymesi*, *B. naticoidea*, and *A. muricola* included the release of 10 larval particles every three hours from each of five seep sites, for a total of 30,000 particles per species simulation per site. The simulations for "*B." childressi* are described in Chapter 2, and included three possible behavioral scenarios. In scenarios two, and three, "*B." childressi* spawning time and date was restricted to simulate observed spawning (C. Young *personal observation*). In Simulation 1, 10 particles were released every three hours for a total of 30,000 particles exhibiting bottom following behavior (i.e., no more than two meters above bottom). In scenarios two and three included the release of 480 particles every three hours during the first week of October for a total of 15,000 particles per site and varied time spent dispersing in surface waters (Table 2). Although the effects of larval behavior and spawning location on potential *"B." childressi* larval dispersal and population connectivity are described in Chapter 2, the LPDF and connectivity matrices for this species are unique to this chapter.

The dispersal paths were quantified using Lagrangian probability functions (LPDFs), which is defined as the probability density of particle displacement (Mitarai et al. 2009):

$$f'_X(\varepsilon;\ \tau, a) = \frac{1}{N}\sum_{n=1}^{N} \delta(X_n(\tau, a) - \ \varepsilon) \qquad (1)$$

Where τ is the advection time scale, ε the space variable, a, the initial position, and the position of the nth particle ($X_n(\tau, a)$), N is the total number of Lagrangian particles, and δ is the Dirac delta function. The Dirac function is defined as the Heaviside function H in a unit

area ($\delta = \frac{dH}{dxdy}$), where H is the unit step function, such that $H(x) = \begin{cases} 0 \; if \; n \; < x \\ 1 \; if \; n \; \geq x \end{cases}$, where n is the grid number integer on the x axis. LPDFs describe the probability density function of particle displacement for a given advection time τ. LPDFs can be utilized to describe expected dispersal patterns using a connectivity matrix, which describe the probability for the event that a particle is transported from site *j* to site *i*. LPDF data for each species simulation from the five methane seep sites were analyzed and quantified in MATLAB (version 2014b).

The latitude and longitude of a particle's position on the last day of its PLD was used to determine if settlement occurred within a 10 km radius for each of the five seep sites, which was then compiled to establish connectivity matrices for each species. Connectivity, $C_{j,i}$, is defined as the probability of a particle moving from source *j* to destination *i* over time interval τ. For a given source location, x_i, and destination location, x_i, the value of $C_{j,i}$ can be defined as:

$$C_{j,i}(\tau) = f_x(\varepsilon = x_i; \tau, \alpha = x_j)(\pi R^2) \quad (2)$$

The data were used to determine the percent of particles settling in a 5 x 5 connectivity matrix, with the exception of *L. luymesi* and *"B." childressi* (simulations 1, 2, and 3), which were released in three out of the five study sites. This is because *L. luymesi* has not been found in the Western Atlantic, and it is not known if recovered mussels from South or Mid Atlantic Bight seeps are actually *"B." childressi*. As a result, particles with *L. luymesi* or *"B." childressi* behavior were not released from Blake Ridge or Cape Fear Diapir.

Larval Particle Behavior

Larval behaviors, such as swimming speed, planktonic larval duration, and vertical distribution in the water column, were determined with a combination of published literature (Young et al. 1996, Van Gaest 2006, Arellano 2008, Young et al. 2012), shipboard observations of larvae, and zooplankton tows while at sea. Planktonic larval durations (PLDs) used in our simulations were determined with a combination of published literature (Young et al. 2012, Arellano 2008, Van Gaest 2006, Young et al. 1996), personal observations, and zooplankton tows using a MOCNESS while at sea. In many cases, PLD was estimated by comparing larval size and known spawning dates of our study species. For example, the gastropod, *B. naticoidea* has an estimated PLD of four months based on morphology of larvae obtained from MOCNESS tows, and has been found at thermocline depths of ~ 100 m (Fig. 2; Young et al. 2012). The larvae of the polychaete, *L. luymesi* have been cultured in laboratories and cold rooms with an estimated PLD of three weeks, and found at thermocline depths of 8^{o}C and 250 meters depth (Fig. 2; Young et al. 2012). Studies of metabolic rates for the chemosynthetic tubeworm, *L. luymesi* larvae also confirm a three-week, lecithotrophic larval period (Leong 1998). *L. luymesi* populations appear to be confined in the Gulf of Mexico due to their relatively short PLD (Young et al. 1996), which is why *L. luymesi* larval dispersal simulations were not released from Blake Ridge or Cape Fear seep sites in the South Atlantic Bight (see below). The deep-sea shrimp, *A. muricola* has an estimated PLD of six months, and disperses near the surface (~100 m to 0 m) (Fig. 2; Nye et al. 2013). In this case, PLD is based on the estimated PLD of other Alvinocarid species,

however, this genus has several dispersal strategies, extended PLDs, and their dispersal depth is not yet fully known (Nye et al. 2013)

The *"Bathymodiolus" childressi* species are found throughout the Gulf of Mexico and Western Atlantic, and at depths from 200 m to more than 3,000 m (Gustafson et al. 1998, Carney et al. 2006, Tyler et al. 2006 and *personal observations*). Molecular phylogeny analysis of "*B." childressi* indicates uncertainty about its taxonomic status, and so followed the recommendation of Jones et al. (2006) and used quotation marks around the genus name. Planktonic larval durations used in our simulations were determined using the best available information from a combination of published literature (Young et al. 2012, Arellano 2008, Van Gaest 2006, Young et al. 1996), personal observations, and zooplankton tows using MOCNESS while at sea. Based on these observations, three possible larval dispersal strategies (simulations) were evaluated: (1) demersal drift of larvae with a PLD of 395 days, (2) variable larval vertical distribution with near surface dispersal, and (3) variable larval vertical distribution with near-surface dispersal.

(1). Protracted spawning and demersal drift. -- The first simulation included the release of 10 larval particles every three hours from three seep sites, for a total of 10,000 particles per species simulation per site in Mid-October. The particles were programmed with demersal drift behavior, which meant all particles stayed within three meters of the sea floor throughout the 395-day PLD (Fig. 2).

(2). Discrete spawning and variable larval vertical distribution with near surface dispersal. -- In the second simulation, 20 particles were released every hour for a total of

14,880 particles released over the period of a week in Mid-October. The behavioral assignments for the larval particles released in Mid-October are extremely specific to match very precise observations of "*B." childressi* larvae over the course of their larval life (*personal observation* and C. Young *personal observation*). Particles were programmed to exhibit no behavior the first two days, followed by weak upward swimming behavior at 0.02 cm s^{-1} from day three to ten. On the tenth day, swimming speed increased to 0.2 cm s^{-1} until particles reached near surface (<100 m). Particles dispersed at near surface for 175 days, and programmed to swim down to the sea floor at 0.2 cm s^{-1} to arrive on bottom by 185^{th} day of their PLD. Particles then drifted within three meters above bottom until the end of the 395-PLD (Fig. 2).

(3). Discrete spawning and variable larval vertical distribution with near-surface dispersal. -- In the third simulation, the programmed spawning occurred in the same manner as described in Simulation 2. Particles exhibited no behavior the first two days, followed by weak upward swimming behavior at 0.02 cm s^{-1} from day three to ten. On the tenth day, swimming speed increased to 0.2 cm s^{-1} until particles reached near surface (<100 meters). There, particles dispersed in surface waters for 385 days, and started swimming down to the sea floor at 0.2 cm s^{-1} in order arrive on bottom by the end of the 395-PLD (Fig. 2).

Hypotheses and Statistical Analyses

I hypothesized that seep species whose larvae had a relatively long PLD and surface seeking larval behavior, would display the greatest level of connectivity, regardless of release site, while particles with low PLD and non-surface seeking behavior would have greater levels of retention. I tested the main and interactive effects of: (1) spawning site, (2) particle behavior,

and (3) PLD on two response variables: (i) LPDFs, and (ii) connectivity between five methane seep sites. LPDFs and connectivity matrices for each species were analyzed using MATLAB (2014b).

RESULTS

Lagrangian Particle Density Functions

There were striking differences in LPDFs among species, larval behavior, and release sites, with a majority of larval particles remaining near their natal site. *A. muricola* and *B. naticoidea* larval particles released from the Alaminos Canyon and Brine Pool sites in the western Gulf of Mexico have the potential to connect with sites in the Western Atlantic Ocean (much less so for *B. naticoidea*), however, it is a weak connection (Fig. 3 and 4). LPDF trajectories for *L. luymesi* and "*B." childressi* Simulation 1 were spatially constrained to the northern and western GOM, with no connection to the Western Atlantic (Fig. 3). Conversely, particles for "*B." childressi* Simulation 2 and 3 readily dispersed throughout the eastern GOM and into the US Western Atlantic, with relatively stronger LPDFs for "*B." childressi* Simulation 2 near their natal sites, as well as off northern Florida, and the central Caribbean (Fig. 3). Note that LPDF quantifies the probability of particles moving through a grid cell in the domain over the course of their PLD, which is distinct from only analyzing dispersal trajectories.

Particles released from Brine Pool, which is located 150 km east of Alaminos Canyon and in shallower water (2200 m vs. 660 m, respectively), displayed dispersal patterns similar to particles released from Alaminos Canyon in the GOM (compare Figs. 3 & 4). Highest

LPDFs occurred near natal sites, irrespective of invertebrate species, with *A. muricola, L. luymesi* and *"B." childressi* Simulation 1 restricted to the GOM, and relatively weak dispersal by *B. naticoidea* and *B." childressi* Simulations 2 and 3 to the Western Atlantic (Fig. 4).

For particles released from Florida Escarpment, located in the eastern GOM and in relatively deep (3300 m) water, there were stronger LPDFs to the Western Atlantic than for particles released from Alaminos Canyon and Brine Pool (compare Figs. 3-5). *A. muricola, B. naticoidea*, and *"B." childressi* simulations 2 and 3 displayed relatively strong LPDFs in the Western Atlantic (Fig. 4). The LPDF trajectories for "*B." childressi* simulations 2 and 3 had relatively high probability of connecting to Blake Ridge and Cape Fear Diapir seep sites in the Western Atlantic (Fig. 5). In contrast, particles of "*B." childressi* Simulation 1 were restricted to the GOM, likely by deep cyclonic currents in the GOM, and there was minimal dispersal of *L. luymesi* particles to the northern region of the Caribbean. There is no available documentation to show if *L. luymesi* tubeworms reside in the northern Caribbean. While other species of tubeworms are known to exist in the Barbados-Accretionary Prism, *L. luymesi* has not been found in the Caribbean.

LPDF results of *A. muricola* released from Blake Ridge and Cape Fear show that the majority (10%) of particles disperse south (this would suggest deep water circulation) of the release sites along the bathymetric contour depth contour to the Caribbean, as well as dispersing north into the central region of the Atlantic where there are no known methane seeps (compare Figs. 6A and 7A). The trajectory results of *B. naticoidea* particles released from Blake Ridge and Cape Fear show a similar north-south trajectory of particles to those

displayed by *A. muricola*, yet with reduced spatial spread of particles (compare Figs. 6B & 7B).

Connectivity Matrices

A connectivity matrix for a given seep species was quantified using the LPDFs for a given larval destination and source location. This matrix illustrates the degree to which any two sites among all possible locations are connected over a particle's PLD. Connectivity matrices were generated for each of the seep invertebrate species, as well as *"B." childressi* simulations 1-3 (Fig. 8). Overall, self-recruitment dominates regardless of PLD, although there are moderately strong connections between GOM sites (i.e. Florida Escarpment) and the Western Atlantic (Cape Fear Diapir) for particles with *B. naticoidea* behavior. The connectivity patterns between the four species varied, with the least amount of connectivity exhibited by *"B." childressi* simulations 2 and 3, and the greatest amount of connectivity by *B. naticoidea* and *A. muricola*. The connectivity matrix for *Alvinocaris muricola* shows weak self-recruitment at Alaminos Canyon and limited connectivity between Alaminos Canyon and Brine Pool, as well as limited connectivity between Alaminos Canyon and Florida Escarpment (Fig. 8). Similarly, connectivity at Brine Pool revealed similar results to Alaminos Canyon, with weak connectivity to Florida Escarpment and limited self-recruitment. Connectivity among seep sites for particles with *A. muricola* behavior released from Blake Ridge exhibited weak signs of self-recruitment, while particles released from Cape Fear displayed a relatively weak connection to Blake Ridge. Connectivity analysis of *B. naticoidea* shows weak self-recruitment at Alaminos Canyon and limited connectivity

between Alaminos Canyon and Brine Pool (Fig. 8). Similarly, connectivity at Brine Pool showed weak connectivity with itself and Florida Escarpment. Particles released from Florida Escarpment also had limited self-recruitment and a weak connection to Cape Fear. *B. naticoidea* particles released from both Blake Ridge and Cape Fear had weak self-recruitment. Connectivity analysis of *L. luymesi* shows no connectivity in the GOM and only self-recruitment with Alaminos Canyon and Florida Escarpment (Fig. 8), although less than one percent of particles successfully settled. Connectivity matrix analysis of *"B." childressi* Simulation 1 shows strong self-recruitment at Alaminos Canyon (Fig. 8); however, particles released from Brine Pool and Florida Escarpment had no connectivity. Connectivity matrix analysis of *"B." childressi* Simulation 2 shows weak self-recruitment at Alaminos Canyon and limited connectivity between Brine Pool and Florida Escarpment (Fig. 8). Despite the extensive dispersal of particles, no other sites exhibited any degree of connectivity. Connectivity matrix analysis of *"B." childressi* Simulation 3 shows weak self-recruitment at Alaminos Canyon and limited connectivity between Alaminos Canyon and Brine Pool, as well as between Alaminos Canyon and Florida Escarpment (Fig. 8), while no other sites exhibited connectivity.

DISCUSSION

This study provides the first characterization of the relative strength of larval dispersal and population connectivity of deep-sea, methane seep invertebrates that is currently in the literature. This study combined ocean circulation and Lagrangian particle-tracking models, with empirical data on larval PLD, swimming speed and vertical distribution in the water

column, to address two fundamental challenges to our understanding of population connectivity: (i) spatial scales of connectivity in the deep sea, and (ii) mechanisms underlying potential connectivity for deep-sea invertebrates. Particles were programmed with species-specific behavior that corresponded to four seep species: *A. muricola*, *B. naticoidea*, *L. luymesi*, and *"B." childressi*, and tracked for five years among five methane seep sites in the GOM and Western Atlantic Margin to determine the dominant dispersal pathways and strength of potential population connectivity in the domain. Interestingly, particles that exhibited broad dispersal behavior had more limited connectivity than those with more limited dispersal, which initially contrasts the notion that greater dispersal enhances potential connectivity. Future research should focus on simulating the total number of methane seeps available in the GOM and WAM to understand the level of connectivity in seep areas as well as discrete seeps. The climatological conditions of the model domain provide an ideal method to understand dispersal patterns under average meteorological conditions. Although data on larval biology of deep-sea invertebrates is very limited, species-oriented studies that focus on behavior (e.g., Young et al. 1996a, Young et al. 1996b Arellano et al. 2014), coupled with ocean circulation models (Cowan et al. 2006, Kough et al. 2013, R. He, unpubl. data), can provide valuable predictions of larval dispersal and population connectivity of methane seep and other unique deep-sea communities.

Caveats

The *USEast* model domain has the capacity to track particles over large areas of the Gulf of Mexico and Western Atlantic Ocean, which provides a convenient platform to study the large-scale dispersal patterns and connectivity of larval particles. The climatological

model is limited by grid scale of 7-10 km, which also corresponded to the size of the grid cell for particles to successfully settle in one of our known seep sites. This somewhat coarse spatial resolution is a necessary trade-off for the immense spatial domain in this study (over 1,000,000 km^2). While the methane seep sites (Alaminos Canyon, Florida Escarpment, etc.) are not 10 km wide, there are several adjacent methane seep communities that make the results biologically relevant. The strength of the connectivity for some species is very weak and low probability of such an occurrence. For example, the strongest connectivity of particles with *"B." childressi* Simulation 3 behavior was 0.03%, while the weakest was 0.0068%. If 14,880 particles are released from a site, then a minimum of 150 particles must successfully settle to reach 1% connection rate. While the probabilities are low, it does not mean that the particles are not settling in other areas where methane seep communities exist. In contrast, the connectivity strength for *"B." childressi* Simulation 1 had 37% self-recruitment with particles released from Alaminos Canyon. Therefore, care should be taken when interpreting the connectivity matrices and the probabilities of particles with a given behavior connecting to another site.

Potential Role of Varying Hydrodynamics on Patterns of Larval Dispersal

The LPDF results highlight the dominant dispersal pathways of larval particles, and while variation exists for each species, there are similar patterns. Based on the LPDF results, eddy shedding likely plays a critical role in the dispersal patterns observed in the GOM for particles with thermocline and near surface seeking behavior, particularly in the western region. Particles released in the western GOM from Alaminos Canyon generally remained in

the region, with many dispersing in an ellipsoid manner over the release site and circling either southeast or southwest. Particles released from Alaminos Canyon also had the highest levels of self-recruitment for all species (*L. luymesi, B. naticoidea, A. muricola,* and *"B." childressi* simulations 1, 2, and 3). These dispersal patterns are likely caused by eddies which shed from the Loop Current, which can separate from the Loop Current at random intervals and drift west (2-5 km/day), and can be 200-400 kilometers in diameter and extend down to 1000 meters (Mooers 1998, Sturges and Leben 2000, Oey et al. 2005). Loop Current Frontal eddies may also have an impact on the dispersal patterns observed in the GOM. For example, cold core cyclonic eddies are approximately 120 kilometers in diameter and typically smaller than the warm core eddies mentioned above (Oey et al. 2005). Therefore, eddies may affect the dispersal direction of particles, as well as influence abiotic factors such as temperature and food availability for larvae. Surface winds also exhibit seasonal variability, which may affect dispersal patterns of particles with surface-seeking behavior and with a PLD of greater than 30 days (Morey et al. 2005). It should also be noted that the upper layer mean flow in the central and northwestern GOM is anticyclonic, while the mean flow below 1000 m is cyclonic. The particle trajectories, particularly the higher self-recruitment from Alaminos Canyon, potentially show the strong effect of eddies with their entrenchment in the western GOM over several months. The model accurately represents eddies at spatial scales >10 km, and it is important to recall that climatological models show seasonal timescales, where changes in eddy patterns can occur. Similarly, particles released from Blake Ridge and Cape Fear may circulate in both cylonic and anti-cyclonic eddies off of the Gulf Stream, showing

that the hydrography of a region is intimately linked to the dispersal patterns of marine larvae.

Particles released from Brine Pool, (shallowest site in this study at 660 m) dispersed east and west of the release site, which was an interesting distribution pattern when compared to other sites with more unidirectional particle dispersal. The particles are likely interacting with eddies shedding off the loop current, as well as river run off from the Mississippi, surface wind driven currents, and the GOM Loop Current. This dispersal pattern may partially be caused by the seasonal variation in the Loop Current that can push deep currents into the GOM near Louisiana's coast before continuing through the Florida Strait. When this pattern occurs, the main current passes very close to Brine Pool, which may explain the observed east and west dispersal patterns in the model domain (DeHann and Sturges 2005).

Florida Escarpment (the deepest site in this study at 3,500 m) is situated at the base of the Florida Platform, where depth changes dramatically from 91 m to 3,500 m. The pressure forced upon the West Florida Shelf by the Loop Current generates a current flowing south that is also driven by the steep topography of the Escarpment. The deep currents near Florida Escarpment form a cyclonic flow, thus, the near surface dispersing particles traveled south through the Florida Strait while near bottom dispersing particles had a northern trajectory. Demersal drifting particles were subjected to the cyclonic flows of the deep currents, which have a mean velocity of 0.5 cm s^{-1}, which is several orders of magnitude slower than the surface current mean velocity of 16 cm s^{-1} (DeHann and Sturges 2005).

In the Western Atlantic Margin (WAM), Blake Ridge and Cape Fear are in relatively close proximity (80 km apart) within the South Atlantic Bight. The Gulf Stream flows from

the south and delivers a constant succession of both cyclonic and anti-cyclonic eddies that peel off the Gulf Stream and travel either west towards land or east to open Atlantic. Coupled with the North Atlantic Gyre, which flows cyclonically from north to south, the near surface waters of the WAM are generally flowing from south to north (McCartney 2003). The deeper waters are exposed to the Deep Western Boundary Current (DWBC), which transports cold arctic water south along the WAM (Dengler et al. 2004). Therefore, particles released from sites in the WAM are first exposed to the DWBC and if they disperse near the surface, many are carried north by the Gulf Stream. Surprisingly, the majority of particles had a 10% probability of dispersing south of the release site, even though both *A. muricola* and *B. naticoidea* drift near the surface and thermocline, respectively. Both Blake Ridge and Cape Fear are on the outer edge of the Gulf Stream, therefore, these particle trajectories are possibly caused by cyclonic counter currents adjacent to the Gulf Stream. It is also possible that the strength and position of the counter currents in the model domain are slightly different than observed patterns, and further research is needed to continue validating the physical characteristics of such a large and relatively new domain.

Comparison and Contrast with Hydrothermal Vents and Shallow Ecosystems

Connectivity in the deep-sea is little studied due to the inherent challenges and difficulties of observing organisms *in situ* over long periods of time. A review by Virjenhoek (2010) assessed the factors regulating connectivity for hydrothermal vents, with the population genetic data of nearly 30 vent species. The bivalve *Bathymodiolus thermophilus* has small (~50 μm), planktotrophic larvae that have very high rates of gene flow in certain regions of

the Galapagos Rift (Lutz et al. 1979, Virjenhoek 2010). In contrast, the clam *Calyptogena magnifica* produces larger lecithotrophic larvae that would be expected to have limited dispersal, yet gene flow is high (>200 km; Lutz et al. 1986). Similar to our study, methane seep species such as *"B." childressi* and *L. luymesi* have very different biological characteristics and potential dispersal distances (*L. luymesi* 171 km vs. 328 km *"B." childressi* Simulation 2 released from Alaminos Canyon), and yet both are found throughout the GOM. The strength of self-recruitment for both species is very similar, which suggests that self-recruitment can happen over PLDs of 21 to 395 days and scales of 171 to 328 km. The large variation in dispersal strategy, yet similar levels of connectivity between these species, highlights the need for more research on the biophysical factors regulating dispersal in the ocean, particularly for deep-sea invertebrates.

In a recent study by Mitarai et al. (2016), the dispersal potential of hydrothermal vent particles in the Pacific Ocean was assessed with a variety of PLDs, but did not include other biological parameters (e.g. larval swimming speeds and vertical distributions). Their model results show high connectivity within hydrothermal vent basins (>300 km) without clear directionality to particle dispersal patterns; however, basin-to-basin dispersal (>1,000 km) appears more infrequent with strong directionality associated with the major currents. Integration of biological parameters into the model by Mitarai et al. (2016) will likely enhance the accuracy of predictions concerning larval dispersal and population connectivity among invertebrates inhabiting hydrothermal vent systems.

There is a much better understanding of the relative strength of larval dispersal and population connectivity in shallow coastal and estuarine systems than in the deep-sea. For

example, a model accurately simulated the larval dispersal of the mussel, *Mytilus edulis* along the California coast which matched the observed dispersal patterns, such as the general patterns of larval transport, scale of dispersal (approximately 30 km), and isolation areas created by physical barriers (Glig and Hilbish 2003). A recent study used a biophysical model to predict meta-population connectivity of the intertidal barnacle *B. glandula* and compared the model results of connectivity with molecular data to investigate factors influencing dispersal (Galindo et al. 2010). The authors conclude that small-scale changes that enhance greater local retention over approximately 15 km successfully predict the observed genetic patterns, and list two factors that may be important to enhance the accuracy of larval simulations: increased local retention and long distance dispersal. The study also highlights the challenges of missing data, both physical and biological, and that modeling is not at a level that can precisely imitate field conditions. In estuarine systems, Hedgecock et al. (2007) found genetic patchiness within an oyster population at spatial scales of 69 km, and Puckett et al. (2014) found that oyster larvae had a mean dispersal distance from 2 to 75 km over a 21-day PLD with the immigration of particles into other many oyster sub-populations.

The limited empirical data in our study makes it difficult to determine the model's accuracy, however the overall dispersal strength, connectivity, and influence of hydrodynamics on larval particles does have some similarities with shallow water results. Both shallow and deep systems show a degree of self-recruitment, connectivity with other sites, and dispersal distances that correspond to their PLD and position in the water column (Cowen et al. 2007, Botsford et al. 2009, Galindo et al. 2010). These studies highlight the

need for increased integration of population genetic data, physical oceanography, and biology in connectivity research in both shallow and deep-water communities.

Future Research

Previous research indicates that marine larvae have relatively high plasticity in their PLD, which can have a strong effect on potential connectivity (Hadfield and Strathmann 1996, Bradbury and Snelgrove 2001, Green and Fisher 2004, Oyarrzun et al. 2011, C. Young *personal communication*). Within physiological limits, larvae can delay settlement until they encounter suitable habitat, or respond to physical cues such as temperature, turbulent shear, biological sounds, or chemical sensors such as sulfide (Gaylord et al. 2013, Lillis et al. 2013). If particles with *B. naticoidea* behavior have the ability to settle on benthic habitat for up to 10 days before the end of their 90-day PLD, the connectivity matrix changes, with more particles encountering and connecting with one of the five seep sites than with a fixed PLD (Appendix 6). It should be noted that 10 days is a conservative value, as some deep-sea larvae have the ability to settle several weeks before their known PLD (C. Young, *personal communication*). Future research should explore how varying PLD within a given seep species affects potential population connectivity. Based on the results from this study, the following hypotheses could be tested regarding the genetic relatedness of four seep invertebrates examined in this study: (1) are the individuals of *"B." childressi* in the Gulf of Mexico one open population, and how does the genetic relatedness compare with *"B." childressi* mussels found in the WAM? (2) Does *L. luymesi* exist in the Caribbean, or does it exist anywhere else outside of the Gulf of Mexico? If *L. luymesi* only exists in the GOM, how genetically isolated are the populations? (3) *A. muricola* is found throughout the

Caribbean, GOM, and WAM; is this an open, connected population? Or, are there physical barriers that prevent the flow of larvae into the Caribbean, GOM, or WAM? (4) *B. naticoidea* is closely associated with *"B." childressi*, but basic genetic data is lacking. Are the gastropods one species, is the species *B. naticoidea*, and are they found in all seeps that contain *"B." childressi*? Exploring these hypotheses can provide greater insight into the biophysical processes driving connectivity patterns for four dominant species commonly found in methane seeps.

ACKNOWLEDGEMENTS

Special thanks to the crews of the *R/V Cape Hatteras, Pelican, Endeavor,* and *Atlantis* for their expertise while at sea, as well as the engineering teams of *Alvin* and *Sentry*. We are also grateful to A. Todd and S. Ricci for their technical support with this project. The funding for this project was provided by NSF OCE-1031050.

REFERENCES

Adams, T.P., R. Proud, K.D. Black. 2015. Connected networks of sea lice populations: dynamics and implications for control. *Aquacult Environ Interact* 6: 273-284.

Adams, D.K., and L.S. Mullineaux. 2008. Supply of gastropod larvae to hydrothermal vents reflects transport from local larval sources. *Limnol and Oceanog* 53(5): 1945-1955.

Arellano, S.M., A.L. Van Gaest, S.B. Johnson, R.C. Vrijenhoek, and C.M. Young. 2014. Larvae from deep-sea methane seeps disperse in surface waters. *Proc R Soc B* 281: 20133276.

Arellano, S.M. 2008. Embryology, larval ecology, and recruitment of *"Bathymodiolus" childressi*, a cold seep mussel from the Gulf of Mexico. Dissertation University of Oregon.

Beedessee G., H. Watanabe, T. Ogura, S. Nemoto, T. Yahagi, S. Nakagawa, K. Nakamura, K. Takai, M. Koonjul, D.E.P. Marie. High connectivity of animal populations in deep-sea hydrothermal vent fields in the central Indian Ridge relevant to its geological setting. *Plos One* 8(12): 1:-11.

Bradbury I.R, and P.V.R. Snelgrove. 2001.Contrasting larval transport in demersal fish and benthic invertebrates: the roles of behaviour and advective processes in determining spatial pattern. *Can J Fish Aquat Sci* 58:811–823.

Botsford, L.W. J.W. White, M.A. Coffroth, C.B. Paris, S. Plines, T.L. Shearer, S.R. Thorrold, G.P. Jones. 2009. Connectivity and resilience of coral reef metapopulations in marine protected areas: matching empirical efforts to predictive needs. *Coral Reefs* 28: 327-337.

Carney, S.L., M.I. Formica, H. Divatia, K. Nelson, C.R. Fisher, and S.W. Schaeffer. 2006. Population structure of the mussel *"Bathymodiolus" childressi* from Gulf of Mexico hydrocarbon seeps. *Deep-Sea Res I* 53: 1061-1072.

Childress, J. J., C.R. Fisher, J. M. Brooks, M. C. Kennicutt II, R. R. Bidigare, and A. E. Anderson. 1986. A methanotrophic marine molluscan (Bivalvia, Mytilidae) symbiosis: mussels fueled by gas. *Science* 233: 1306-1308.

Cordes, E. E., S. Carney, S. Hourdez, R.S. Carney, J.M. Brooks, and C.R. Fisher. 2007. Cold seeps of the deep Gulf of Mexico: community structure and biogeographic comparisons to Atlantic equatorial belt seep communities. *Deep Sea Research Part I: Oceanographic Research Papers* 54(4): 637-653.

Cowen, R.K., K.M. Lwiza, S. Sponaugle, C.B. Paris, D.B. Olson. 2000. Connectivity of marine populations: open or closed? *Sci* 287: 857-859.

Cowen, R.K., C.B. Paris, and A. Srinivasan. 2006. Scaling of connectivity in marine populations. *Sci* 311: 522-527.

Cowen, R.K., G. Gawarkiewicz, J. Pineda, S.R. Thorrold, and F.E. Werner. 2007. Population connectivity in marine systems. *Oceanog* 20(3):14-21.

Cowen, R.K., and S. Sponaugle. 2009. Larval dispersal and marine population connectivity. *Ann Rev Mar Sci* 1:443-466.

Dengler, M., Schott, F. A., Eden, C., Brandt, P., Fischer, J., & Zantopp, R. J. 2004. Break-up of the Atlantic deep western boundary current into eddies at 8 S. *Nature* 432(7020):1018-1020.

Eggleston, D.B., R.N. Lipcius, L.S. Marshall, S.G. Ratchford. 1998. Spatiotemporal variation in post larval recruitment of the Caribbean spiny lobster in the central Bahamas: lunar and seasonal periodicity, spatial coherence, and wind forcing. *Mar Ecol Prog Ser* 174: 33-49.

Fairall, C. W., E.F. Bradley, J.E. Hare, A.A. Grachev, and J.B. Edson. 2003. Bulk parameterization of air-sea fluxes: Updates and verification for the COARE algorithm. *J of Clim*, 16(4), 571-591.

France, S.C., R.R. Hessler, and R.C. Vrijenhoek. 1992. Genetic differentiation between spatially-disjunct populations of the deep-sea, hydrothermal vent-endemic amphipod *Ventiella sulfuris*. *Mar Biol* 114: 551-559.

Galindo H.M. A.S. Pfeiffer-Herbert, M.A. McManus, Y. Chao, and F. Chai. 2010. Seascape genetics along a steep cline: using genetic patterns to test predictions of marine larval dispersal. *Mol Ecol* 19:3692-3707.

Galindo, H.M., D.B. Olson, and S.R. Palumbi. 2006. Seascape genetics: a coupled oceanographic-genetic model predicts population structure of Caribbean corals. *Curr Biol* 16: 1622-1626.

Gaylord B, J. Hodin, and M.C. Ferner. 2013. Turbulent shear spurs settlement in larval sea urchins. *PNAS* 110: 6901–6906.

Gilg, M. R., T. J. Hilbish. 2003. The geography of marine larval dispersal: coupling genetics with fine- scale physical oceanography. *Ecol* 84: 2989–2998.

Gustafson, R.G., R.D. Turner, R.A. Lutz, R.C. Vrijenhoek. 1998. A new genus and five species of mussels (Bivalvia Mytilidae) from deep-sea sulfide/hydrocarbon seeps in the Gulf of Mexico. *Malacologia* 40: 63-112.

Green, B. S. and R. Fisher. 2004. Temperature influences swimming speed, growth and larval duration in coral reef fish larvae. *Journal of Experimental Marine Biology and Ecol* 299(1): 115-132.

Hadfield, M. G., and M.F. Strathmann. 1996. Variability, flexibility and plasticity in life histories of marine invertebrates. *Oceanologica acta* 19(3-4):323-334.

Hedgecock, D., P.H. Barber, and S. Edmands. 2007. Genetic approaches to measuring connectivity. *Oceanogr* 20(3): 70-80.

Hilario, A. A. Metaxas, S. M. Gaudron, K.L. Howell, A. Mercier, N. C. Mestre, R. E. Ross, A.M. Thurnherr, and C. Young. 2015. Estimating dispersal distance in the deep sea: challenges and applications to marine reserves. *Front Mar Sci* 2(6): 1-14.

Hunt, H. L., A. Metaxas, R.M. Jennings, K.M. Halanych, and L.S. Mullineaux. 2004. Testing biological control of colonization by vestimentiferan tubeworms at deep-sea hydrothermal vents (East Pacific Rise, 9 50′ N). *Deep Sea Research Part I: Oceanographic Research Papers*, 51(2), 225-234.

Jones, G.P., G.R. Almany, G.R. Russ, P.F. Sale, R.S. Steneck, M.J.H. van Oppen, and B.L. Willis. 2009. Larval retention and connectivity among populations of corals and reef fishes: history, advances, and challenges. *Coral Reefs* 28: 307-325.

Jones, W. J. and R.C. Vrijenhoek. 2006. Evolutionary relationships within the "Bathymodiolus " childressi group. *Cah. Biol. Mar.* 47: 403–407.

Kinlan, B.P., S.D. Gaines, S.E. Lester. 2005. Propagule dispersal and scales of marine community process. *Diversity Distrib* 11: 139-148.

Kough, A.S. and C.B. Paris. 2015. The influence of spawning periodicity on population connectivity. *Coral Reefs* 34.3 : 753-757.

Kroll, I., A. Poray, B. Puckett, D. Eggleston, J. Fodrie. 2016. Environmental effects on elemental signatures in the shells of the Eastern oyster, *Crassostrea virginica*: implications for the use of geochemical tagging to assess population connectivity. *Mar. Ecol. Prog. Ser*. 543:173-186, doi:10.3754/meps/11549.

Lefebvre, A. C. Ellien, D. Davoult, E. Thiebaut, J.C. Salomon. 2003. Pelagic dispersal of the brittle-star *Ophiothrix fragilis* larvae in a megatidal area (English Channel, France) examined using an advection-diffusion model. *Est Coast Shelf Sci* 57: 421-433.

Lester, S.E., B.I. Ruttenberg, S.D. Gaines, B.P. Kinlan. 2007. The relationship between dispersal ability and geographic range size. *Ecol Lett* 10: 745-758.

Levin, L.A. 2013. Recent progress in understanding larval dispersal: new directions and digressions. *Integ Compar Biol* 46(3): 282-297.

Levin, L.A. 2005. Ecology of cold seep sediments: interactions of fauna with flow, chemistry, and microbes. *Oceanog and Mar Biol: Ann Rev* 43: 1-46.

Levin, L.A. 2006. Recent progress in understanding larval dispersal: new directions and digressions. *Integ and Compar Biol* 46(3): 282-297.

Lillis, A., D.B. Eggleston, and D.R. Bohnenstiehl. 2013. Oyster larvae settle in response to habitat-associated underwater sounds. *PloS one* 8(10), e79337.

Marshall, D.J, P.D. Steinberg. 2014. Larval size and age affect colonization in a marine invertebrate. *J Exper Biol* 217: 3891-3987.

Marsh, A. G., L.S. Mullineaux, C.M. Young and D.T. Manahan. 2001. Larval dispersal potential of the tubeworm Riftia pachyptila at deep-sea hydrothermal vents. *Nature*, 411(6833), 77-80.

McCartney, M. S. 1993. Crossing of the equator by the deep western boundary current in the western Atlantic Ocean. *Journal of Physical Oceanog* 23(9), 1953-1974.

McGillicuddy, D. J., J.W. Lavelle, A.M. Thurnherr, V.K. Kosnyrev and L.S. Mullineaux. 2010. Larval dispersion along an axially symmetric mid-ocean ridge. *Deep Sea Research Part I: Oceanographic Research Papers* 57(7): 880-892.

Metaxas, A. 2011. Spatial patterns of larval abundance at hydrothermal vents on seamounts: evidence for recruitment limitation. *Mar. Ecol. Prog. Ser*, 437(10).

Mitarai, S., H. Watanabe, Y. Nakajima, A.F. Shchepetkin, and J.C. McWilliams. 2016. Quantifying dispersal from hydrothermal vent fields in the western Pacific Ocean. *PNAS* 113(11): 2976-2981.

Mooers, C. 1998. Intra-Americas circulation. The sea. The global coastal ocean. Regional Studies and Syntheses. John Wiley and Sons 183-208.

Mullineaux, L. S., D.K. Adams, S.W. Mills and S.E. Beaulieu. 2010. Larvae from afar colonize deep-sea hydrothermal vents after a catastrophic eruption. *Proc Natal Acad Sci* 107(17): 7829-7834.

North, E.W., R.R. Hood, S-Y Chao, L.P. Sanford. 2006. Using a random displacement model to simulate turbulent particle motion in a baroclinic frontal zone: A new implementation scheme and model performance tests. *J Mar Sys* 60: 365-80

Nye, V., J.T. Copley, and P.A. Tyler. 2013. Spatial variation in the population structure and reproductive biology of *Rimicaris hybisae* (Caridea: Alvinocarididae) at hydrothermal vents on the mid-cayman spreading centre. *Plos One* 8(3): 1:15.

Oey, L. T. Ezer, and H. Lee. 2005. Rings and related circulation in the Gulf of Mexico: a review of numerical models and future challenges. *Geophys Monograph Ser* 161: 31-56.

Olu-LeRoy, K, R. von Cosel, S. Hourdez, S.L. Carney, and D. Jollivet. 2007. Amphi-Atlantic cold-seep Bathymodiolus species complexes across the equatorial belt. *Deep-Sea Res I* 54:1890-911.

Oyarzun, F. X. and R.R. Strathmann. 2011. Plasticity of hatching and the duration of planktonic development in marine invertebrates. *Integ Compar Biol* 51(1):81-90.

Palumbi, S.R. 2004. Marine reserves and ocean neighborhoods: the spatial scale of marine populations and their management. *Ann Rev Environ Resources* 29: 31-68.

Paris, C.B. and R.K. Cowen. 2004. Direct evidence of a biophysical retention mechanism for coral reef larvae. *Limnol Oceanogr* 49: 1964-1979.

Pile, A.J. and C.M. Young. 1999. Plankton availability and retention efficiencies of cold-seep symbiotic mussels. *Limnol Oceanogr* 44:1833-1839.

Puckett, B. J. and D. B. Eggleston. 2016. Metapopulation dynamics guide marine reserve design: importance of connectivity, demographics, and stock enhancement *Ecosphere* (in press).

Puckett, B.J., D.B. Eggleston, P.C. Kerr and R.A. Luettich Jr. 2014. Larval dispersal and population connectivity among a network of marine reserves. *Fish and Oceanogr 23*(4), 342-361.

Qian, H., Y. Li, R. He, and D.B. Eggleston. 2015. Connectivity in the Intra-American seas and implications for potential larval transport. *Coral Reefs* 34(2), 403-417.

Schlag, Z. R., and E. W. North. 2012. Lagrangian TRANSport (LTRANS) v.2 model User's Guide. Technical Report of the University of Maryland Center for Environmental Science Horn Point Laboratory. Cambridge, MD. 183 p.

Shank, T.M., D.J. Fornari, K.L. Von Damm, M.D. Lilley, R.M. Haymon and R.A. Lutz. 1998. Temporal and spatial patterns of biological community development at nascent deep-sea hydrothermal vents (9 50′ N, East Pacific Rise). *Deep Sea Research Part II: Topical Studies in Oceanography* 45(1): 465-515.

Siegel, D.A., S. Mitarai, C.J. Costello, S.D. Gaines, B.E. Kendall, R.R. Warner, K.B. Winters. 2008. The stochastic nature of larval connectivity among nearshore marine populations. *Proc Nationl Acad Sci USA* 105: 8974-8979.

Sturges, W. and R. Leben. 2000. Frequency of ring separations from the loop current in the Gulf of Mexico: a revised estimate. *J Phys Oceanog* 30(7): 1814-1819.

Treml, E.A., J.J. Roberts, Y. Chao, P.N. Halpin, H.P. Possingham, and C. Riginos. 2012. Reproductive output and duration of the pelagic larval stage determine seascape-wide connectivity of marine populations. *Integ and Compar Biol* 52(4): 525-537.

Teixeira, S., K. Olu, C. Decker, R.L. Cunha, S. Fuchs, S. Hourdez, E.A. Serrao, S. Arnaud-Haond. 2013. High connectivity across the fragmented chemosynthetic ecosystems of the deep Atlantic Equatorial Belt: efficient dispersal mechanisms or questionable endemism? *Molec Ecol* 22(18): 4663-4680.

Thaler, A.D., K. Zelnio, W. Saleu, T.F. Schultz, J. Carlsson, C. Cunningham, R.C. Vrijenhoek, and C.L. Van Dover. 2011. The spatial scale of genetic subdivision in populations of *Ifremeria nautilei*, a hydrothermal vent gastropod from the southwest Pacific. *BMC Evol Biol* 11(372): 1-12.

Treml, E.A., J.J. Roberts, Y. Chao, P.N. Halpin, H.P. Possingham, and C. Riginos. 2012. Reproductive output and duration of the pelagic larval stage determine seascape-wide connectivity of marine populations. *Integ Compar Biol* 52(4): 525-537.

Tunnicliffe, V., R.W. Embley, J.F. Holden, D.A. Butterfield, G.J. Massoth and S.K. Juniper. 1997. Biological colonization of new hydrothermal vents following an eruption on Juan de Fuca Ridge. *Deep Sea Research Part I: Oceanographic Research Papers* 44(9): 1627-1644.

Tyler, P., C. M. Young, E. Dolan, S. M. Arellano, S. D. Brooke, and M. Baker. 2006. Gametogenic periodicity in the chemosynthetic cold-seep mussel *"Bathymodiolus" childressi. Mar. Biol.* 150 (5): 829-840.

Van Dover, C.L., C.R. German, K.G. Speer, L.M. Parson, and R.C. Vrijenhoek. 2002. Evolution and biogeography of deep-sea vent and seep invertebrates. *Science* 295(5558): 1253-1257.

Van Gaest and A. Lea. 2006. Ecology and early life history of Bathynerita naticoidea: evidence for long-distance larval dispersal of a cold seep gastropod.

Virjenhoek, R.C. 1997. Gene flow and genetic diversity in naturally fragmented metapopulations of deep-sea hydrothermal vent animals. *J Hered* 88(4): 285-293.

Vrijenhoek, R.C. 2010. Genetic diversity and connectivity of deep-sea hydrothermal vent metapopulations. *Molec Ecol* 19: 4391-4411

Weatherly, G.L., N. Wieders, and A. Romanou. 2005. Intermediate-depth circulation in the Gulf of Mexico estimated from direct measurements. In *Circulation in the Gulf of Mexico: Observations and Models*. W. Sturges, and A. Lugo-Fernandez, Eds., AGU Geophysical Monograph 161. American Geophysical Union, 315-324.

Young, C.M., P.A. Tyler, and J.D. Gage. 1996 (a). Vertical distribution correlates with pressure tolerances of early embryos in the deep-sea asteroid Plutonaster bifrons. *Journal of the Marine Biological Association of the United Kingdom* 76(3): 749-757.

Young, C.M., M.G. Devin, W. Jaeckle, S.U.K Ekaratne, S.B. George. 1996 (b). The potential for ontogenetic vertical migration by larvae of bathyal echinoderms. *Oceanol Acta* 19: 263-271.

Young, C.M., R. He, R.B. Emlet, Y. Li, H. Qian, S.M. Arellano, A.Van Gaest, K.C. Bennett, M. Wolf, T.I. Smart, and M.E. Rice. 2012. Dispersal of deep-sea larvae from Intra-American Seas: simulations of trajectories using ocean models. *Integ and Compar Biol* 52(4): 483-496.

TABLES

Table 1. Methane seep sites in the Gulf of Mexico and U.S. Western Atlantic Ocean

Site Name	Site Latitude (N)	Site Longitude (W)	Site Depth (m)
Alaminos Canyon	26 21'17"	94 29'48"	1300
Florida Escarpment	26 1'48"	84 54'54"	3300
Brine Pool	27 43'23"	91 16' 30"	660
Blake Ridge	32 29'45"	76 11'30"	2150
Cape Fear	32 58'45"	75 55'30"	2500

Table 2. Species-specific Pelagic Larval Duration (PLD) and dispersal behavior for larval particles in this study. *Bathymodiolus childressi* has three possible dispersal strategies, which are designated as 1, 2, and 3.

Species	PLD (days)	Dispersal Behavior
Lamellibrachia luymesi	21	Thermocline
Bathynerita naticoidea	90	Thermocline
Alvinocaris muricola	186	Near-surface
Bathymodiolus childressi (1)	395	Demersal drift
Bathymodiolus childressi (2)	395	175 days near-surface followed by demersal drift
Bathymodiolus childressi (3)	395	Near-surface

FIGURES

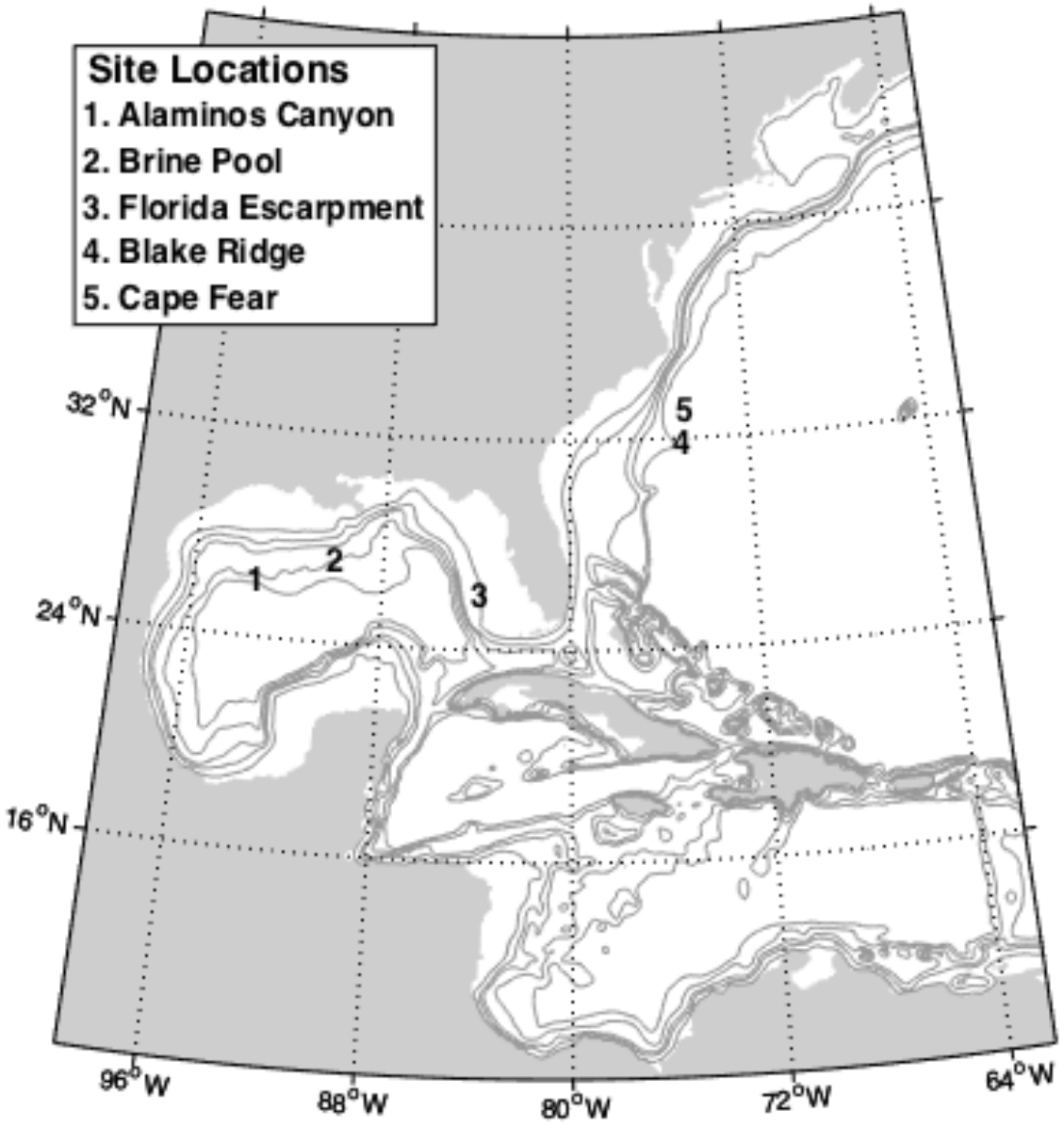

Figure 1. Spatial domain of *USEast* circulation model. Methane seep study sites are plotted on the model domain to match latitude, longitude, and depth of the actual locations: Alaminos Canyon, Brine Pool, Florida Escarpment, Blake Ridge, and Cape Fear.

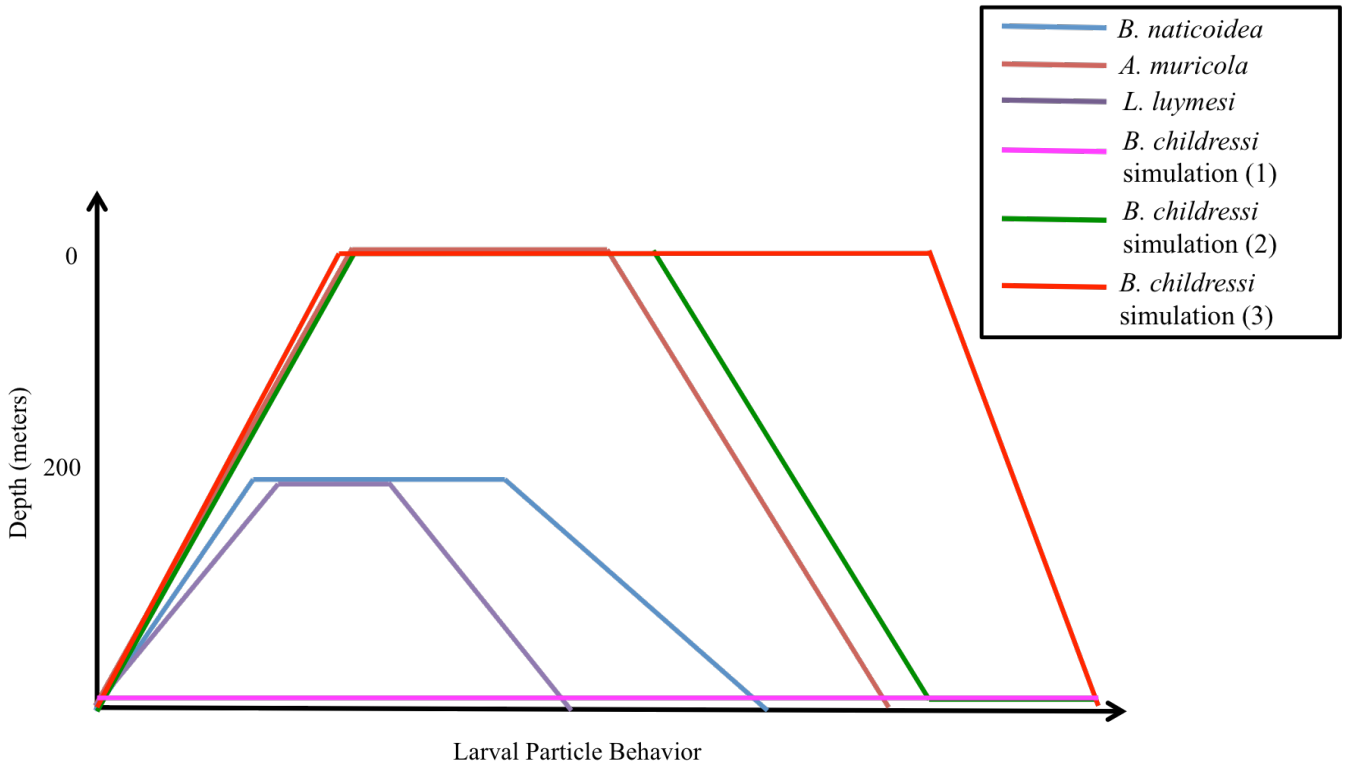

Figure 2. Schematic diagram of programmed species-specific behavior. Particles of *B. naticoidea* and *L. luymesi* dispersed at thermocline over the duration of their PLD, while *A. muricola* dispersed at the surface. Three behavior simulations for *"B." childressi* are shown as dispersing near bottom, 175 days at the surface, and 395 days at the surface. All particles were programmed to arrive on sea floor and settle by the end of their specific PLD.

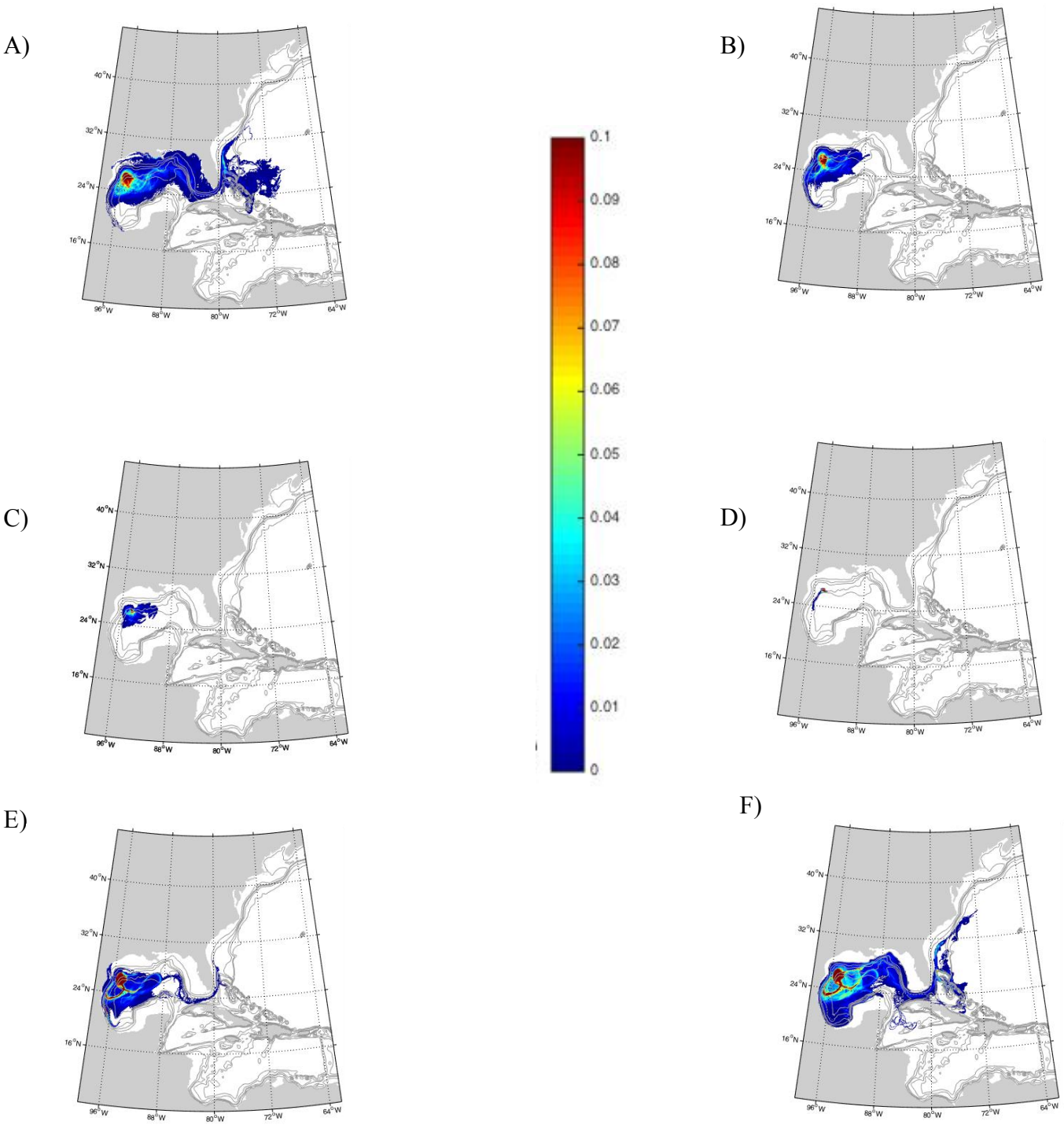

Figure 3. Lagrangian Particle Density Functions (LPDFs) for a single release site, Alaminos Canyon, (site 1 as shown in Fig. 1) based on the trajectories of (A) *Alvinocaris muricola*, (B) *Bathynerita naticoidea*, (C) *Lamellibrachia luymesi*, (D) *Bathymodiolus childressi* Simulation 1, (E) *Bathymodiolus childressi* Simulation 2, and (F) *Bathymodiolus childressi*

Simulation 3. Warmer colors indicate a higher probability (for example, 10%) of a particle dispersing through a particular grid cell in the model domain, whereas cooler colors signify lower probabilities of particles dispersing through the grid cell.

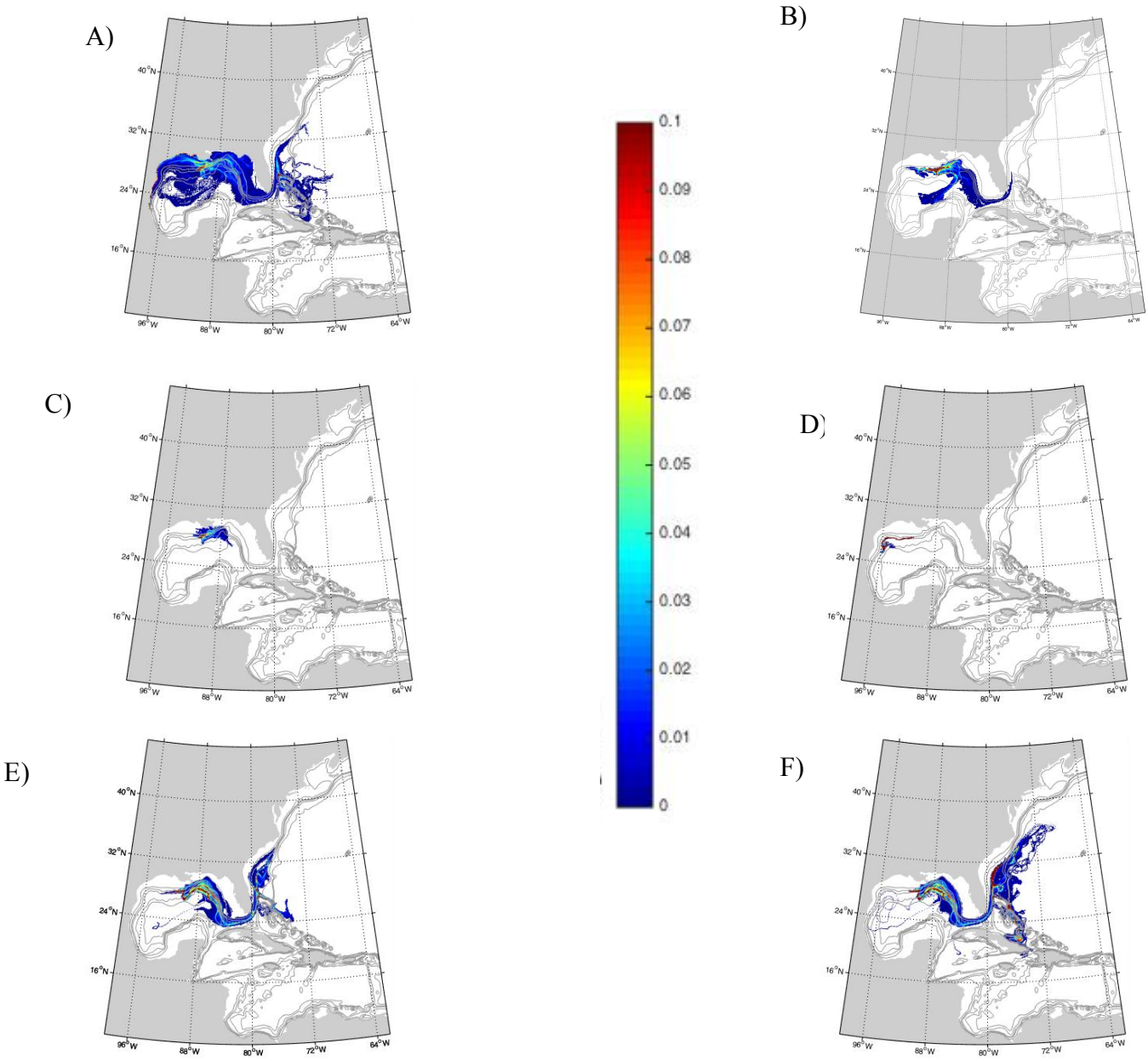

Figure 4. Lagrangian Particle Density Functions (LPDFs) for a single release site, Brine Pool, (site 2 as shown in Fig. 1) based on the trajectories of (A) *Alvinocaris muricola*, (B) *Bathynerita naticoidea*, (C) *Lamellibrachia luymesi*, and (D) *Bathymodiolus childressi* Simulation 1, (E) *Bathymodiolus childressi* Simulation 2, and (F) *Bathymodiolus childressi*

Simulation 3. Warmer colors indicate a higher probability (for example, 10%) of a particle dispersing through a particular grid cell in the model domain, whereas cooler colors signify lower probabilities of particles dispersing through the grid cell.

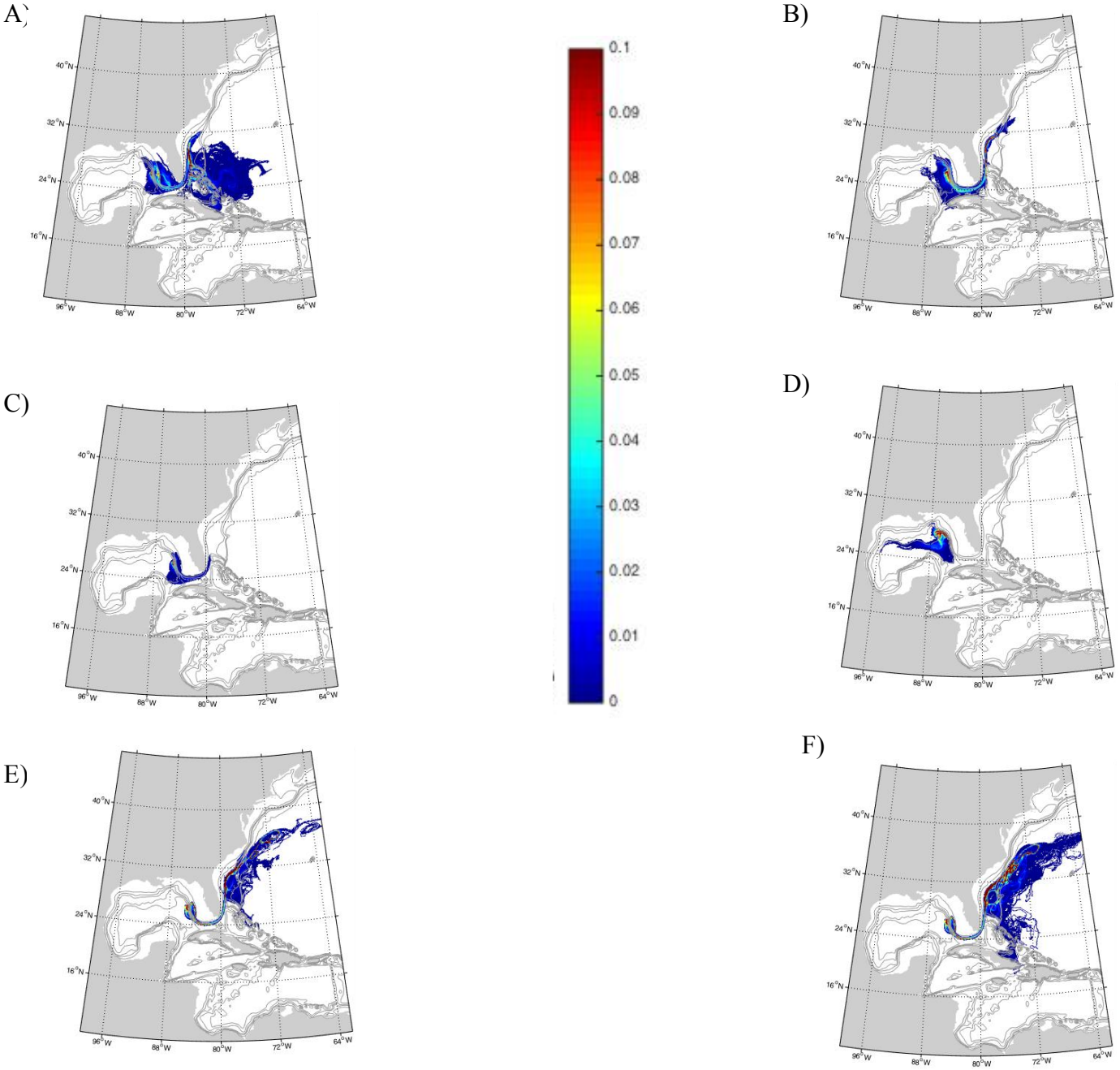

Figure 5. Lagrangian Particle Density Functions (LPDFs) for a single release site, Florida Escarpment, (site 3 as shown in Fig. 1) based on the trajectories of (A) *Alvinocaris muricola*, (B) *Bathynerita naticoidea*, (C) *Lamellibrachia luymesi*, and (D) *Bathymodiolus childressi*

Simulation 1, (E) *Bathymodiolus childressi* Simulation 2, and (F) *Bathymodiolus childressi* Simulation 3. Warmer colors indicate a higher probability (for example, 10%) of a particle dispersing through a particular grid cell in the model domain, whereas cooler colors signify lower probabilities of particles dispersing through the grid cell.

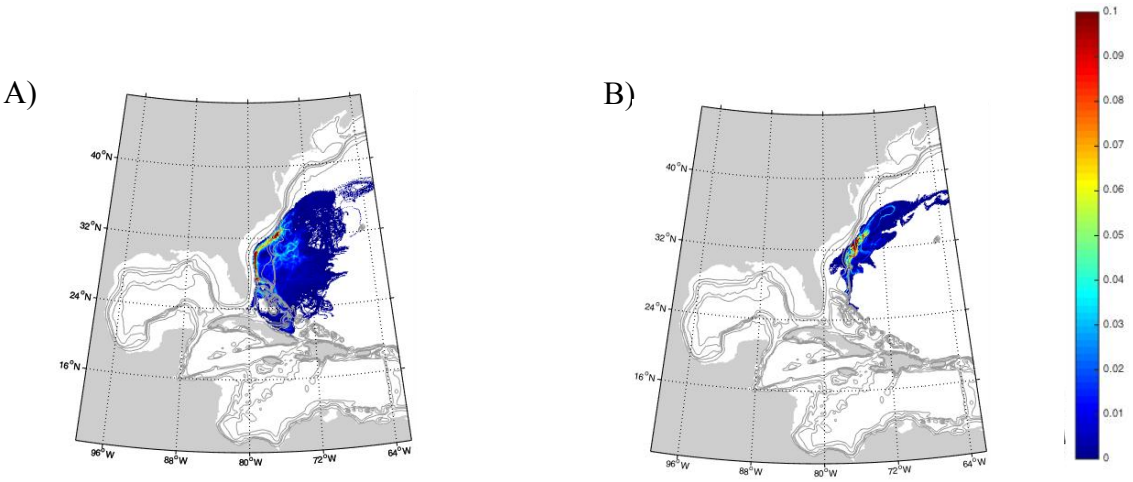

Figure 6. Lagrangian Particle Density Functions (LPDFs) for a single release site, Blake Ridge, (site 4 as shown in Fig. 1) based on the trajectories of (A) *Alvinocaris muricola*, and (B) *Bathynerita naticoidea*. Warmer colors indicate a higher probability (for example, 10%) of a particle dispersing through a particular grid cell in the model domain, whereas cooler colors signify lower probabilities of particles dispersing through the grid cell.

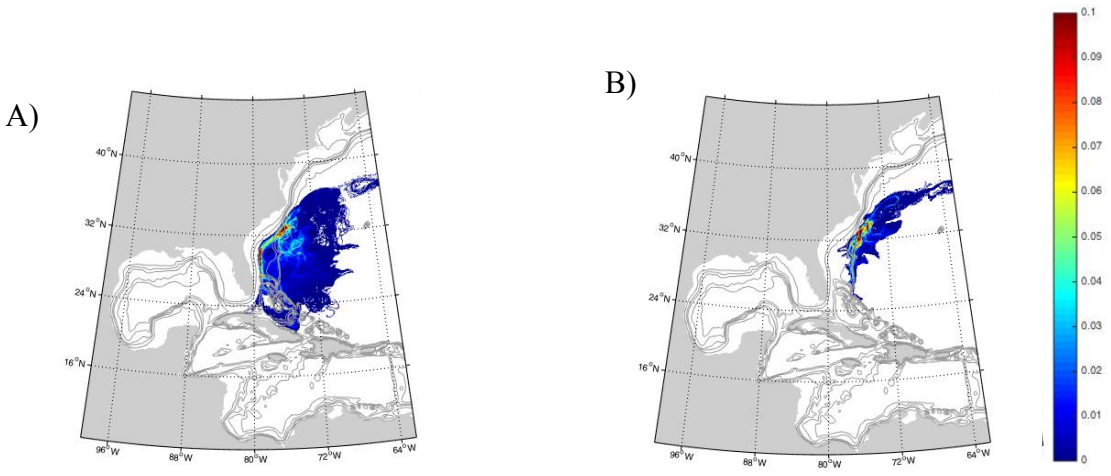

Figure 7. Lagrangian Particle Density Functions (LPDFs) for a single release site, Cape Fear, (site 5 as shown in Fig. 1) based on the trajectories of (A) *Alvinocaris muricola*, (B) *Bathynerita naticoidea*. Warmer colors indicate a higher probability (for example, 10%) of a particle dispersing through a particular grid cell in the model domain, whereas cooler colors signify lower probabilities of particles dispersing through the grid cell.

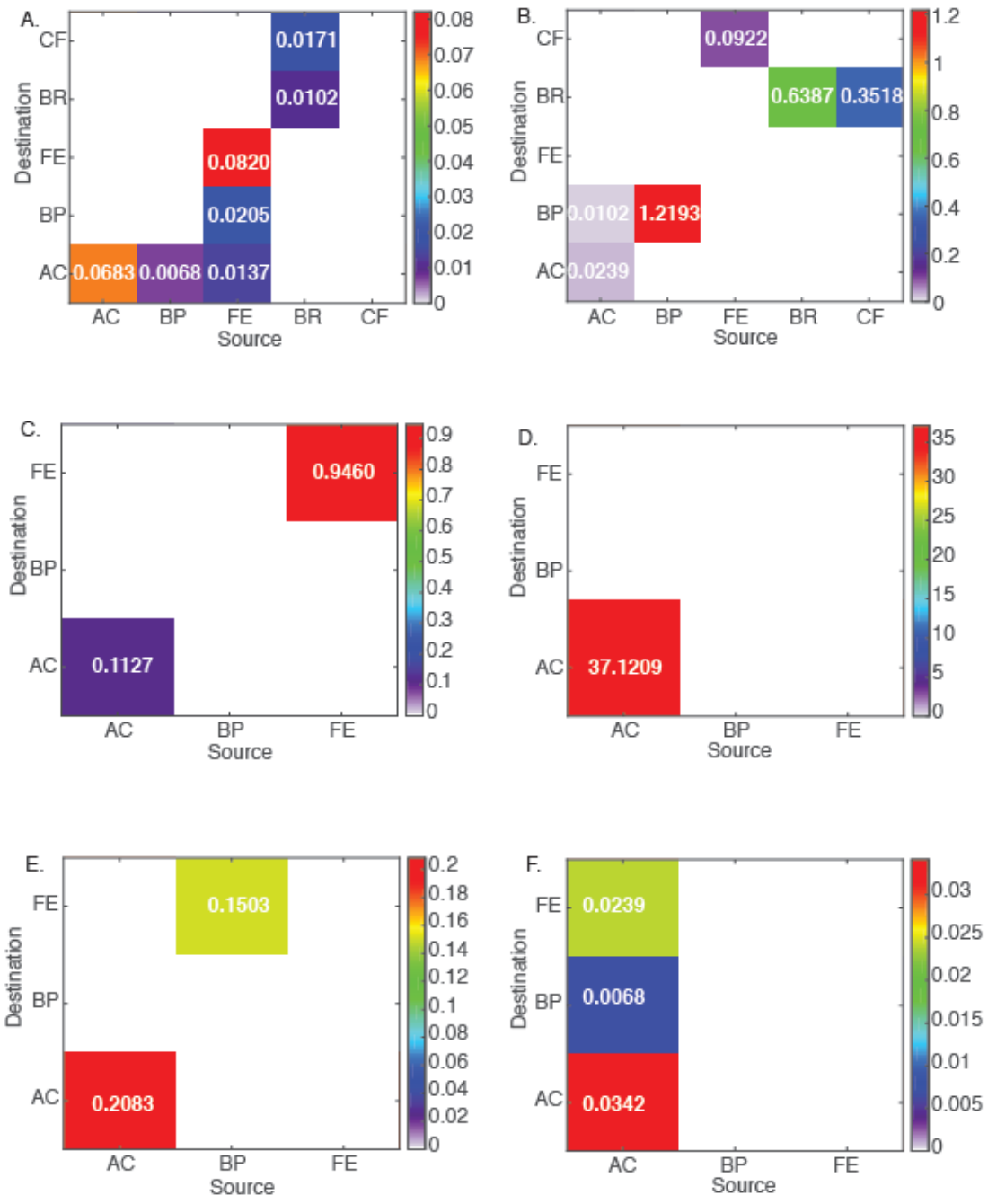

Figure 8. Average connectivity matrices indicating proportional exchange of larvae between natal seep sites (rows) and settlement seep sites (columns) for (A) *Alvinocaris muricola* (PLD = 186 days), (B) *Bathynerita naticoidea* (PLD = 90 days), (C) *Lamellibrachia luymesi* (PLD = 21 days), and (D) *Bathymodiolus childressi* Simulation 1 (PLD = 395 days), (E) *Bathymodiolus childressi* Simulation 2 (PLD = 395 days), and (F) *Bathymodiolus childressi*

Simulation 3 (PLD = 395 days. To determine average connectivity, the total number of particles that successfully connected to a site were divided by the total number of released particles and multiplied by 100 to get the actual percent value for each scenario. The magnitude of local retention and inter-site connectivity is depicted by the color bar. Warmer colors indicate a stronger percent connection between sties, while cooler colors denote a weaker connection. For ease of interpreting the data, the actual percent of connectivity for each species is depicted in every box. Care should be taken when interpreting the strength of connectivity for each species, as the color bar strength is specific to each species. To interpret the figure, begin first on the x axis (Source) and for connectivity with itself or another site on the y axis (Destination).

CONCLUSIONS

Studies of larval dispersal long considered larvae to be passive planktonic particles, completely subject to physical oceanographic processes, but in recent decades the roles of larval behavior in dispersal and settlement outcomes have become increasingly recognized (Levin 2006, Metaxas 2011). This study provides the first detailed characterization of the relative strength of larval dispersal and population connectivity of deep-sea, methane seep invertebrates that is known. Through the combination of ocean circulation and Lagrangian particle-tracking models, with empirical data on larval PLD, swimming speed and vertical distribution in the water column, this study addresses two fundamental challenges to our understanding of population connectivity: (i) spatial scales of connectivity in the deep sea, and (ii) mechanisms underlying potential connectivity for deep-sea invertebrates. Particles were programmed with species-specific behavior that corresponded to four seep species: *A. muricola*, *B. naticoidea*, *L. luymesi*, and *"B." childressi*, and tracked for five years among five methane seep sites in the GOM and Western Atlantic Margin to determine the dominant dispersal pathways and strength of potential population connectivity in the domain. The climatological conditions of the model domain provide an ideal method to understand dispersal patterns under average meteorological conditions. Although data on larval biology of deep-sea invertebrates are very limited, species-oriented studies that focus on behavior (e.g., Young et al. 1996a, Young et al. 1996b Arellano et al. 2014), coupled with ocean circulation models (Cowan et al. 2007, Kough et al. 2015, R. He, unpubl. data), can provide valuable predictions of larval dispersal and population connectivity of methane seep and

other unique deep-sea communities. The effects of spawning location and behavior on potential dispersal distances for three seep species (Chapter 1), combined with an in depth analysis of three potential larval behaviors for *"B." childressi* mean dispersal (Chapter 2), were quantified using LPDFs (Lagrangian Particle Density Function) and connectivity matrices to determine potential connectivity in the GOM and WAM (Chapter 3). Very few studies have attempted to model larval dispersal in the deep sea, and most have been limited by the availability of reliable estimates of biological parameters, including planktonic larval duration and larval behavior (Cowen and Sponaugule 2009, Young et al. 2012, Mitarai et al. 2016). The present study highlights how incorporating biological traits greatly influences larval dispersal trajectories and distances travelled, and why more biologically accurate simulations are necessary. Obtaining values of the relevant physiological and behavioral parameters of larvae that can be integrated into biophysical models should continue to take high priority in the study of deep-sea invertebrates and predictions of population connectivity. This dissertation advances our awareness of incorporating species-specific behavior in coupled biophysical models and increases our understanding of potential population connectivity of methane seep invertebrates.

REFERENCES

Arellano, S.M., A.L. Van Gaest, S.B. Johnson, R.C. Vrijenhoek, and C.M. Young. 2014. Larvae from deep-sea methane seeps disperse in surface waters. *Proc R Soc B* 281: 20133276.

Cowen, R.K. and S. Sponaugle. 2009. Larval dispersal and marine population connectivity. *Annu Rev Mar Sci* 1: 443-466.

Kough, A.S. and C.B. Paris. 2015. The influence of spawning periodicity on population connectivity. *Coral Reefs* 34(3): 753-757.

Levin, L. A. 2006. Recent progress in understanding larval dispersal: new directions and digressions. *Integr. Comp. Biol.* 46: 282-297.

Metaxas, A. 2011. Spatial patterns of larval abundance at hydrothermal vents on seamounts: evidence for recruitment limitation. *Mar. Ecol. Prog. Ser*, 437(10).

Mitarai, S., H. Watanabe, Y. Nakajima, A.F. Shchepetkin, and J.C. McWilliams. 2016. Quantifying dispersal from hydrothermal vent fields in the western Pacific Ocean. *PNAS* 113(11): 2976-2981.

Young, C.M., R. He, R.B. Emlet, Y. Li, H. Qian, S.M. Arellano, A.Van Gaest, K.C. Bennett, M. Wolf, T.I. Smart, and M.E. Rice. 2012. Dispersal of deep-sea larvae from Intra-American Seas: simulations of trajectories using ocean models. *Integ and Compar Biol* 52(4): 483-496.

Young, C.M., P.A. Tyler, and J.D. Gage. 1996 (a). Vertical distribution correlates with pressure tolerances of early embryos in the deep-sea asteroid Plutonaster bifrons. *Journal of the Marine Biological Association of the United Kingdom* 76(3): 749-757.

Young, C.M., M.G. Devin, W. Jaeckle, S.U.K Ekaratne, S.B. George. 1996 (b). The potential for ontogenetic vertical migration by larvae of bathyal echinoderms. *Oceanol Acta* 19: 263-271.

APPENDICES

APPENDIX 1

Sample script of LTRANS code used in behavior simulations for *Alvinocaris muricola* and *"B." childressi* simulation 2. Code is written in Fortan90 and provides the behavior regimes at the different larval stages. Particles exhibited no behavior the first two days, followed by weak upward swimming behavior at 0.02 cm s^{-1} from day three to ten. On the tenth day, swimming speed increased to 0.2 cm s^{-1} until particles reached near surface (<100 meters). There, particles dispersed in surface waters for 385 days, and started swimming down to the sea floor at 0.2 cm s^{-1} in order arrive on bottom by the end of the 395-PLD.

.f90 *Alvinocaris muricola* code

```
!TYPE 8: Alvinocaris.  Swim at 20.76 cm/min for first day, then
! try to swim near the surface until just before 3 months, then swim downward.
IF(P_behave(n) .EQ. 8) THEN
   btest = 0   !switch to control behavior

   !Particle swims up if deeper than 1.0 m below surface
   IF (P_zc .LT. (P_zetac-1.0)) THEN
      parBehav=P_swim(n,3)
      btest = 1
   END IF

   ! If within 1 m of surface, swim randomly (50% chance of swimming up)
   IF (btest.EQ.0) THEN
      negpos = 1.0
      dev1=genrand_real1()
      switch = 0.5
      IF (dev1.GT.switch) negpos = -1.0
      devB=genrand_real1()
      parBehav=negpos*devB*P_swim(n,3)
   END IF

   ! Make particle swim downward at deadage
   IF (P_age .GE. P_deadage(n)) THEN
      parBehav=-1.0*swimfast
   END IF
END IF
!-------------------------------------------------------------------------------
```

.f90 *"B." childressi* Simulation 2 code.

```
!TYPE 8:  Bathymodiolus childressi - type 2.
   ! Passive for first 2 days
   ! Days 3-10, swim upward @ 0.02 cm/s
   ! Days 10+, swim upward until reaching 100 m depth
   ! Passive until day 365.
   ! Swim downward at 0.2 cm/s
   IF(P_behave(n) .EQ. 8) THEN
     btest = 0   !switch to control behavior
     parBehav = 0.0

     ! If day 3-10, start swimming at swimslow
     IF (P_age .GE. swimstart) THEN
       parBehav=swimslow
     END IF

     !  If > 10 days, swim faster
     IF (P_age .GE. pediage) THEN
       parBehav=swimfast
     END IF

    ! If shallower than 100m, swim downward
     if (P_zc .GT. -100.0) then
       parBehav=-1.0*swimfast
     else if (P_zc .LT. -100.0) then
       parBehav= swimfast
     end if

     ! Time to swim down?  At 365 days (31536000.0 sec).
     IF (P_age .GE. 31536000.0) THEN
       parBehav=-1.0*swimfast

       ! If particle greater than 1.0 m from bottom, swim down
       IF (P_zc .LT. (P_depth+1.0)) THEN
         parBehav=0.0
       END IF
     END IF

     btest=1

   END IF
!-------------------------------------------------------------------------------
```

APPENDIX 2

Closer view of the Lagrangian Particle Density Functions (LPDFs) for a single release site, Alaminos Canyon, (site 1 as shown in Fig. 1) based on the trajectories of (A) *Alvinocaris muricola*, (B) *Bathynerita naticoidea*, (C) *Lamellibrachia luymesi*, (D) *Bathymodiolus childressi* Simulation 1, (E) *Bathymodiolus childressi* Simulation 2, and (F) *Bathymodiolus childressi* Simulation 3.

A)

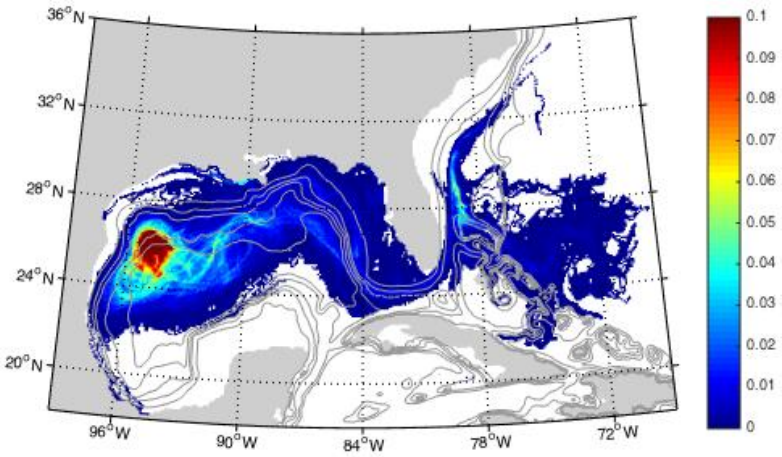

B)

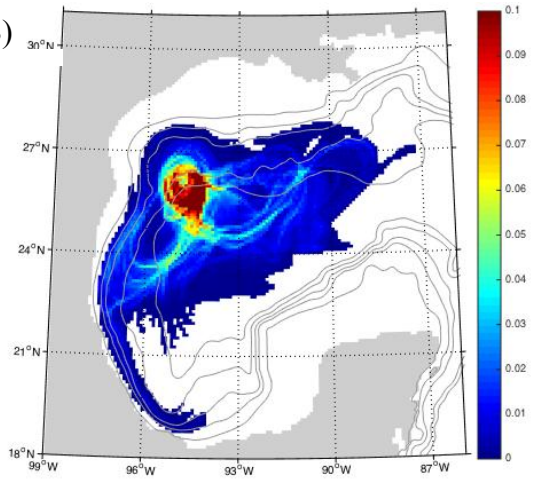

C)

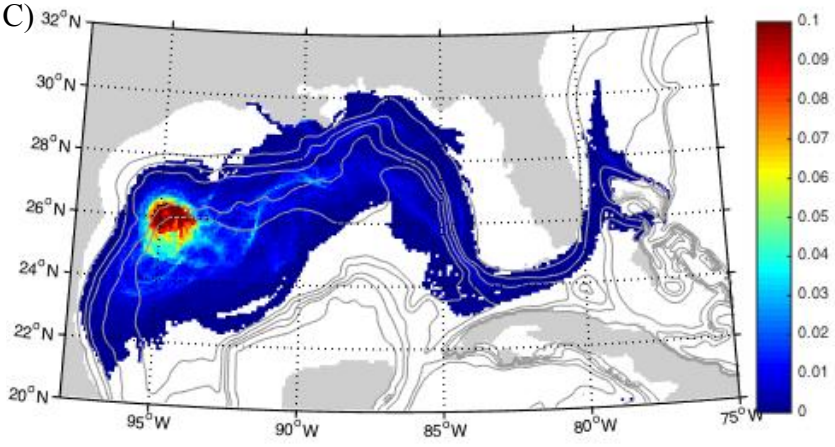

D)

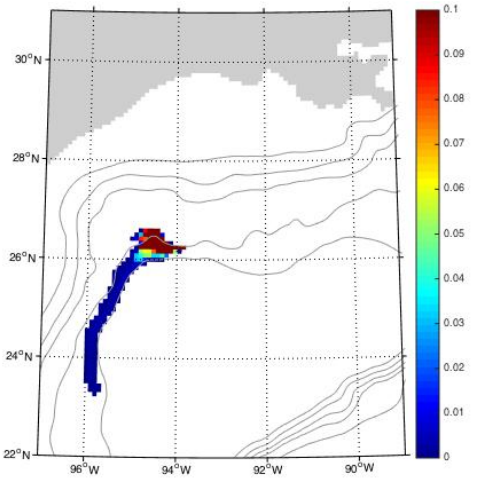

E)

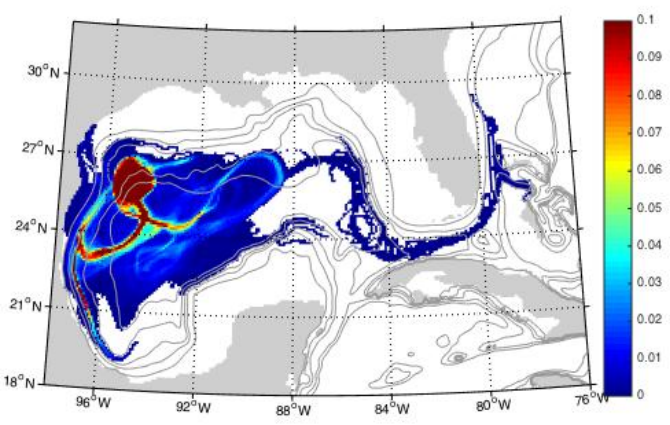

F)

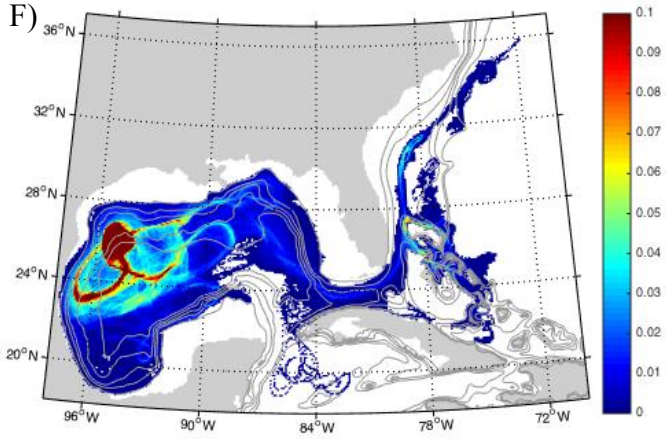

APPENDIX 3

Closer view of the Lagrangian Particle Density Functions (LPDFs) for a single release site, Brine Pool, (site 2 as shown in Fig. 1) based on the trajectories of (A) *Alvinocaris muricola*, (B) *Bathynerita naticoidea*, (C) *Lamellibrachia luymesi*, and (D) *Bathymodiolus childressi* Simulation 1, (E) *Bathymodiolus childressi* Simulation 2, and (F) *Bathymodiolus childressi* Simulation 3.

A)

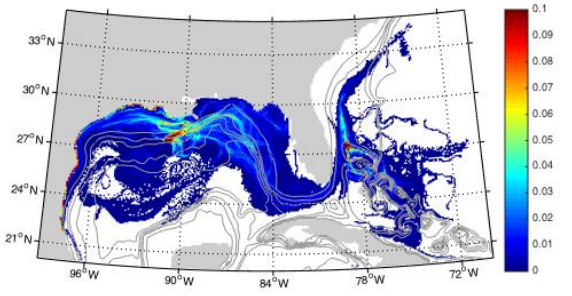

B)

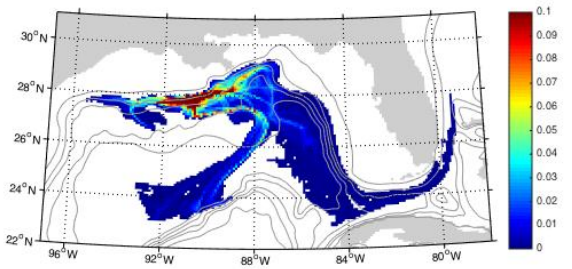

C)

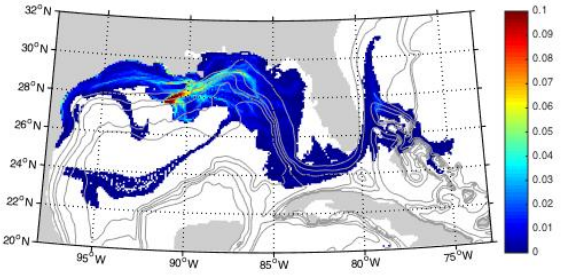

D)

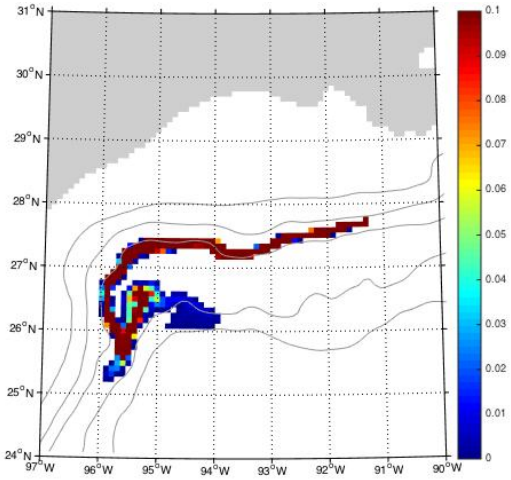

E)

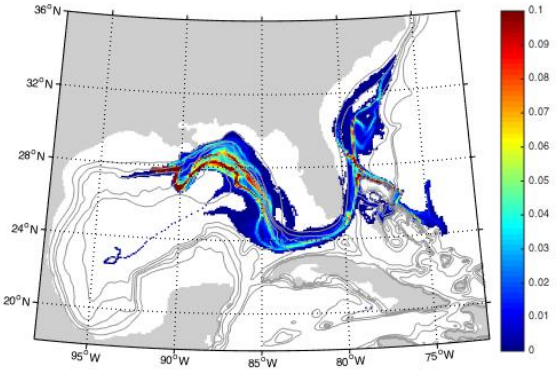

F)

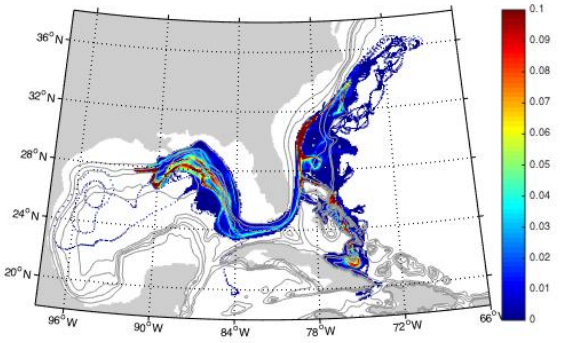

APPENDIX 4

Closer view of the Lagrangian Particle Density Functions (LPDFs) for a single release site, Florida Escarpment, (site 3 as shown in Fig. 1) based on the trajectories of (A) *Alvinocaris muricola*, (B) *Bathynerita naticoidea*, (C) *Lamellibrachia luymesi*, and (D) *Bathymodiolus childressi* Simulation 1, (E) *Bathymodiolus childressi* Simulation 2, and (F) *Bathymodiolus childressi* Simulation 3.

A)

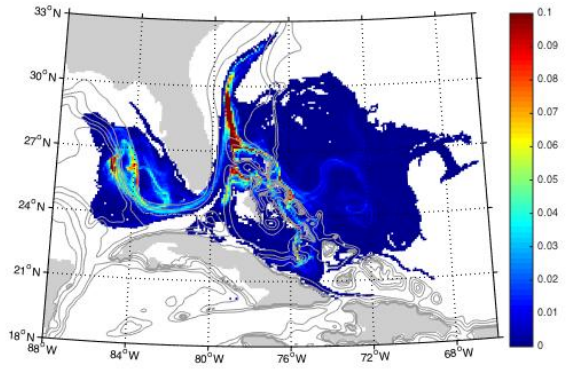

B)

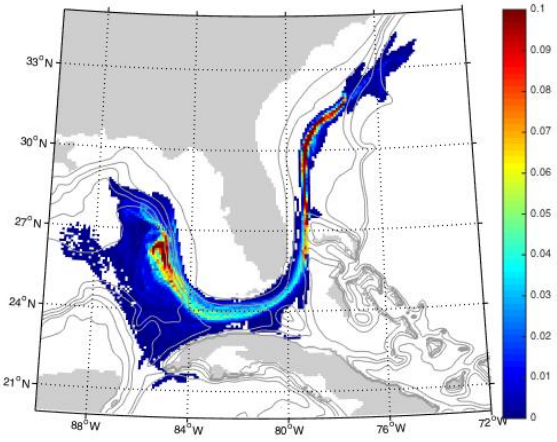

C)

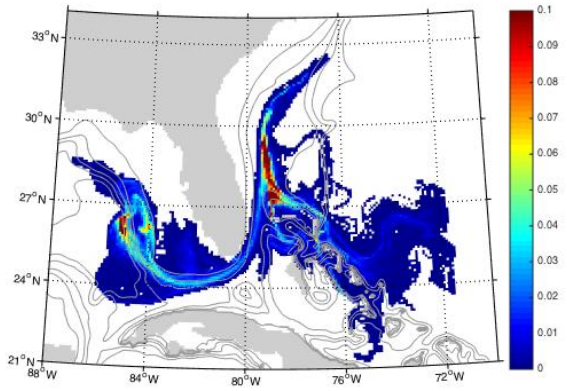

D)

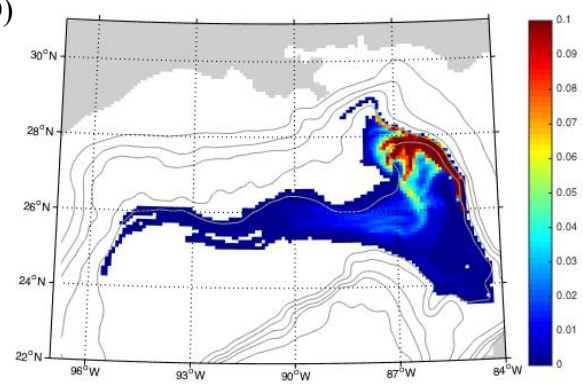

E)

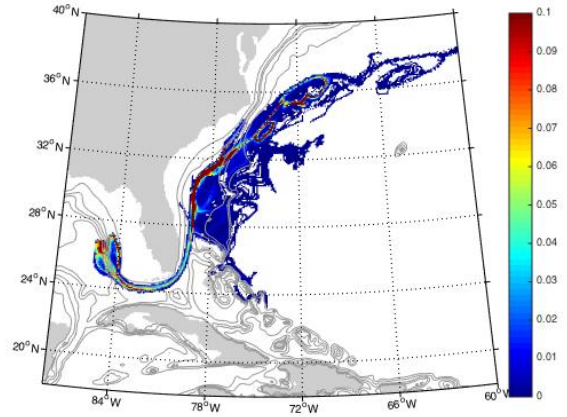

F)

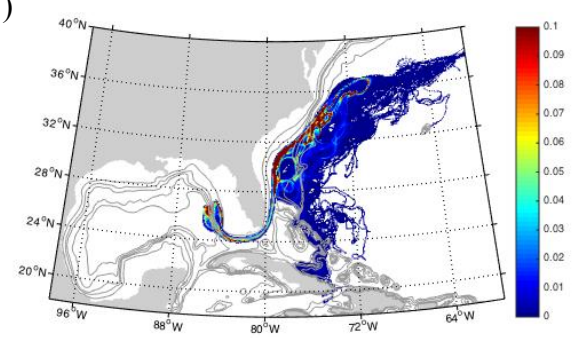

APPENDIX 5

A closer view of the Lagrangian Particle Density Functions (LPDFs) for a single release site, Blake Ridge, (site 4 as shown in Fig. 1) based on the trajectories of (A) *Alvinocaris muricola*, and (B) *Bathynerita naticoidea*.

A)

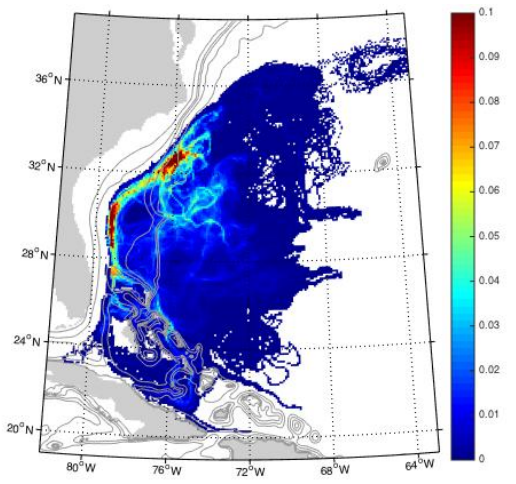

B)

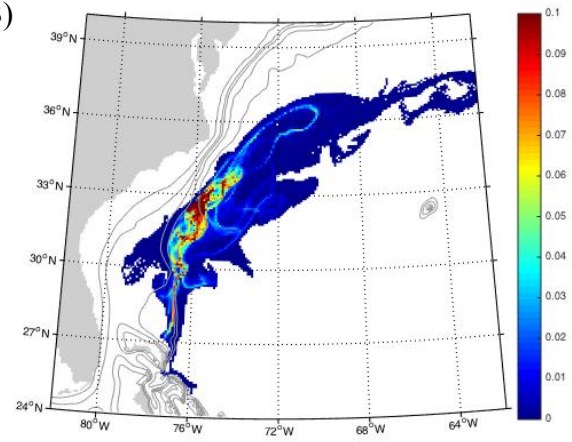

APPENDIX 6

A closer view of the Lagrangian Particle Density Functions (LPDFs) for a single release site, Cape Fear, (site 5 as shown in Fig. 1) based on the trajectories of (A) *Alvinocaris muricola*, and (B) *Bathynerita naticoidea*.

A)

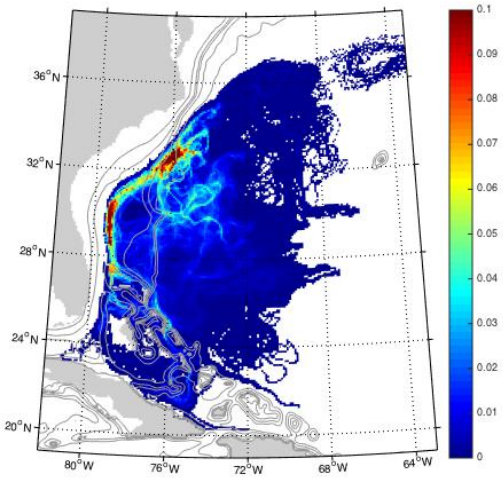

B)

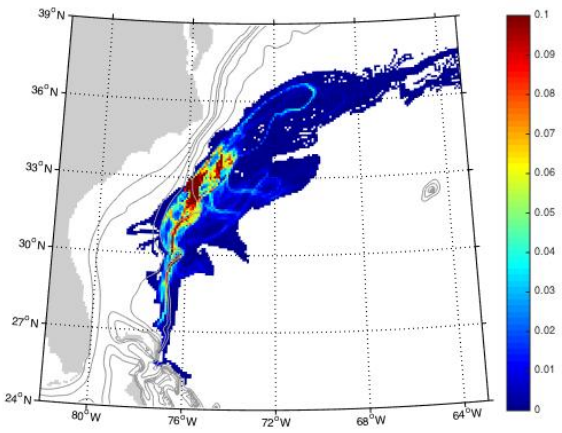

APPENDIX 7

Average connectivity matrix indicating proportional exchange of larvae between natal seep sites (rows) and settlement seep sites (columns) for *Bathynerita naticoidea* (PLD = 90 days) with the ability to connect with a site up to 10 days before the end of their 90-day PLD. To determine average connectivity, the total number of particles that successfully connected to a site were divided by the total number of released particles and multiplied by 100 to get the actual percent value for each scenario. The magnitude of local retention and inter-site connectivity is depicted by the color bar. Warmer colors indicate a stronger percent connection between sties, while cooler colors denote a weaker connection. For ease of interpreting the data, the actual percent of connectivity for each species is depicted in every box. Care should be taken when interpreting the strength of connectivity for each species, as the color bar strength is specific to each species. To interpret the figure, begin first on the x axis (Source) and for connectivity with itself or another site on the y axis (Destination).